# Analysis and Synthesis of Semi-Markov Jump Linear Systems and Networked Dynamic Systems

by

Ji Huang
B.Sc., Northwestern Polytechnical University, 2008

A Dissertation Submitted in Partial Fulfillment of the
Requirements for the Degree of

DOCTOR OF PHILOSOPHY

in the Department of Mechanical Engineering

Analysis and Synthesis of Semi-Markov Jump Linear Systems and Networked Dynamic Systems

by

Ji Huang
B.Sc., Northwestern Polytechnical University, 2008

Supervisory Committee

---

Dr. Yang Shi, Supervisor
(Department of Mechanical Engineering)

---

Dr. Daniela Constantinescu, Departmental Member
(Department of Mechanical Engineering)

---

Dr. Xiaodai Dong, Outside Member
(Department of Electrical and Computer Engineering)

**Supervisory Committee**

---

Dr. Yang Shi, Supervisor
(Department of Mechanical Engineering)

---

Dr. Daniela Constantinescu, Departmental Member
(Department of Mechanical Engineering)

---

Dr. Xiaodai Dong, Outside Member
(Department of Electrical and Computer Engineering)

## ABSTRACT

Physical processes which are governed by differential equations or difference equations with discontinuous behavior can be modeled as jump systems. An important type of jump systems is the one evolving linearly among the discrete events; this type of systems is called jump linear systems. A common analysis approach is to employ stochastic processes to describe the sequences, switches, and statistic properties of the discrete events. In this thesis, the jump linear systems to be studied are governed by semi-Markov processes. This type of jump linear systems is called the semi-Markov jump linear system. Due to the nature of the jump linear system, it finds many applications in networked control systems, fault tolerant control systems, and other systems subject to abrupt changes. It is worthwhile to mention that the well studied Markov jump linear system is a special case of the semi-Markov jump linear system.

The thesis consists of two parts: The analysis and synthesis of semi-Markov jump linear systems and networked dynamic systems. In Chapter 2 and Chapter 3, the stochastic stability and optimal control for semi-Markov jump linear systems with or without time delays are investigated. In Chapter 4, a novel fault tolerant control scheme is proposed based on the semi-Markov jump linear system stability conditions. Chapter 5 to Chapter 7 discuss the networked dynamic systems analysis via jump linear system approaches.

The stochastic stability conditions for semi-Markov jump linear systems are firstly derived. The Lyapunov theory is used to establish the sufficient stability conditions by deriving the infinitesimal generator of the Lyapunov function. Since in practice, almost all the system models could not be identified precisely, robust control problems for systems with uncertainties are investigated based on the established stability conditions. Considering the potential applications on networked systems where time delays are inevitable, optimal control problems for systems with time-varying delays have been studied. In the fault tolerant control design, the semi-Markov process is ideal to characterize time-varying failure rates of the system components whose life time is not exponentially distributed. The designed controller is capable of maintaining the stability when an actuator malfunctions.

In the networked control system analysis, stochastic processes are used to model time delays and sensor scheduling rules. Network limitations are compensated by considering more historical information or planning for all possible delays that happen in the future. Both simulations and experiments show the improvements of the control performance by using the proposed techniques. A networked haptic system is investigated via the switching system approach. In the haptic system, the avatar interacts one-dimensionally with a multi-material virtual wall in the virtual environment. The random trajectory along which the avatar moves upon the wall is modeled by stochastic processes, then the multi-material virtual wall rendering is achieved.

Finally, the thesis work is summarized and two future research topics are proposed. One is on the networked control system design where delays are modeled by semi-Markov processes, and the other one is on the event-trigger scheme design for networked dynamic systems.

# Contents

**Supervisory Committee** **ii**

**Abstract** **iii**

**Table of Contents** **v**

**List of Tables** **viii**

**List of Figures** **ix**

**Acknowledgements** **xii**

**Acronyms** **xiii**

**1 Introduction** **1**

1.1 Jump Linear Systems . . . . . 1

1.2 Networked Control Systems . . . . . 5

1.3 Research Motivations . . . . . 11

1.4 Contributions and Thesis Organization . . . . . 12

**2 Stability and Control of Semi-Markov Jump Linear Systems** **15**

2.1 Introduction . . . . . 15

2.2 Problem Formulation . . . . . 17

2.3 Stochastic Stability Analysis of S-MJLS . . . . . 19

2.4 Robust State Feedback Control for S-MJLS . . . . . 25

2.5 Illustrative Examples . . . . . 30

2.6 Conclusion . . . . . 33

**3 $H_\infty$ State-Feedback Control for Semi-Markov Jump Linear Systems with Time-Varying Delays** **35**

3.1 Introduction . . . . . 35
3.2 Problem Formulation . . . . . 37
3.3 Main Results . . . . . 39
3.3.1 Stochastic Stability Condition for Delayed S-MJLS . . . . . 39
3.3.2 $H_\infty$ Controller Design for Delayed S-MJLS . . . . . 42
3.3.3 Conservativeness Reduction . . . . . 49
3.4 Numerical Example . . . . . 50
3.5 Conclusion . . . . . 52

**4 Active Fault Tolerant Control Systems by the Semi-Markov Model Approach 54**
4.1 Introduction . . . . . 54
4.2 Problem Formulation . . . . . 56
4.3 Main Results . . . . . 60
4.3.1 Stochastic Stability . . . . . 61
4.3.2 Control Performance . . . . . 63
4.4 Numerical Examples . . . . . 66
4.5 Conclusions . . . . . 72

**5 Networked Control System Design Using Historical Data 74**
5.1 Introduction . . . . . 74
5.2 Problem Formulation . . . . . 76
5.3 Main Results . . . . . 79
5.4 Numerical Examples . . . . . 83
5.5 Conclusions . . . . . 86

**6 Networked Control System Design: A Haptic Example 88**
6.1 Introduction . . . . . 88
6.2 System Identification and the Stochastic Model . . . . . 90
6.2.1 System Identification . . . . . 91
6.2.2 Stochastic Model . . . . . 92
6.3 Stability Analysis . . . . . 93
6.4 Transparent Virtual Coupler Design . . . . . 97
6.5 Simulation and Experimental Results . . . . . 101
6.5.1 Simulation . . . . . 101
6.5.2 Experiment . . . . . 101

6.6 Conclusion and Future Work . . . . . 103

**7 Robust Tracking Control of Networked Control Systems: Application to a Networked DC Motor 105**

7.1 Introduction . . . . . 105
7.2 Problem Statement . . . . . 108
7.3 Robust $H_2$ and $H_\infty$ Optimal Tracking . . . . . 113
7.3.1 Reformulating the NCS as MJLS . . . . . 113
7.3.2 Robust $H_2$ Tracking Control . . . . . 116
7.3.3 Robust $H_\infty$ Tracking Control . . . . . 119
7.3.4 Mixed $H_2/H_\infty$ Tracking Control Design . . . . . 121
7.4 Simulation and Experimental Results . . . . . 121
7.4.1 Numerical Example on a VTOL System . . . . . 122
7.4.2 Numerical Simulation on a Networked DC Motor System . . . 124
7.4.3 Experimental Test on the Networked DC Motor System . . . . 126
7.5 Conclusions . . . . . 129

**8 Conclusions and Future Work 131**

8.1 Summary of the Thesis . . . . . 131
8.2 Future Work . . . . . 133
8.2.1 S-MJLSs Applied in NCSs . . . . . 133
8.2.2 Event-Triggered S-MJLSs . . . . . 134

# List of Tables

Table 2.1 ± Standard deviation. . . . . 33

Table 3.1 VTOL parameters depending on the speed. . . . . 51

Table 7.1 Sum of squared tracking errors over 0-5s (VTOL example). . . . 124
Table 7.2 Sum of squared tracking errors (DC motor example). . . . . 127

# List of Figures

Figure 1.1 Typical setup of an NCS. . . . . 6
Figure 1.2 Two main research streams of NCSs. . . . . 7
Figure 1.3 Depictions of S-C delays and C-A delays in NCSs. . . . . 9
Figure 1.4 Road map of the research. . . . . 12

Figure 2.1 Beginning and ending time for each sections. . . . . 29
Figure 2.2 One run simulation and Monte Carlo simulation. . . . . 32
(a) Comparison by using Corollary 2.2 and techniques in [1, 2] (S2003). 32
(b) Monte Carlo simulation with different semi-Markov processes for 20 runs by using Corollary 2.2. . . . . 32
Figure 2.3 Average results and statistics of the Monte Carlo simulation (10000 runs). . . . . 33
(a) Average system trajectories by using Monte Carlo simulation (10000 runs). . . . . 33
(b) Statistics of the settling time by using two methods (10000 runs). 33
Figure 2.4 Convergence of Monte Carlo simulation. . . . . 34
(a) Convergence of Monte Carlo simulation (Mean). . . . . 34
(b) Convergence of Monte Carlo simulation (Std). . . . . 34

Figure 3.1 The relationship among the jump linear systems, S-MJLSs, and MJLSs. . . . . 36
Figure 3.2 The state trajectories of the closed-loop S-MJLS using the proposed controller in (3.27). . . . . 51

Figure 4.1 Life time PDFs with different number of redundant components. 56
Figure 4.2 Transition rates with different number of redundant components. 56
Figure 4.3 Fault occurrence trajectory. . . . . 69
Figure 4.4 State trajectories by using the proposed controller (4.30). . . . 70
Figure 4.5 State trajectories by using the proposed controller (4.31). . . . 70

Figure 4.6 Average system trajectories (Monte Carlo simulation (100 runs)) by using the proposed controller (4.30). . . . . 71
Figure 4.7 Average system trajectories (Monte Carlo simulation (100 runs)) by using the proposed controller (4.31). . . . . 71
Figure 4.8 $\|y_t\|/\|\omega_t\|$ for the 100 simulations. . . . . 72

Figure 5.1 NCSs with multi-sensors. . . . . 76
Figure 5.2 State information to be used by the controller. . . . . 78
Figure 5.3 State trajectories by using controller without historical information. . . . . 86
Figure 5.4 State trajectories by using the proposed controller. . . . . 86

Figure 6.1 Phantom Omni device modeling. . . . . 91
Figure 6.2 A part of the mixed virtual environment. . . . . 92
Figure 6.3 Schematic diagram of the haptic system. . . . . 94
Figure 6.4 Block diagram of the haptic system. . . . . 96
Figure 6.5 Block diagram representation of $W(z)\cdot\left(\frac{G_i(z)}{1+G_i(z)C_i(z)}z^{-(\tau_1+\tau_2)}-G_i(z)\right)$. 98
Figure 6.6 Block diagram representation of $W(z)\cdot\left(\frac{\bar{G}_i(z)}{1+\bar{G}_i(z)\bar{C}_i(z)}z^{-(\tau_1+\tau_2)}-G_i(z)\right)$. 99
Figure 6.7 Configuration of the Phantom Omni Haptic System. . . . . 101
Figure 6.8 Penetration response by applying a constant force on each material. 102
Figure 6.9 The 3D avatar trajectory at different view points. . . . . 103
Figure 6.10 The trajectory of the avatar on the mixed virtual wall. . . . . 103

Figure 7.1 Diagram of a networked control system. . . . . 109
Figure 7.2 Step response in NCSs using the proposed robust $H_2$ controller and the local robust $H_2$ controller. . . . . 123
Figure 7.3 Step response using the proposed robust $H_\infty$ controller and the local robust $H_\infty$ controller. . . . . 123
Figure 7.4 Simulation results using the proposed $H_\infty$ controller, $H_2$ controller, and Smith predictor for the networked DC motor system under a simulated network environment. . . . . 126
Figure 7.5 The experimental setup of the networked DC motor system. . . 127
Figure 7.6 Experimental and simulation results using the proposed $H_\infty$ controller for the networked DC motor system under a simulated network environment. . . . . 128

Figure 7.7 Experimental and simulation results using the proposed $H_2$ controller for the networked DC motor system under a simulated network environment. . . . . 128
Figure 7.8 Simulation and experimental results using the local controller for the networked DC motor system under a simulated network environment. . . . . 129

Figure 8.1 The idea illustration of the semi-Markov process based NCS. . . 134
Figure 8.2 The idea illustration for event-trigger scheme based on the error between adjacent measurements. . . . . 135

# ACKNOWLEDGEMENTS

First and foremost, I would like to express my most gratitude to my supervisor Dr. Yang Shi for his patience, encouragement, intelligence, guidance, and support. During the PhD studies, he showed and taught me how to do research from wisely selecting appropriate research papers to effectively and efficiently reading the literature, from rigorously deriving theoretical results to accurately conducting experiments, and from professionally writing technical papers to comprehensively replying to reviewers' questions. Beyond that, he is also a true mentor who shares his own experiences from which I learned why and how to become a considerate person.

I would like to thank the thesis committee members, Dr. Daniela Constantinescu and Dr. Xiaodai Dong. I enjoy sitting in Dr. Constantinescu's course and Dr. Dong's constructive comments and advice that have inspired me a lot in this thesis work.

My gratitude also goes to my coauthors: Bo Yu, Jian Wu, and Fuqiang Liu. It has always been great to collaborate with them. Without their help, it would take a much longer time to solve some research challenges.

I would also like to thank the friends within and outside of the Applied Control and Information Processing Lab. Yang Lin and Wutao Yin offered great help on transportations. Huazhen Fang could always come up with solutions for mathematical problems. Hui Zhang helped me with LMI problems. Huiping Li contributed to this thesis on efficient optimization techniques. The days with group members, Qiao Zhang, Lili Han, Jie Ding, and Shurong Chen in Saskatoon were memorable. The days with group members, Xiaotao Liu, Mingxi Liu, Bingxian Mu, Yanjun Liu, Wenbai Li, Dr. Yinyan Zhao, Ping Cheng, Dr. Fang Fang, Dr. Le Wei, Dr. Zexu Zhang, and Xue Zhang in Victoria will become memorable. My sincere thanks go to Jing Qian.

I feel grateful to work in MPC Consulting Ltd as a Co-op student. My supervisor at MPC, Mr. Paul Bulmer, guided me on the professional way of doing engineering projects. His suggestions were always insightful and applicable. I enjoy every single day with my colleagues: Lori Fitzgerald, Jazz Harding, Mark Bragg, Afshin Safa, Michael Marek, Dwaine Williams, and Dave Dolomont, for their support, kindness, and training. Thank Dr. Shi again for providing me the Co-op opportunity.

Lastly, I would like to thank my mother Qiaojun Chen and my father Rongyu Huang for all their trusts on whatever choices I have made. I am very lucky and happy to meet my wife Ying Dai. I also greatly appreciate the understanding from her family, which inspires me to finish the study.

# Acronyms

**BIBO** Bounded-input bounded-output

**CDF** Cumulative distribution function

**HIL** Hardware-in-the-loop

**LMI** Linear matrix inequality

**LTI** Linear time-invariant

**MIMO** Multiple-input and multiple-output

**MJLS** Markov jump linear system

**MPC** Model predictive control

**NCS** Networked control system

**PDF** Probability distribution function

**PID** Proportional integral derivative

**SIQC** Stochastic integral quadratic constraint

**SISO** Single-input and single-output

**S-MJLS** Semi-Markov jump linear system

**VTOL** Vertical take-off and landing

**ZOH** Zero-order hold

# Chapter 1

# Introduction

## 1.1 Jump Linear Systems

Jump linear systems, sometimes referred to as hybrid systems, are mathematical models of the practical dynamic systems or processes that are governed by differential equations or difference equations with discontinuous behavior [3]. A jump linear system consists of a set of linear systems, and the overall system switches among discrete events. It is assumed that the dynamics between discrete events is linear, because 1) linear systems have been well studied and many results have been reported during the past decades; 2) many practical processes can be well modeled in the framework of jump linear systems, such as systems subject to component failures and systems with parameter shifting [4].

Depending on different time domains, jump linear systems can be classified: Discrete-time jump linear systems and continuous-time jump linear systems. A review of the two categories is as follows.

For discrete-time jump linear systems, a popular treatment for the switching of the discrete-time stochastic process is to assume that the process switches at each time step. The applications of discrete-time Bernoulli jump linear systems have been reported extensively, though the terminology – Bernoulli switching system was not explicitly adopted. For instance, Gupta *et al.* provided an example on the Bernoulli jump linear system in [5], where the measurements from sensors are transmitted through unreliable communication links subject to Bernoulli distributed dropouts; as a result, the closed-loop dynamics exhibits a Bernoulli switching pattern. In Bernoulli processes, it only allows two possible states, taking either 1 or 0. This intrinsic

property of Bernoulli processes coincides with the nature of the fault isolation and fault tolerant control, where the operating modes are "working" and "failure". If the probability of a successful transmission is $p$ and the probability of an unsuccessful transmission is $1-p$, then the overall system in the closed-loop form jumps according to a Bernoulli process. This type of systems has been studied for decades in the area of fault isolation and fault tolerant control [6].

The analysis and synthesis of continuous-time jump linear systems are more complicated and mathematically involved. Some features and characteristics in continuous-time systems do not have direct analogies to discrete-time systems. A big challenge lies in that the variations of the system dynamics may occur at any time during the operation in continuous-time systems, while discrete-time systems could only jump at specific time instants [7, 8]. Since both continuous state variables of a plant or a process, such as displacement, velocity, or accelerations, and discrete state variables of the governing processes co-exist, continuous-time jump linear systems are sometimes called "hybrid systems". This type of "hybrid systems" can be employed to model many practical systems, such as, electrical power systems and the solar thermal central receiver [9]. The continuous-time switching model has brought in many benefits in the stability analysis and controller design. In [10], the Markov process has been employed to model a vertical take-off and landing (VTOL) aircraft; consequently, a less restrictive stability condition was established.

Other classifications of jump linear systems are based on the underlying stochastic processes. Depending on the governing stochastic processes, jump linear systems can be classified as Bernoulli jump linear systems, Markov jump linear systems (MJLSs), semi-Markov jump linear systems (S-MJLSs), and other jump linear systems. As a result, the characteristics and system dynamics highly depend on the properties of the underlying stochastic processes. Among all types of jump linear systems, the MJLS has been intensively investigated in the control community [11, 12, 13]. Two main reasons have motivated the use of Markov processes instead of Bernoulli processes. Firstly, in the analysis of NCSs, the transmission delays could be represented by the modes of stochastic processes; for networked control systems (NCSs) with time-varying delays, usually two or more delays need to be modeled and represented. Markov processes, even finite-state Markov processes, are able to handle two or more operating modes. Secondly, the future states of jump linear systems usually depend on the current state. Take the weather system for an example. It can be regarded as a jump system where the mode represents the status of the weather, i.e., sunny

and rainy; in some areas around the world, it tends to be sunny tomorrow if today is sunny, and vice versa. A Bernoulli random variable is not suitable for characterizing the relation between the prediction and the current state, whereas Markov processes draw attention with the ability to predict the states in future steps based on the current state. The study of MJLSs started in 1960s when Dynkin firstly derived the infinitesimal operators for differential systems with Markov switching patterns [14]. The motivations on the study of semi-Markov process after the study of Markov process are two-fold. Firstly, the Markov process is a special case of the semi-Markov process. Secondly, lots of system behavior could be better captured by semi-Markov process. Detailed explanations and analysis are given in Chapters 2, 3, and 4.

The parameters of stochastic processes in jump linear systems can be determined by experiments. For example, in the fault tolerant control systems, the stochastic process parameters can be obtained according to the life time of system components. The procedure of determining/obtaining the stochastic process parameters is called statistical model identification [15]. A traditional yet practical way is to employ the maximum likelihood methods. It should be realized that there is usually a deviation between the true values and the identified results. Considering the imperfection of the parameter estimation, analysis and synthesis on jump linear systems with partially known parameters are studied and reported in [16, 17].

The stability analysis results of jump linear systems have been summarized in a comprehensive survey [18]. Early work on the stability analysis stems from [19]. In recent years, with the fast development of optimization techniques and programming tools, lots of stability problems have been converted to optimization problems which could be solved by linear matrix inequalities (LMIs) [20, 21]. With the established results on the stability analysis, researchers' attention has shifted to the control design problems of jump linear systems. In 1990, Ji *et al.* analyzed the controllability and the stabilizability of continuous-time MJLSs [22], where new definitions for controllability, observability, stabilizability, and detectability were constructed. Another contribution of [22] is to construct a stability condition which is not only sufficient but also necessary.

Following the established stability conditions, researchers have always been pursuing improvement in control performance. Optimal control is mathematically a minimization problem, in which different optima are calculated for meeting specific goals. These goals are often called performance indexes or criteria, according to which various optimal control schemes could be proposed. An early work on optimal control

of MJLSs was reported in 1969 [7], where the control performance is optimized in the quadratic sense. With the development of the $H_\infty$ theory since 1980s, $H_\infty$ optimal controllers for jump linear systems were designed for a VTOL vehicle [10]; the optimal control problem has been formulated as an LMI optimization problem, which is readily solvable by using Matlab LMI Control Toolbox [23]. In [10], another popular and widely applied optimal control algorithm, $H_2$ control algorithm, was proposed. Other results on $H_2$ optimal control systems could be found in [24] and the references therein. Aside from the aforementioned systems operating under ideal conditions, often the state variables and control signals are constrained by physical limitations, such as operating work space limitations or the maximal power of the actuator, so optimal control problems with constraints were examined in [25]. In this thesis, the $H_\infty$ and $H_2$ controllers for MJLSs with delays and for a networked DC motor system are discussed.

In all the aforementioned work, the system dynamics is always assumed to be exactly known to the designer and the operator, which is not always the case in practice, due to the system identification challenges or because of different system dynamics obtained based on different assumptions. In order to tackle the problem of uncertain system parameters, the robust control theory has been developed. Two types of model uncertainties are mainly examined in the literature: Polytopic uncertainties and norm-bounded uncertainties. For polytopic uncertainties, the system parameters are assumed to belong to convex sets of polytopic vertices. The advantage of using a polytope to describe model uncertainties is that the resulting system could be represented by a linear combination of a set of linear time-invariant (LTI) systems; the disadvantage of using the polytopic type representation is that the computational load would increase significantly with the increase of the polytope vertex number. Robust stability and control problems for a class of jump linear systems with polytopic uncertainties were examined in [26]. Moving one step further, de Souza reported the stability analysis and control design problems for jump linear systems where polytopic uncertainties were not only considered for system dynamics but also for the parameters of the stochastic processes in [27]. The other approach is to use norm-bounded matrices to characterize the model uncertainties. In this approach, the perturbations are confined within a predetermined unit ball in a particular metric [28]. For example, the stability and control for jump linear systems with norm-bounded uncertainties were studied in [29] and the references therein.

To investigate the more general stochastic systems with non-Markov jumps, it

is natural to relax the assumptions introduced by the Markov process. In a jump linear system, the duration $h$ between two consecutive jumps is called sojourn-time, which is usually a random variable [30]. In continuous-time jump linear systems, the sojourn-time $h$ is a random variable governed by the continuous probability distribution $F$. For instance, $F$ is an exponential distribution in the continuous-time MJLS. The continuous stochastic process whose sojourn-time does not follow an exponential distribution is referred to as a continuous semi-Markov process. Accordingly, the jump linear system whose parameters switch according to a semi-Markov process is termed as an S-MJLS [1]. A stability condition for the S-MJLS controller design was obtained in [1] where the MJLS stability condition was adopted to design the controller. Although the condition was verified on a bunch-train cavity interaction system, the sojourn-time distribution was just "nearly exponential", which indicated that the S-MJLS was nearly MJLS and the time-varying information of the transition rate was not considered in the controller design. Hou *et al.* addressed the stochastic stability for the linear system with semi-Markov jump parameters and similar results have been obtained as those in Markov jump systems [31]. In [31], due to the density property of phase-type distributions of all probability distributions on $[0, +\infty)$, the phase-type semi-Markov process was firstly defined and the stability of simple linear systems with phase-type semi-Markov jump parameters was addressed.

## 1.2 Networked Control Systems

NCSs are control systems where actuators, sensors, and controllers are spatially distributed. The research on NCSs has attracted increasing attention in the past decades. In the control community, many special issues in scientific journals have been published on NCSs, for example, IEEE Transactions on Automatic Control Guest Editorial Special Issue on Networked Control Systems (2004), Proceedings of the IEEE Special Issue on Technology of Networked Control Systems (2007), International Journal of Systems, Control and Communications Special Issue on Progress in Networked Control Systems (2011), and IEEE Transactions on Industrial Informatics Special Section on Advances in Theories and Industrial Applications of NCSs (2012). Also, the NCS has been introduced and discussed in a lot of research workshops, for example, Workshop on Networked Embedded Sensing and Control (2005 USA), Global Centers of Excellence Workshop on Networked Control Systems (2008 Japan), and First International Workshop on Wireless Networked Control Systems (2011 Canada).

In addition, the two flagship conferences in the control community, IEEE Conference on Decision and Control (IEEE-CDC) and American Control Conference (ACC), have been holding many special sections on NCSs. In 2012, IEEE-CDC and ACC organized five and six Special Sections on "Networked Control Systems", respectively.

The NCS differs from the traditional control systems on signal channels between system components. Traditional formulations assume that all components are interconnected by ideal channels [32, 33]. The ideal link/connection puts no limitations on the transmission time, bandwidth, nor transmission faults such as data missing or wrong data. In practice, control systems with distributed components have existed in many fields such as chemical processes [34], mobile sensor networks among vehicles [35], tele-surgeries [36], plant monitoring [37], spacecrafts [38], and unmanned aerial vehicles [39]. In those applications, control signals and sensor outputs are transmitted over various communication networks to the actuator and to the controller, respectively.

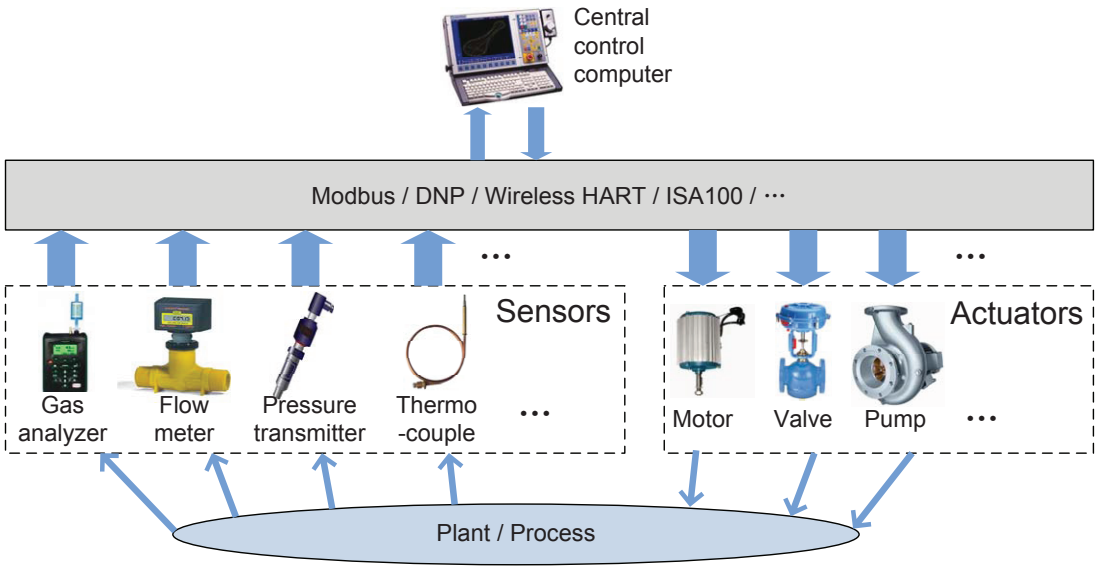


Figure 1.1: Typical setup of an NCS.

A typical NCS diagram is shown in Figure 1.1. As can be seen, the states of the plant/process are measured by various sensors, such as gas analyzers, flow meters, pressure transmitters, and thermocouples. The sensors send measurements to the central control computer via control networks, such as Modbus, DNP, WirelessHART, and ISA100. The control algorithm is implemented in the central control computer. Control actions calculated by the central control computer are sent to different

actuators; possible actuators are motors, valves, and pumps, etc.

As indicated in Figure 1.2, two main research streams on studying NCSs are: 1) Control of networks, and 2) control over networks.

- "Control of networks" concentrates on the property of the network itself; for example, the bit rate, the bandwidth, the protocol design and so on. The research results from sensor networks have also been applied to NCS studies [40]. In the process control and automation industry, improvements on current wireless protocols for NCSs are being extensively studied [41]. It should be pointed out that this type of research falls into the communication and network research fields.

- "Control over networks" focuses on the control strategy design for NCSs where particular communication protocols have been selected for NCSs. In engineering applications, due to the existing devices, cost consideration, or environmental concerns, only specific communication protocols could be used. Therefore, the system designer should customize the control laws or strategies to accommodate network constraints. This type of research falls into the system control community. It is worth mentioning that there is a trend in the co-design of the network and controller for NCSs [42, 43, 44].

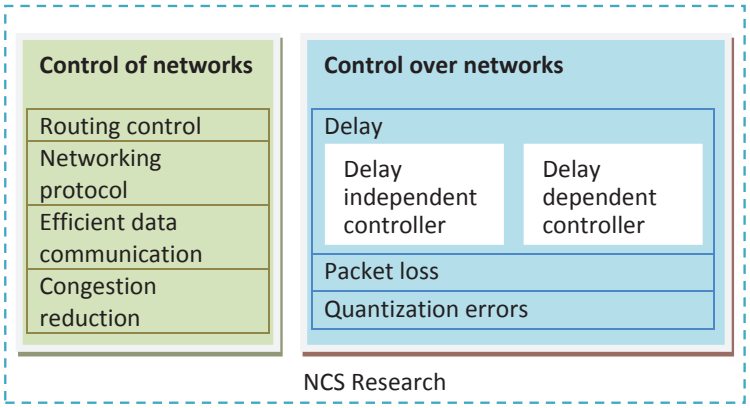


Figure 1.2: Two main research streams of NCSs.

The spatial distribution property brings in several advantages for NCSs: 1) Reducing wirings, 2) ease of system installation, diagnosis, and maintenance, 3) low cost, and 4) sharing data effectively [45]. With these features, NCSs would be implemented with less redundant wires, or even no wires by utilizing industrial wireless networks;

the easy installation enhances the system agility, for example, additional components could be installed modularly, and failed components could be replaced without shutting down the whole system. Challenges come along with the advantages. The major constraints caused by the introduced network are: 1) Time delays, 2) packet dropouts, 3) sampling and quantization errors, and 4) bandwidth limitations [45]. Among those challenges, sampling and quantization issues have been studied for computer control systems with analog-to-digital and digital-to-analog conversions; bandwidth limitation which slows down the sampling rate has been studied in sampled-data control systems. Therefore, time delays and packet dropouts become the major concerns in the system design. To deal with these two issues, in the communication community, new internet transport protocols were developed for teleoperation tasks; meanwhile, new methods that can guarantee the stability and certain performance criteria for NCSs were proposed in the control community. In this thesis, we will also focus on the time delay and packet dropout issues.

During the past years, there was a trend to employ the stochastic system approach to study NCSs, because closed-loop NCSs can be modeled by switching systems. In the 1990s, Nilsson modeled the real-time control system with delays using Markov chains [46]. According to Nilsson's thesis, the original idea was to model the delayed system using jump linear systems; the reasons of using Markov chains to model delays were provided and some preliminary results were reported. After Nilsson's work, Xiao *et al.* modeled the control systems with random but bounded time delays by finite-dimensional, discrete-time jump linear systems [47]. Based on Nilsson's and Xiao *et al.*'s results, various approaches have been proposed for NCSs [24, 48, 49, 50]. The timing mechanism and design approaches are reviewed as follows.

The timing mechanism of NCSs is the core aspect in the stability analysis and the control strategy design. Two communication links are involved with the timing mechanism: The sensor-to-controller (S-C) link, and the controller-to-actuator (C-A) link. In each communication link, the transmitted data packages may be subject to delays or dropouts. Such phenomenon would significantly alter the system dynamics [51]. The two delays are depicted in Figure 1.3. A commonly used assumption is that the delay is upper bounded, and in such cases the packet dropout could be addressed in the delay framework [52]. If the designed controller ignores the effects caused by delays, this type of controller is often termed as the "mode-independent controller" [53]. Similarly, controllers considering one or two side delays, are called "one-mode dependent controllers" or "two-mode dependent controllers", respective-

ly. In the controller design, taking more delay information into consideration would improve the control performance both intuitively and theoretically [47].

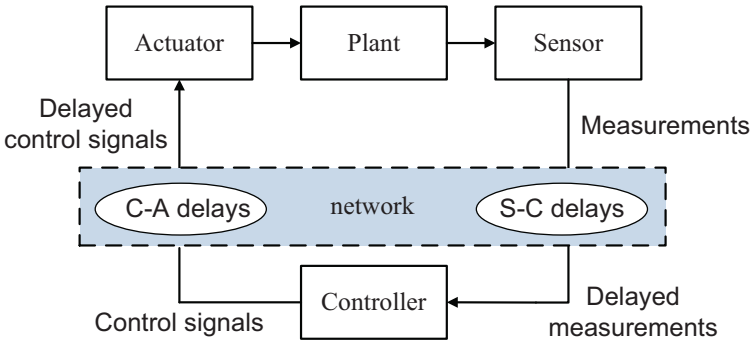


Figure 1.3: Depictions of S-C delays and C-A delays in NCSs.

The S-C delay is relatively easy to deal with, since the controller could compensate for the S-C delay in the control signal calculation. The compensation has been achieved through many approaches. In [47], both the mode-independent controller and the one-mode dependent controller were designed for NCSs where transmission delays were modeled by finite-state discrete-time Markov processes. Furthermore, Seiler *et al.* have built an $H_\infty$ optimal controller considering the S-C delays based on the bounded real lemma [50]. An early work dealing with the C-A communication link introduced buffers to handle the C-A packet dropouts [54]. To study the C-A delays, some strong assumptions were made. For instance, a two-mode dependent controller was developed given that the current S-C delay and the one step previous C-A delay were accessible by the controller at every sampling instant [55]. However, the one step previous C-A delay may not always be accessible by the controller. Indeed, when the controller receives and calculates the one step previous delay information will depend on the S-C delays. A thorough explanation regarding the relation between S-C and C-A delays could be found in [53], where an output feedback controller was designed considering two side delays. By taking the model uncertainties into account, the mixed $H_2/H_\infty$ control problems were examined in [56]. Both one-mode dependent controllers and two-mode dependent controllers are working with a buffer type actuator. With such actuators, only the most recent control signal from the controller will be implemented on the plant. The actuator by itself does not have any intelligence on evaluating the control signals based on the delay information or making appropriate compensations for the detected C-A delays. The rationale behind which the controller could easily compensate for the S-C delay is that the controller

could immediately measure the most updated S-C delay; analogously, the actuator is the ideal system component to compensate for the C-A delays, because the actuator could immediately determine the C-A delay once it happens. The remaining tasks are to develop smart actuators and to adapt control strategies accordingly, which will be discussed later in this thesis.

The main approaches in this thesis are based on Lyapunov theory, or the corollaries stemmed from the Lyapunov theory. Before addressing the stability of systems switching under Bernoulli processes or semi-Markov processes, a brief review of stability analysis for systems with arbitrary switching is summarized. It is shown that the arbitrary switching systems may not be stable even if all sub-systems are stable. The stability of each sub-system becomes a sufficient condition for the overall system stability only in some special cases, for example, when the $A$ matrices of the sub-system state-space models are symmetric [57], or when the sub-systems are pairwise commutative [58]. Nevertheless, the existence of a common Lyapunov function for all the sub-systems is able to guarantee the overall stability with arbitrary switching [59]. Following the idea of searching for a common Lyapunov function and with the developments of numerical toolboxes, such as LMI Toolbox [28] and YALMIP [60], lots of results have been reported for NCSs via switching system approaches. A controller was designed for NCSs in [61]; the NCSs under investigation were subject to network-induced packet dropouts and time-varying delays. Based on the constructed common Lyapunov functions, sufficient conditions in terms of LMIs are obtained. For more results on NCSs stability and control using common Lyapunov functions, please refer to [62] and the references therein. The study on non-common Lyapunov functions for the NCSs has two reasons: Firstly, stability conditions using the common Lyapunov functions are often conservative. Secondly, common Lyapunov functions are used to verify the switching system stability with arbitrary jumps. In such cases, the switching Lyapunov functions are developed, where different Lyapunov function parameters are constructed corresponding to different conditions in the NCS. Although a less conservative stability condition could be obtained via switching Lyapunov functions, the conditions are still only sufficient not necessary. In the NCS applications, switching Lyapunov functions are constructed depending on time-varying delays [63]. As mentioned before, the common switching Lyapunov function is a special case of the switching Lyapunov function. Therefore in [63], the delay and dropout dependent controller is less conservative. In this thesis, the switching Lyapunov function approach has been extensively utilized to reduce the conservativeness in the stability

analysis and the controller design.

## 1.3 Research Motivations

Though many results on jump linear systems and NCSs were reported, the analysis and synthesis of S-MJLSs have not been fully addressed and clearly reported. The motivations of this research are two-fold.

- **Switching system analysis.**

  As discussed in previous sections, some results on S-MJLSs have been reported. These results are either directly approximated from the results for MJLSs, or with computational defects which preclude their engineering applications. So the first part of the thesis is to provide the stability condition for S-MJLSs, especially the numerically testable conditions which are ready for engineering applications within acceptable computational time. Considering the modeling errors in the system identification, the stability problem for systems with uncertainties should be studied. In order to apply the theory to NCSs, stability conditions are further studied for S-MJLSs with time-varying delays. Another research motivation comes from the fault tolerant control community. The life time of a system component may not follow an exponential distribution. Thus a semi-Markov process should be applied to model the system faults.

- **Networked dynamic system analysis.**

  Based on the proposed stability conditions for jump linear systems and for systems with uncertainties or delays, different applications should be studied. In NCSs, the control signal from the controller to the actuator is subject to network-induced delays. This delay information is not accessible by the controller when the control signal is calculated. Therefore, a "send all, apply one" scheme is proposed by allowing the actuator to freely choose an appropriate control signal in the plant side. Another approach to compensate for time delays is to consider more historical measurements of the plant in NCSs. To further verify some of the established results, a haptic device is used as an experimental testing tool.

The road map of the research can be summarized in Figure 1.4. To investigate the two fundamental problems for the NCS: 1) Time delays and 2) packet dropouts,

the switching system is studied. The switching system serves as a bridge between the system (NCSs) and the problems (delays and packet dropouts).

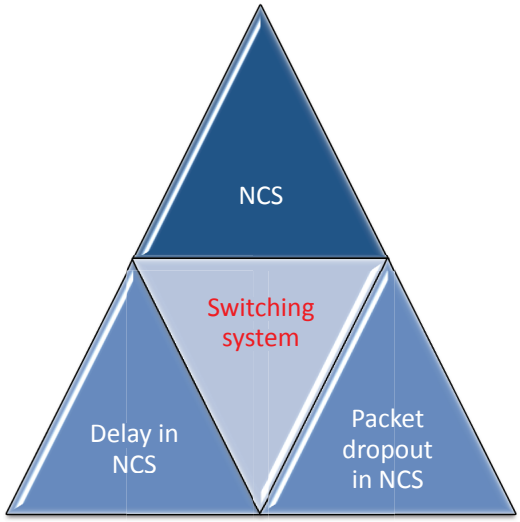


Figure 1.4: Road map of the research.

## 1.4 Contributions and Thesis Organization

The thesis is organized as follows. In Chapter 1, the fundamental concepts and existing results of jump linear systems and NCSs, research motivations, and main research approaches have been reviewed. Then the research contributions of this PhD thesis are presented.

The stability and control problems for S-MJLSs are discussed in Chapter 2. The S-MJLS is more general than the MJLS in terms of modeling some practical systems. Unlike the constant transition rates in the MJLS, the transition rates of the S-MJLS are *time-varying*. This chapter focuses on the robust stochastic stability condition and the robust control design problem for the S-MJLS with norm-bounded uncertainties. The infinitesimal generator for the constructed Lyapunov function is derived. Numerically solvable sufficient conditions for the stochastic stability of S-MJLSs are then established in terms of LMIs. In order to reduce the conservativeness of the stability conditions, we propose to incorporate the upper and lower bounds of the transition rate and apply a new partition scheme at the same time. The robust state feedback controller is accordingly developed. Simulation studies and comparisons demonstrate the effectiveness and advantages of the proposed methods. With the developed the-

orems in this chapter, numerically testable stability conditions and controller design approaches are established for S-MJLSs for the first time.

Chapter 3 discusses the $H_\infty$ control problem for a class of S-MJLSs with time-varying delays. The sojourn-time partition technique is proposed for the delayed stochastic switching system. A sufficient condition for designing a state feedback controller is then established. Moreover, the sufficient condition is expressed as a set of LMIs which can be readily solved.

Chapter 4 investigates the active fault tolerant control problem via the $H_\infty$ state feedback controller. Due to the limitations of Markov processes, we apply semi-Markov process in the system modeling. Two random processes are involved in the system: the failure process and the fault detection and identification process. Therefore, two corresponding semi-Markov processes are integrated in the closed-loop system. This framework is able to accommodate different types of system faults, including the randomly happening sensor faults and actuator faults. A controller is designed to guarantee the closed-loop stability with a prescribed noise/disturbance attenuation level. The controller parameters are solved by using convex optimization techniques.

In Chapter 5, the NCS with multiple physically distributed sensors is considered. The state information of the discrete-time plant with multiple state delays is sent to the controller by communication networks. By setting a sensor scheduling algorithm, the controller receives the measurement from one sensor at each time step. The guaranteed cost state feedback controller is proposed which considers not only the most up-to-date state information, but also the historical information of the state. In addition, according to the sensor scheduling scheme, we design and implement different control gains, i.e., the so-called sensor-dependent controller.

The application of NCS theory on a haptic system is investigated in Chapter 6. In this chapter, a virtual coupler is designed for the Phantom Omni Haptic System in the networked environment with one degree-of-freedom interaction. The manipulator and the control computer are connected through wireless communication links over which the position of the manipulator and the torque of the motor are transmitted. The virtual environment consists of multiple materials with different stiffness and damping, and it is termed the mixed virtual wall. The contact point between the avatar and the virtual wall switches among different materials, where the movement is characterized by a stochastic process. To achieve the free oscillation for the haptic device with the human operator, the stability condition is established based on the

passivity theory. After transforming the transparent virtual coupler design problem into an $H_\infty$ optimization problem for a delayed jump linear system, we propose a design scheme for the switching virtual coupler. The performance of the proposed virtual coupler is verified and tested on the Phantom Omni Haptic System.

Chapter 7 investigates robust $H_2$ and $H_\infty$ step tracking control methods for NCSs subject to random time delays modeled by Markov chains. To make full use of the delay information, the proposed two-mode dependent output feedback controller depends on both sensor-to-controller and controller-to-actuator delays. To actively compensate for the controller-to-actuator delays, we propose the "send all, apply one" scheme: Sending a sequence of control signals, then at the actuator/plant node, applying the appropriate control signal according to the actual controller-to-actuator delay. Using the augmentation method, the resulting closed-loop system can be formulated as a discrete-time MJLS. The $H_2$ and $H_\infty$ step tracking problems are tackled by solving a set of LMIs with nonconvex constraints. Both numerical simulations and experiments on a networked DC motor system are conducted to illustrate the effectiveness of the proposed methods.

The concluding remarks and a few topics deserving future research attention are presented in Chapter 8.

The notations in the thesis are fairly standard. The superscripts "T" and "$-1$" stand for matrix transposition and matrix inverse, respectively. $\mathbb{R}^n$ denotes the $n$-dimensional Euclidean space and the notation $P > 0$ means that $P$ is real symmetric and positive definite. $\dim\{v\}$ represents the dimension of vector $v$. $\det(A)$ denotes the determinant of the square matrix $A$. tr means the trace of a matrix. $\|\cdot\|_2$ refers to the Euclidean norm for vectors and induced 2-norm for matrices. $\mathbb{E}\{\cdot\}$ stands for the mathematical expectation. $\Pr\{A\}$ denotes the probability of event $A$. $\otimes$ is the notation for the Kronecker product. "$*$" is an ellipsis for terms that are induced by symmetry in square matrices.

# Chapter 2

# Stability and Control of Semi-Markov Jump Linear Systems

## 2.1 Introduction

The past years have witnessed extensive research on the Markov jump linear systems (MJLSs). Modeled by a set of linear systems with the transitions among the linear systems governed by the Markov chain, the MJLSs can be used to characterize and model different types of systems subject to abrupt changes [64]. Hence, the MJLS finds many applications in control systems, such as fault tolerant systems, target tracking systems, manufactory processes, NCSs, and multiagent systems; see, e.g., [12, 13, 65]. Many important results on MJLSs have been addressed in the literature. For instance, the stability analysis, filter and control design problems were investigated in [16, 22, 66], and the optimal control and filter design for MJLSs were discussed in [11, 67, 68]. Furthermore, nonlinear systems with Markov jumping parameters were addressed in [69, 70]. Besides the aforementioned theoretical studies, MJLSs also found applications in practical systems, such as networked DC motor systems [71].

In general, the MJLS belongs to the class of jump linear systems. In jump linear systems, the duration $h$ between two successive jumps is referred to as **sojourn-time** which is usually a random variable [30]. In continuous-time jump linear systems, the sojourn-time $h$ is a random variable governed by the continuous probability distribution $F$. For instance, $F$ is an exponential distribution in the continuous-time MJLS. Depending on $F$, the transition rate $\lambda_{ij}(h)$ is the speed/rate that the system jumps from mode $i$ to mode $j$. The transition rate is also called the failure rate or the hazard

rate in different applications [72]. From the memoryless property of the exponential distribution, $\lambda_{ij}(h) \equiv \lambda_{ij}$ is a constant, meaning that the jump speed is independent of the past/history of the stochastic process. In fact, among all the continuous-time probability distributions, exponential distribution is the only one that possesses the memoryless property [72]. As a result, if the MJLS is applied to describe the stochastic system of interest, the transition rate should be assumed to be constant. This requirement, however, is too restrictive, because the transition rates for many practical systems are not constants [73, 74]. For example, in the fault tolerant control systems, the bathtub curve is widely used to describe a particular form of the transition rate function which consists of three parts: a) decreasing, b) constant (roughly), c) increasing [75]. Obviously, the jumping of such process cannot be modeled by an MJLS. A typical transition rate in the bathtub shape in the reliability analysis was reported in [76]. The application of semi-Markov processes in fault-tolerant control systems was discussed in [77], and it was shown that when a practical system does not satisfy the so-called memoryless restriction, the widely used Markov switching scheme would not be applicable.

In a more general setting, the transition rate $\lambda_{ij}(h)$ is usually time-varying instead of a constant $\lambda_{ij}$ [74]. A continuous stochastic process whose sojourn-time is non-exponentially distributed is often termed as a continuous semi-Markov process. Accordingly, the jump linear system which switches according to a semi-Markov process is termed as a semi-Markov jump linear system (S-MJLS) [1]. It is known that the MJLS is a special case of S-MJLSs that can be used to model and characterize a wider range of practical stochastic systems. Therefore, it is of both theoretical merit and practical interest to investigate the stochastic stability and robust stabilization problems of S-MJLS, which is the focus of this chapter.

Compared to the rich literature on MJLSs, there are relatively few research efforts devoted to S-MJLSs. In [1], a stochastic stability condition and the controller design method for the S-MJLS were presented, and further the results were verified on a bunch-train cavity interaction system. Yet, it is worthwhile to point out that the sojourn-time distribution was "nearly exponential"; this indicates that the S-MJLS was nearly an MJLS and the time-varying information of the transition rate was not fully characterized in the control design problem. Hou *et al.* discussed the stochastic stability for the linear system with semi-Markov jump parameters and similar results were obtained for the Markov jump systems [31]. Due to the density property of phase-type (PH) distributions, the PH semi-Markov process was defined and the stability

condition of linear systems with PH semi-Markov jump parameters was established in [31, 78]. Shmerling *et al.* studied the stochastic stability for differential equations with semi-Markov jump parameters [79], where the mean square asymptotic stability of the system was verified by checking the existence of a set of positive definite matrices. The condition in [79] was expressed in an integration form which is difficult to check. It is noticed that, although the stability and control design problems for S-MJLSs have been receiving increasing interest, little attention has been paid to developing numerically testable stochastic stability conditions, and little research was devoted to the controller design for S-MJLSs. The limitation of the MJLS and the wide application of the S-MJLS motivate the current research. The main objectives of this chapter are three-fold:

- To establish sufficient stochastic stability conditions for a class of uncertain S-MJLSs.
- To propose a new partition scheme by dividing the range of the transition rate (from the lower bound to the upper bound) in order to effectively reduce the conservativeness of the stability conditions.
- To propose a robust state feedback controller design for the S-MJLSs with norm-bounded uncertainties.

The remainder of this chapter is organized as follows. The problem formulation is presented in Section 2.2. In Section 2.3, the sufficient conditions for the stochastic stability of S-MJLSs are established. The robust stabilization problem is discussed in Section 2.4. Finally, simulation studies illustrate the effectiveness of the proposed methods in Section 2.5. Some concluding remarks are made in Section 2.6.

## 2.2 Problem Formulation

Consider the following unforced continuous-time S-MJLS with norm-bounded uncertainties,

$$\mathscr{S}_1: \begin{array}{ll} \dot{x}(t) & = [A(r(t)) + E(r(t))\delta(t)F_A(r(t))]x(t), \\ x(0) & = x_0, \quad r(0) = r_0, \end{array} \tag{2.1}$$

where $\{r(t), t \geq 0\}$ is a continuous-time semi-Markov process taking values in a finite space $\mathcal{S} = \{1, 2, \ldots, N\}$, $x(t) \in \mathbb{R}^n$ is the state vector. $x_0 \in \mathbb{R}^n$ is the initial state

at $t = 0$, and $r_0 \in \mathcal{S}$ is the initial mode in the semi-Markov process at $t = 0$. $A(r(t))$, $r(t) = i \in \mathcal{S}$ are system matrices with compatible dimensions which depend on $r(t)$, and $E(r(t))$ and $F_A(r(t))$, $i \in \mathcal{S}$ are known real constant matrices. $\delta(t)$ is an unknown real matrix function with Lebesgue-measurable elements, satisfying $\delta^{\mathrm{T}}(t)\delta(t) \leq I$ with $I$ being the identity matrix. For the convenience of notations, we write $A(r(t))$, $E(r(t))$, and $F_A(r(t))$ as $A_i$, $E_i$, and $F_{A,i}$, respectively when $r(t) = i$ and omit the arguments of those functions without any confusion. The similar notations will be used in the sequel except in special statements.

The evolution of the semi-Markov process $\{r(t), t \geq 0\}$ is governed by the following probability transitions:

$$\Pr\{r(t+h) = j | r(t) = i\} = \begin{cases} \lambda_{ij}(h)h + o(h), & r(t) \text{ jumps from mode } i \text{ to mode } j, \\ 1 + \lambda_{ii}(h)h + o(h), & r(t) \text{ stays at mode } i, \end{cases}$$

where $\lambda_{ij}(h)$ is the transition rate from mode $i$ to mode $j$ at $t$ when $i \neq j$ and $\lambda_{ii}(h) = -\sum_{j=1, j\neq i}^{N} \lambda_{ij}(h)$. $o(h)$ is the little-$o$ notation defined by $\lim_{h\to 0} o(h)/h = 0$. In practice, the transition rate $\lambda_{ij}(t)$ is generally bounded by $\underline{\lambda}_{ij}$ and $\bar{\lambda}_{ij}$ ($\underline{\lambda}_{ij} \leq \bar{\lambda}_{ij}$) [80].

**Remark 2.1** The sojourn-time $h$ is the time elapsed from the most recent system jumps, which is different from $t$. Therefore, $h$ is set to be 0 whenever the system jumps. The transition rate $\lambda_{ij}(h)$ depends only on $h$.

For the stochastic stability, we adopt the following definition. For more details, please refer to [81, 82, 83] and the references therein.

**Definition 2.1.** *The system in (2.1) with all modes and all $t \geq 0$ is said to achieve stochastic stability with semi-Markov jump parameters if there exists a finite positive constant $T(x_0, r_0)$ such that the following holds for any initial condition $(x_0, r_0)$:*

$$\mathbb{E}\left\{\int_0^\infty \|x(t)\|^2 dt | (x_0, r_0)\right\} \leq T(x_0, r_0), \tag{2.2}$$

*where $\mathbb{E}\{\cdot|\cdot\}$ is the expectation conditioning on the initial value of $(x_0, r_0)$.*

## 2.3 Stochastic Stability Analysis of S-MJLS

Before proceeding further, we recall the following lemma which will be used in the proof of the robust stochastic stability of the S-MJLS.

**Lemma 2.1.** *[84, 85] If $F^{\mathrm{T}}F \leq I$, then there exist constant matrices $H$ and $E$, and scalar $\varepsilon > 0$ such that the following inequality holds:*

$$HFE + E^{\mathrm{T}}F^{\mathrm{T}}H^{\mathrm{T}} \leq \varepsilon HH^{\mathrm{T}} + \varepsilon^{-1}E^{\mathrm{T}}E. \tag{2.3}$$

**Theorem 2.1.** *The S-MJLS in (2.1) is stochastically stable if there exist a set of matrices $P(i) > 0$, $i \in \mathcal{S}$, and a set of scalars $\varepsilon_{A,i} > 0$, $i \in \mathcal{S}$ such that the following inequalities hold for all admissible uncertainties:*

$$\begin{bmatrix} J_i(h) & P(i)E_i \\ E_i^{\mathrm{T}}P(i) & -\varepsilon_{A,i}I \end{bmatrix} < 0, \quad i \in \mathcal{S}, \tag{2.4}$$

*where $J_i(h) = A_i^{\mathrm{T}}P(i) + P(i)A_i + \sum_{j=1}^{N}\lambda_{ij}(h)P(j) + \varepsilon_{A,i}F_{A,i}^{\mathrm{T}}F_{A,i}$.*

*Proof.* Consider the following quadratic Lyapunov function

$$V(x(t), r(t)) = x^{\mathrm{T}}(t)P(r(t))x(t), \tag{2.5}$$

where $P(r(t)) > 0$ denotes the positive symmetric matrix. The infinitesimal generator $\tilde{A}$ can be considered as a derivative of the Lyapunov function $V(x(t), r(t))$ along the trajectory of the semi-Markov process $\{r(t), t \geq 0\}$ at the point $\{x(t), r(t)\}$ at time $t$ [86]. The MJLS and the S-MJLS are governed by different stochastic processes, so the infinitesimal generator of the Lyapunov function for the S-MJLS is essentially *different* from the one for the MJLS. We need to derive the infinitesimal generator $\tilde{A}$ of $V(x(t), r(t))$ first of all. According to the definition of $\tilde{A}$ [14], we have

$$\tilde{A}V(x(t), r(t)) = \lim_{\Delta \to 0} \frac{\mathbb{E}\left\{V(x(t+\Delta), r(t+\Delta))|x(t), r(t)\right\} - V(x(t), r(t))}{\Delta}.$$

Here, $\Delta$ is a small positive number. Conditioning on $r(t) = i$, and applying the law of total probability and conditional expectation yield

$$\lim_{\Delta \to 0} \frac{1}{\Delta}\left[\sum_{j=1, j\neq i}^{N} \Pr\{r(t+\Delta) = j | r(t) = i\}\, x^{\mathrm{T}}(t+\Delta)P(j)x(t+\Delta)\right.$$

$$
\begin{aligned}
&+ \Pr\{r(t+\Delta)=i|r(t)=i\}x^{\mathrm{T}}(t+\Delta)P(i)x(t+\Delta) - x^{\mathrm{T}}(t)P(i)x(t)\Big] \\
&= \lim_{\Delta\to 0}\frac{1}{\Delta}\Bigg[\sum_{j=1,j\neq i}^{N}\frac{\Pr\{r(t+\Delta)=j,r(t)=i\}}{\Pr\{r(t)=i\}}\,x^{\mathrm{T}}(t+\Delta)P(j)x(t+\Delta) \\
&\quad + \frac{\Pr\{r(t+\Delta)=i,r(t)=i\}}{\Pr\{r(t)=i\}}x^{\mathrm{T}}(t+\Delta)P(i)x(t+\Delta) - x^{\mathrm{T}}(t)P(i)x(t)\Bigg].
\end{aligned} \tag{2.6}
$$

For MJLSs, due to the memoryless property, $\Pr\{r(t+\Delta)=j,r(t)=i\}=\Pr\{r(\Delta)=j,r(0)=i\}$ and $\Pr\{r(t+\Delta)=i,r(t)=i\}=\Pr\{r(\Delta)=i,r(0)=i\}$. However, for S-MJLSs, the above two equalities do not hold; instead, they are functions depending on the sojourn-time $h$. Therefore, Equation (2.6) can be equivalently rewritten as

$$
\begin{aligned}
&\lim_{\Delta\to 0}\frac{1}{\Delta}\Bigg[\sum_{j=1,j\neq i}^{N}\frac{q_{ij}(G_i(h+\Delta)-G_i(h))}{1-G_i(h)}\,x^{\mathrm{T}}(t+\Delta)P(j)x(t+\Delta) \\
&\quad + \frac{1-G_i(h+\Delta)}{1-G_i(h)}x^{\mathrm{T}}(t+\Delta)P(i)x(t+\Delta) - x^{\mathrm{T}}(t)P(i)x(t)\Bigg],
\end{aligned} \tag{2.7}
$$

where $h$ is the time elapsed when the system stays at mode $i$ from the last jump; $G_i(t)$ is the cumulative distribution function (CDF) of the sojourn-time when the system remains in mode $i$, and $q_{ij}$ is the probability intensity of the system jump from mode $i$ to mode $j$. Given that $\Delta$ is small, the first order approximation of $x(t+\Delta)$ is $x(t+\Delta)=\left[A_i\Delta+E_i\delta(t)F_{A,i}\Delta+I\right]x(t)+o(\Delta)$. Then the infinitesimal generator becomes

$$
\tilde{A}V(x(t),r(t)) = x^{\mathrm{T}}(t)Q(i,t,h)x(t),
$$

where

$$
\begin{aligned}
&Q(i,t,h) \\
&= \lim_{\Delta\to 0}\frac{1}{\Delta}\Bigg[\sum_{j=1,j\neq i}^{N}\frac{q_{ij}(G_i(h+\Delta)-G_i(h))}{1-G_i(h)}\left[A_i\Delta+E_i\delta(t)F_{A,i}\Delta+I\right]^{\mathrm{T}}P(j) \\
&\qquad \left[A_i\Delta+E_i\delta(t)F_{A,i}\Delta+I\right] \\
&\quad + \frac{1-G_i(h+\Delta)}{1-G_i(h)}\left[A_i\Delta+E_i\delta(t)F_{A,i}\Delta+I\right]^{\mathrm{T}}P(i)\left[A_i\Delta+E_i\delta(t)F_{A,i}\Delta+I\right]-P(i)\Bigg] \\
&= \sum_{j=1,j\neq i}^{N}q_{ij}P(j)\lim_{\Delta\to 0}\frac{G_i(h+\Delta)-G_i(h)}{(1-G_i(h))\Delta} + P(i)\lim_{\Delta\to 0}\frac{G_i(h)-G_i(h+\Delta)}{(1-G_i(h))\Delta}
\end{aligned}
$$

$$+\sum_{j=1,j\neq i}^{N} q_{ij}\left[(A_i+E_i\delta(t)F_{A,i})^{\mathrm{T}}P(j)+P(j)(A_i+E_i\delta(t)F_{A,i})\right]$$
$$\lim_{\Delta\to 0}\frac{G_i(h+\Delta)-G_i(h)}{1-G_i(h)}$$
$$+\left[(A_i+E_i\delta(t)F_{A,i})^{\mathrm{T}}P(i)+P(i)(A_i+E_i\delta(t)F_{A,i})\right]\lim_{\Delta\to 0}\frac{1-G_i(h+\Delta)}{1-G_i(h)}.$$

Using the property of the CDF, we have

$$\lim_{\Delta\to 0}\frac{G_i(h+\Delta)-G_i(h)}{(1-G_i(h))\Delta}=\lambda_i(h),\ \lim_{\Delta\to 0}\frac{G_i(h+\Delta)-G_i(h)}{1-G_i(h)}=0.$$

Therefore,

$$Q(i,t,h)$$
$$=\sum_{j=1,j\neq i}^{N} q_{ij}P(j)\lambda_i(h)+\left[(A_i+E_i\delta(t)F_{A,i})^{\mathrm{T}}P(i)+P(i)(A_i+E_i\delta(t)F_{A,i})\right]-P(i)\lambda_i(h).$$

Define $\lambda_{ij}(h):=q_{ij}\lambda_i(h)$ for $i\neq j$ and $\lambda_{ii}(h):=-\sum_{j=1,j\neq i}^{N}\lambda_{ij}(h)$, then we obtain

$$\begin{aligned}Q(i,t,h)=&(A_i+E_i\delta(t)F_{A,i})^{\mathrm{T}}P(i)+P(i)(A_i+E_i\delta(t)F_{A,i})+\sum_{j=1}^{N}P(j)\lambda_{ij}(h)\\ =&A_i^{\mathrm{T}}P(i)+P(i)A_i+F_{A,i}^{\mathrm{T}}\delta^{\mathrm{T}}(t)E_i^{\mathrm{T}}P(i)+P(i)E_i\delta(t)F_{A,i}+\sum_{j=1}^{N}P(j)\lambda_{ij}(h).\end{aligned}$$

Using Lemma 2.1, we get

$$F_{A,i}^{\mathrm{T}}\delta^{\mathrm{T}}(t)E_i^{\mathrm{T}}P(i)+P(i)E_i\delta(t)F_{A,i}\leq\varepsilon_{A,i}F_{A,i}^{\mathrm{T}}F_{A,i}+\varepsilon_{A,i}^{-1}P(i)E_iE_i^{\mathrm{T}}P(i),$$

where $\varepsilon_{A,i}$ is a positive scalar. Hence,

$$Q(i,t,h)\leq\tilde{Q}(i,h),$$

where

$$\tilde{Q}(i,h)=A_i^{\mathrm{T}}P(i)+P(i)A_i+\varepsilon_{A,i}F_{A,i}^{\mathrm{T}}F_{A,i}+\varepsilon_{A,i}^{-1}P(i)E_iE_i^{\mathrm{T}}P(i)+\sum_{j=1}^{N}P(j)\lambda_{ij}(h).$$

Based on the Schur complement, $\tilde{Q}(i,h) < 0$, $i \in \mathcal{S}$ implies

$$\begin{bmatrix} J_i(h) & P(i)E_i \\ E_i^{\mathrm{T}}P(i) & -\varepsilon_{A,i}I \end{bmatrix} < 0,$$

where $J_i(h)$ is given by

$$J_i(h) = A_i^{\mathrm{T}}P(i) + P(i)A_i + \varepsilon_{A,i}F_{A,i}^{\mathrm{T}}F_{A,i} + \sum_{j=1}^{N} P(j)\lambda_{ij}(h).$$

Thus

$$\tilde{A}V(x(t), r(t)) \leq x^{\mathrm{T}}(t)\tilde{Q}(i,h)x(t) \leq \max_{i\in\mathcal{S},h}\left\{\lambda_{\max}\tilde{Q}(i,h)\right\} x^{\mathrm{T}}(t)x(t).$$

Here, we will show that $\max_{i\in\mathcal{S},h}\left\{\lambda_{\max}\tilde{Q}(i,h)\right\}$ exists. Denote

$$\tilde{Q}(i,h) = \tilde{Q}_1(i) + \tilde{Q}_2(i,h), \tag{2.8}$$

where $\tilde{Q}_1(i)$ and $\tilde{Q}_2(i,h)$ are given as follows

$$\begin{aligned} \tilde{Q}_1(i) =& A_i^{\mathrm{T}}P(i) + P(i)A_i + \varepsilon_{A,i}F_{A,i}^{\mathrm{T}}F_{A,i} + \varepsilon_{A,i}^{-1}P(i)E_iE_i^{\mathrm{T}}P(i), \\ \tilde{Q}_2(i,h) =& \sum_{j=1}^{N} P(j)\lambda_{ij}(h). \end{aligned} \tag{2.9}$$

It is obvious that $\max_{i\in\mathcal{S}}\left\{\lambda_{\max}\tilde{Q}_1(i)\right\}$ and $\lambda_{\max}P(j)$ exist. Since $\lambda_{ij}(h)$ is positive and upper bounded by $\bar{\lambda}_{ij}$, the following inequalities hold

$$\tilde{Q}_1(i) - I\max_{i\in\mathcal{S}}\left\{\lambda_{\max}\tilde{Q}_1(i)\right\} \leq 0, \quad \tilde{Q}_2(i,h) - I\sum_{j=1}^{N}\lambda_{\max}P(j)\bar{\lambda}_{ij} \leq 0, \tag{2.10}$$

where $(\cdot) \leq 0$ indicates negative semi-definite matrix. Hence,

$$\tilde{Q}(i,h) - I\max_{i\in\mathcal{S}}\left\{\lambda_{\max}\tilde{Q}_1(i)\right\} - I\sum_{j=1}^{N}\lambda_{\max}P(j)\bar{\lambda}_{ij} \leq 0. \tag{2.11}$$

Therefore, $\max_{i\in\mathcal{S},h}\left\{\lambda_{\max}\tilde{Q}(i,h)\right\}$ always exists.

By the generalized Dynkin's formula [87], we have

$$\begin{aligned}\mathbb{E}\{V(x(t),r(t))\}-V(x_0,r_0)=&\mathbb{E}\left\{\int_0^t \tilde{A}V(x(s),r(s))ds\middle|(x_0,r_0)\right\}\\ \leq&\max_{i\in\mathcal{S},h}\left\{\lambda_{\max}\tilde{Q}(i,h)\right\}\mathbb{E}\left\{\int_0^t x^{\mathrm{T}}(s)x(s)ds\middle|(x_0,r_0)\right\}.\end{aligned}$$

The last inequality implies

$$\begin{aligned}&-\max_{i\in\mathcal{S},h}\left\{\lambda_{\max}\tilde{Q}(i,h)\right\}\mathbb{E}\left\{\int_0^t x^{\mathrm{T}}(s)x(s)ds\middle|(x_0,r_0)\right\}\\ \leq&V(x_0,r_0)-\mathbb{E}\left\{V(x(t),i)\right\}\\ \leq&V(x_0,r_0).\end{aligned}$$

Furthermore, the condition in (2.4) indicates $\max_{i\in\mathcal{S},h}\left\{\lambda_{\max}\tilde{Q}(i,h)\right\}<0$, so

$$\mathbb{E}\left\{\int_0^t x^{\mathrm{T}}(s)x(s)ds\middle|(x_0,r_0)\right\}\leq-\frac{V(x_0,r_0)}{\max_{i\in\mathcal{S},h}\left\{\lambda_{\max}\tilde{Q}(i,h)\right\}}$$

holds for any $t>0$. Letting $t$ go to infinity, then we know that

$$\mathbb{E}\left\{\int_0^\infty x^{\mathrm{T}}(s)x(s)ds\middle|(x_0,r_0)\right\}$$

is bounded by the following constant

$$T(x_0,r_0)=-\frac{V(x_0,r_0)}{\max_{i\in\mathcal{S},h}\left\{\lambda_{\max}\tilde{Q}(i,h)\right\}}>0.$$

According to Definition 2.1, the system in (2.1) is stochastically stable. This ends the proof. □

To this end, the sufficient conditions of the stochastic stability for S-MJLSs have been established in Theorem 2.1. However, due to the time-varying term $\lambda_{ij}(h)$ in (2.4), solving the conditions (2.4) in Theorem 2.1 will unavoidably involve testing infinitely many LMIs, which is very time-consuming, if not impossible, from the perspective of the numerical computation. Therefore, a question arises naturally: How to develop the numerically testable conditions of the stochastic stability for S-MJLSs? In the following, Theorem 2.2 will address this question.

**Theorem 2.2.** *The S-MJLS in (2.1) is stochastically stable if there exist a set of matrices $P(i) > 0$, $i \in \mathcal{S}$ and a set of scalars $\varepsilon_{A,i} > 0$, $i \in \mathcal{S}$ such that the following inequalities hold for all admissible uncertainties:*

$$(a) \begin{bmatrix} \underline{J}_i & P(i)E_i \\ E_i^{\mathrm{T}}P(i) & -\varepsilon_{A,i}I \end{bmatrix} < 0, \ (b) \begin{bmatrix} \bar{J}_i & P(i)E_i \\ E_i^{\mathrm{T}}P(i) & -\varepsilon_{A,i}I \end{bmatrix} < 0, \quad i \in \mathcal{S}. \tag{2.12}$$

*Here, $J_i^0 = A_i^{\mathrm{T}}P(i) + P(i)A_i + \varepsilon_i F_{A,i}^{\mathrm{T}}F_{A,i}$, $\underline{J}_i = J_i^0 + \sum_{j=1}^{N} \underline{\lambda}_{ij}P(j)$, and $\bar{J}_i = J_i^0 + \sum_{j=1}^{N} \bar{\lambda}_{ij}P(j)$, $i \in \mathcal{S}$.*

*Proof.* According to Theorem 2.1, the jump linear system is stochastically stable with transition rate $\lambda_{ij}(h)$ if there exist $P(i) > 0$, $i \in \mathcal{S}$ such that the condition in (2.4) holds. For a specific $h$, $\lambda_{ij}(h)$ can be written as the linear combination $\lambda_{ij}(h) = \theta_1\underline{\lambda}_{ij} + \theta_2\bar{\lambda}_{ij}$ where $\theta_1 + \theta_2 = 1$ and $\theta_1, \theta_2 > 0$. Multiplying (2.12-$a$) by $\theta_1$ and (2.12-$b$) by $\theta_2$, the summation yields

$$\begin{bmatrix} \theta_1\underline{J}_i + \theta_2\bar{J}_i & P(i)E_i \\ E_i^{\mathrm{T}}P(i) & -\varepsilon_{A,i}I \end{bmatrix} < 0.$$

By tuning $\theta_1$ and $\theta_2$, all possible $\lambda_{ij}(h) \in [\underline{\lambda}_{ij} \ \bar{\lambda}_{ij}]$ can be achieved. Therefore the condition in (2.1) holds uniformly, which implies that the system in (2.1) is stochastically stable. □

Theorem 2.2, it has been moved one step further towards the numerically solvable conditions by making use of the upper and lower bounds of the transition rate. However, the derived sufficient condition in Theorem 2.2 is relatively conservative. Then another critical question arises here: How to reduce the conservativeness of the stability conditions while keeping it numerically testable? To reduce the conservativeness, we propose to partition the sojourn-time $h$ into $M$ sections in every working mode. Since the transition rates $\lambda_{ij}(h)$ are time-varying, denote $\underline{\lambda}_{ij,m}$ and $\bar{\lambda}_{ij,m}$ as the lower and the upper bounds of the transition rates during the $m^{\text{th}}$ section. Such a way of performing partition can effectively reduce the conservativeness, as more of the transition rate information can be incorporated into the analysis and synthesis.

**Corollary 2.1.** *For the S-MJLS in (2.1), if there exist a set of matrices $P(i, m) > 0$,*

*$i \in \mathcal{S}$, $m \in \mathcal{M}$ that the following set of linear matrix inequalities hold*

$$\begin{bmatrix} \underline{J}_{i,m} & P(i,m)E_i \\ E_i^{\mathrm{T}}P(i,m) & -\varepsilon_{i,m}I \end{bmatrix} < 0, \begin{bmatrix} \bar{J}_{i,m} & P(i,m)E_i \\ E_i^{\mathrm{T}}P(i,m) & -\varepsilon_{i,m}I \end{bmatrix} < 0, \quad i \in \mathcal{S}, \tag{2.13}$$

*where*

$$\underline{J}_{i,m} = A_i^{\mathrm{T}}P(i,m) + P(i,m)A_i + \sum_{j=1}^{N} \underline{\lambda}_{ij,m}P(j,m) + \varepsilon_{i,m}F_{A,i}^{\mathrm{T}}F_{A,i},\ i \in \mathcal{S},\ m \in \mathcal{M}, \tag{2.14}$$

$$\bar{J}_{i,m} = A_i^{\mathrm{T}}P(i,m) + P(i,m)A_i + \sum_{j=1}^{N} \bar{\lambda}_{ij,m}P(j,m) + \varepsilon_{i,m}F_{A,i}^{\mathrm{T}}F_{A,i},\ i \in \mathcal{S},\ m \in \mathcal{M}. \tag{2.15}$$

*Here, $\mathcal{M} = \{1, 2, \ldots, M\}$. Then the S-MJLS is stochastically stable.*

Partitioning the sojourn-time into $M$ sections, the original S-MJLS in (2.1) in each section can be regarded as an individual S-MJLS with the time-varying transition rate varying in a narrowed range. Applying Theorem 2.2 for the individual S-MJLS in the $m^{\text{th}}$ section, and substituting $\underline{\lambda}_{ij}$ and $\bar{\lambda}_{ij}$ by $\underline{\lambda}_{ij,m}$ and $\bar{\lambda}_{ij,m}$, this corollary can be readily proved.

## 2.4 Robust State Feedback Control for S-MJLS

In this section, we discuss how to design the robust state feedback control law for the following S-MJLS:

$$\mathscr{S}_2: \quad \begin{array}{ll} \dot{x}(t) & = [A_{i,0} + E_i\delta(t)F_{A,i}]\,x(t) + [B_{i,0} + E_i\delta(t)F_{B,i}]\,u(t), \\ x(0) & = x_0, \quad r(0) = r_0, \end{array} \tag{2.16}$$

where $A_{i,0}$ and $B_{i,0}$ are nominal values with appropriate dimensions. $\delta(t)$ is a known real matrix satisfying $\delta^{\mathrm{T}}(t)\delta(t) \leq I$ and $E_i$, $F_{A,i}$, $F_{B,i}$ are known real constant matrices with appropriate dimensions. The robust state feedback control law to be designed is

$$u(t) = K(r(t))x(t). \tag{2.17}$$

**Theorem 2.3.** *If there exist a set of matrices $X(i) > 0$, $Y(i)$, $i \in \mathcal{S}$, and a set of scalars $\varepsilon_{A,i}, \varepsilon_{B,i} > 0$, $i \in \mathcal{S}$ such that the following LMIs hold. Then the controller*

*$K(i) = Y(i)X^{-1}(i)$ can stabilize the system.*

$$\begin{bmatrix} \tilde{J}_i(h) & X(i)F_{A,i}^{\mathrm{T}} & Y(i)^{\mathrm{T}}F_{B,i}^{\mathrm{T}} & \Xi_i(h) \\ * & -\varepsilon_{A,i}I & 0 & 0 \\ * & * & -\varepsilon_{B,i}I & 0 \\ * & * & * & -\mathcal{X}_i \end{bmatrix} < 0, \quad i \in \mathcal{S}. \tag{2.18}$$

*Here, * represents the blocks that are induced by symmetry and*

$$\begin{aligned} \tilde{J}_i(h) =& X(i)A_{i,0}^{\mathrm{T}} + A_{i,0}X(i) + Y^{\mathrm{T}}(i)B_{i,0}^{\mathrm{T}} + B_{i,0}Y(i) + (\varepsilon_{A,i} + \varepsilon_{B,i})E_iE_i^{\mathrm{T}} + \lambda_{ii}(h)X(i), \\ \Xi_i(h) =& \left[\sqrt{\lambda_{i1}(h)}X(i) \ \cdots \ \sqrt{\lambda_{i,i-1}(h)}X(i) \quad \sqrt{\lambda_{i,i+1}(h)}X(i) \ \cdots \ \sqrt{\lambda_{iN}(h)}X(i)\right], \\ \mathcal{X}_i =& \mathrm{diag}\left[X(1) \ \cdots \ X(i-1) \quad X(i+1) \ \cdots \ X(N)\right]. \end{aligned}$$

*Proof.* Using the robust control law in (2.17) for the system $\mathscr{S}_2$ in (2.16), the closed-loop system becomes

$$\dot{x}(t) = \left[\bar{A}_{i,0} + E_i\delta(t)\bar{F}_i\right]x(t), \tag{2.19}$$

where

$$\bar{A}_{i,0} = A_{i,0} + B_{i,0}K(i), \ \bar{F}_i = F_{A,i} + F_{B,i}K(i).$$

Applying the stochastically stable condition in Theorem 2.1, we know that the following inequality holds

$$\begin{aligned} &A_{i,0}^{\mathrm{T}}P(i) + K^{\mathrm{T}}(i)B_{i,0}^{\mathrm{T}}P(i) + F_{A,i}^{\mathrm{T}}\delta^{\mathrm{T}}(t)E_i^{\mathrm{T}}P(i) + K^{\mathrm{T}}(i)F_{B,i}^{\mathrm{T}}\delta^{\mathrm{T}}(t)E_i^{\mathrm{T}}P(i + P(i)A_{i,0} \\ &\quad + P(i)B_{i,0}K(i) + P(i)E_i\delta(t)F_{A,i} + P(i)E_i\delta(t)F_{B,i}K(i) + \sum_{j=1}^{N}\lambda_{ij}(h)P(j) < 0. \end{aligned}$$

Applying Lemma 2.1 leads to the following inequalities:

$$F_{A,i}^{\mathrm{T}}\delta^{\mathrm{T}}(t)E_i^{\mathrm{T}}P(i) + P(i)E_i\delta(t)F_{A,i} \le \varepsilon_{A,i}^{-1}F_{A,i}^{\mathrm{T}}F_{A,i} + \varepsilon_{A,i}P(i)E_iE_i^{\mathrm{T}}P(i),$$

$$\begin{aligned} &K^{\mathrm{T}}(i)F_{B,i}^{\mathrm{T}}\delta^{\mathrm{T}}(t)E_i^{\mathrm{T}}P(i) + P(i)E_i\delta(t)F_{B,i}K(i) \\ \le& \varepsilon_{B,i}^{-1}K^{\mathrm{T}}(i)F_{B,i}^{\mathrm{T}}F_{B,i}K(i) + \varepsilon_{B,i}P(i)E_iE_i^{\mathrm{T}}P(i). \end{aligned}$$

So the closed-loop S-MJLS in (2.19) is stochastically stable if the following inequality

holds

$$A_{i,0}^{\mathrm{T}}P(i)+P(i)A_{i,0}+K^{\mathrm{T}}(i)B_{i,0}^{\mathrm{T}}P(i)+P(i)B_{i,0}K(i)+\sum_{j=1}^{N}\lambda_{ij}(h)P(j)$$
$$+\varepsilon_{A,i}^{-1}F_{A,i}^{\mathrm{T}}F_{A,i}+(\varepsilon_{A,i}+\varepsilon_{B,i})P(i)E_iE_i^{\mathrm{T}}P(i)+\varepsilon_{B,i}^{-1}K^{\mathrm{T}}(i)F_{B,i}^{\mathrm{T}}F_{B,i}K(i)<0$$

Denote $X(i)=P^{-1}(i)$ and $Y(i)=K(i)X(i)$. Pre- and post- multiplying the last inequality by $X(i)$ yields

$$X(i)A_{i,0}^{\mathrm{T}}+A_{i,0}X(i)+Y^{\mathrm{T}}(i)B_{i,0}^{\mathrm{T}}+B_{i,0}Y(i)+X(i)\left[\sum_{j=1}^{N}\lambda_{ij}(h)P(j)\right]X(i)$$
$$+\varepsilon_{A,i}^{-1}X(i)F_{A,i}^{\mathrm{T}}F_{A,i}X(i)+(\varepsilon_{A,i}+\varepsilon_{B,i})E_iE_i^{\mathrm{T}}+\varepsilon_{B,i}^{-1}Y^{\mathrm{T}}(i)F_{B,i}^{\mathrm{T}}F_{B,i}Y(i)<0$$

Using the Schur complement, the last inequality is equivalent to (2.18). This ends the proof. □

Testing the conditions in Theorem 2.3 involves solving infinitely many LMIs which is not numerically possible. We apply the same idea in the stability analysis in Section 2.3 by denoting the lower and upper bounds of the transition rate $\lambda_{ij}(h)$ with $\underline{\lambda}_{ij}$ and $\bar{\lambda}_{ij}$. Therefore, we have the following Theorem.

**Theorem 2.4.** *If there exist a set of matrices $X(i)>0$, $Y(i)$, $i\in\mathcal{S}$, and a set of scalars $\varepsilon_{A,i},\varepsilon_{B,i}>0$, $i\in\mathcal{S}$ such that the following LMIs hold. Then the controller $K(i)=Y(i)X^{-1}(i)$ stabilizes the system. For $i\in\mathcal{S}$*

$$\begin{bmatrix}\underline{\tilde{J}}_i & X(i)F_{A,i}^{\mathrm{T}} & Y^{\mathrm{T}}(i)F_{B,i}^{\mathrm{T}} & \Xi_i\\ * & -\varepsilon_{A,i}I & 0 & 0\\ * & * & -\varepsilon_{B,i}I & 0\\ * & * & * & -\mathcal{X}_i\end{bmatrix}<0,\quad\begin{bmatrix}\bar{\tilde{J}}_i & X(i)F_{A,i}^{\mathrm{T}} & Y^{\mathrm{T}}(i)F_{B,i}^{\mathrm{T}} & \bar{\Xi}_i\\ * & -\varepsilon_{A,i}I & 0 & 0\\ * & * & -\varepsilon_{B,i}I & 0\\ * & * & * & -\mathcal{X}_i\end{bmatrix}<0,\tag{2.20}$$

*where*

$$\underline{\tilde{J}}_i=X(i)A_{i,0}^{\mathrm{T}}+A_{i,0}X(i)+Y^{\mathrm{T}}(i)B_{i,0}^{\mathrm{T}}+B_{i,0}Y(i)+(\varepsilon_{A,i}+\varepsilon_{B,i})E_iE_i^{\mathrm{T}}+\underline{\lambda}_{ii}X(i),$$
$$\bar{\tilde{J}}_i=X(i)A_{i,0}^{\mathrm{T}}+A_{i,0}X(i)+Y^{\mathrm{T}}(i)B_{i,0}^{\mathrm{T}}+B_{i,0}Y(i)+(\varepsilon_{A,i}+\varepsilon_{B,i})E_iE_i^{\mathrm{T}}+\bar{\lambda}_{ii}X(i),$$
$$\Xi_i=\left[\sqrt{\underline{\lambda}_{i1}}\ \cdots\ \sqrt{\underline{\lambda}_{i,i-1}}\ \ \sqrt{\underline{\lambda}_{i,i+1}}\ \cdots\ \sqrt{\underline{\lambda}_{iN}}\right]X(i),$$

$$\bar{\Xi}_i = \left[\sqrt{\bar{\lambda}_{i1}} \ \cdots \ \sqrt{\bar{\lambda}_{i,i-1}} \quad \sqrt{\bar{\lambda}_{i,i+1}} \ \cdots \ \sqrt{\bar{\lambda}_{iN}}\right] X(i),$$
$$\mathcal{X}_i = \mathrm{diag}\left[X(1) \ \cdots \ X(i-1) \quad X(i+1) \ \cdots \ X(N)\right].$$

Applying the sojourn-time partition technique from the stochastic stability analysis in Section 2.3, the following Corollary can be readily established.

**Corollary 2.2.** *If there exist a set matrices $X(i,m) > 0$, $Y(i,m)$, $i \in \mathcal{S}$, $m \in \mathcal{M}$ and a set of scalars $\varepsilon_{A,i,m}, \varepsilon_{B,i,m} > 0$, $i \in \mathcal{S}$, $m \in \mathcal{M}$ such that the following LMIs hold. Then the controller $K(i,m) = Y(i,m)X^{-1}(i,m)$ stabilizes the system.*

$$\begin{bmatrix} \underline{\tilde{J}}_{i,m} & X(i,m)F_{A,i}^{\mathrm{T}} & Y^{\mathrm{T}}(i,m)F_{B,i}^{\mathrm{T}} & \underline{\Xi}_{i,m} \\ * & -\varepsilon_{A,i,m}I & 0 & 0 \\ * & * & -\varepsilon_{B,i,m}I & 0 \\ * & * & * & -\mathcal{X}_{i,m} \end{bmatrix} < 0,$$
$$\begin{bmatrix} \bar{\tilde{J}}_{i,m} & X(i,m)F_{A,i}^{\mathrm{T}} & Y^{\mathrm{T}}(i,m)F_{B,i}^{\mathrm{T}} & \bar{\Xi}_{i,m} \\ * & -\varepsilon_{A,i,m}I & 0 & 0 \\ * & * & -\varepsilon_{B,i,m}I & 0 \\ * & * & * & -\mathcal{X}_{i,m} \end{bmatrix} < 0, \quad i \in \mathcal{S}, \tag{2.21}$$

*where for $m = 1, 2, \ldots, M$*

$$\underline{\Xi}_{i,m} = \left[\sqrt{\underline{\lambda}_{i1,m}} \ \cdots \ \sqrt{\underline{\lambda}_{i,i-1,m}} \quad \sqrt{\underline{\lambda}_{i,i+1,m}} \ \cdots \ \sqrt{\underline{\lambda}_{iN,m}}\right] X(i,m),$$
$$\bar{\Xi}_{i,m} = \left[\sqrt{\bar{\lambda}_{i1,m}} \ \cdots \ \sqrt{\bar{\lambda}_{i,i-1,m}} \quad \sqrt{\bar{\lambda}_{i,i+1,m}} \ \cdots \ \sqrt{\bar{\lambda}_{iN,m}}\right] X(i,m),$$
$$\mathcal{X}_{i,m} = \mathrm{diag}\left[X(1,m) \ \cdots \ X(i-1,m) \quad X(i+1,m) \ \cdots \ X(N,m)\right],$$
$$\underline{\tilde{J}}_{i,m} = \tilde{J}_{i,m}^0 + \underline{\lambda}_{ii,m}X(i,m), \quad \bar{\tilde{J}}_{i,m} = \tilde{J}_{i,m}^0 + \bar{\lambda}_{ii,m}X(i,m),$$

*where*

$$\tilde{J}_{i,m}^0 = X(i,m)A_{i,0}^{\mathrm{T}} + A_{i,0}X(i,m) + Y^{\mathrm{T}}(i,m)B_{i,0}^{\mathrm{T}} + B_{i,0}Y(i,m) + (\varepsilon_{A,i,m} + \varepsilon_{B,i,m})E_iE_i^{\mathrm{T}}.$$

Following the same techniques used in Theorem 2.2 and Corollary 2.1, Theorem 2.4 and Corollary 2.2 can be readily proved and hence the proof is omitted here.

**Remark 2.2** The partition strategy of the sojourn-time plays a significant role in the stochastic stability analysis and the corresponding robust controller design for

the S-MJLS. As shown in [88], the conservativeness of the sufficient condition will be reduced with more partitions. In this chapter, the sojourn-time is partitioned such that for the $m^{\text{th}}$ ($m \in \mathcal{M}$) section

$$\Pr\{h_{m-1} \leq h < h_m\} = \frac{1}{M}, \quad m = 1, 2, \ldots, M. \tag{2.22}$$

Here, $h_{m-1}$ and $h_m$ are the beginning and ending time for section $m$, when the system operating on a specific mode. An illustration of the beginning and ending time is given in Figure 2.1. In this figure, totally $M$ sections are set for mode 3. The S-MJLS switches from mode 3 to mode 1 after $h_{M-2}$ and before $h_{M-1}$, i.e., the system switches at section $M-1$. Different from the currently used partition technique,

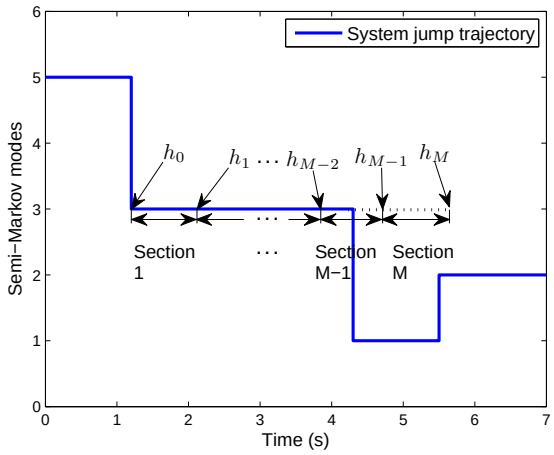


Figure 2.1: Beginning and ending time for each sections.

we can also propose other partition methods. For example, partition each section uniformly, i.e.,

$$h_m - h_{m-1} = \frac{h_M - h_0}{M}, \quad m = 1, 2, \ldots, M, \tag{2.23}$$

or, putting constraints on the variation of the transition rates for each section, i.e.,

$$\bar{\lambda}_{ij,m} - \underline{\lambda}_{ij,m} \leq \texttt{Threshold}. \tag{2.24}$$

In fact, the effect of using a) different number of partitions ($M$) and b) different sojourn-time partition strategies on the stability analysis and controller design has not been fully investigated yet, and this issue deserves further exploration and is our current research topic.

**Remark 2.3** In [88], by studying jump linear systems where the sojourn-time follows the Weibull distribution, the difference between the time-varying transition rate and the constant transition rate was analyzed and explained; furthermore, the numerically testable sufficient condition for ensuring the stability of the S-MJLS was established. However, the model uncertainties were not considered in [88]. In this chapter, we have extended the stability analysis and the corresponding robust control design for S-MJLSs with norm-bounded uncertainties. In addition, the statistic characteristic of the control performance of the stochastic switching system is analyzed and presented in Section 2.5.

## 2.5 Illustrative Examples

Consider a continuous-time S-MJLS $\mathscr{S}_2$ in (2.16) operating on 2 modes with the following system matrices:

$$A_1(t) = \begin{bmatrix} 1.1555 & -0.4006 + 0.1\sigma(t) \\ -0.4470 & -0.7930 \end{bmatrix}, \; A_2(t) = \begin{bmatrix} -0.0274 & 0.0249 \\ -0.3835 & 0.3026 + 0.7\rho(t) \end{bmatrix},$$

$$B_1(t) = \begin{bmatrix} 1 & 1 \end{bmatrix}^{\mathrm{T}}, \; B_2(t) = \begin{bmatrix} 1 & 0.1\rho(t) \end{bmatrix}^{\mathrm{T}}.$$

The nominal system matrices are

$$A_{1,0} = \begin{bmatrix} 1.1555 & -0.4006 \\ -0.4470 & -0.7930 \end{bmatrix}, \; B_{1,0} = \begin{bmatrix} 1 \\ 1 \end{bmatrix},$$
$$A_{2,0} = \begin{bmatrix} -0.0274 & 0.0249 \\ -0.3835 & 0.3026 \end{bmatrix}, \; B_{2,0} = \begin{bmatrix} 1 \\ 0 \end{bmatrix},$$

and the matrices describing the norm-bounded uncertainties are

$$E_1 = E_2 = \begin{bmatrix} 1 & 0 \\ 0 & 1 \end{bmatrix}, \; \delta(t) = \begin{bmatrix} \sigma & 0 \\ 0 & \rho \end{bmatrix}, \; F_{A,1} = \begin{bmatrix} 0.2 & 0.1 \\ 0.1 & 0 \end{bmatrix}, \; F_{A,2} = \begin{bmatrix} 0 & 0 \\ 0.1 & 0 \end{bmatrix},$$

$$F_{B,1} = \begin{bmatrix} 0 & 0 \end{bmatrix}^{\mathrm{T}}, \; F_{B,2} = \begin{bmatrix} 0 & 0.1 \end{bmatrix}^{\mathrm{T}}, \tag{2.25}$$

where $\sigma$ and $\rho$ are uncertain real parameters such that $|\sigma| \leq 1$, $|\rho| \leq 1$. Depending on sojourn-time $h$, the transition rate function $\lambda_{ij}(h)$ is a continuous piecewise function

described as follows:

$$\lambda_{ij}(h) = \begin{cases} \underline{h}, & h < \underline{h}, \\ h, & \underline{h} \leq h \leq \bar{h}, \\ \bar{h}, & h > \bar{h}, \end{cases} \tag{2.26}$$

where $\underline{h} = 0.1000$s and $\bar{h} = 4.6000$s. Considering that the switching system jumps from mode $i$ to mode $j$, if the sojourn-time follows Weibull distribution with the scale parameter $\alpha = 1$ and the shape parameter $\beta = 2$, the transition rate function is $\lambda_{ij}(h) = h$. Therefore, the transition rate function (2.26) can be regarded as an approximation when the sojourn-time follows Weibull distribution at a high confidence level. If the sojourn-time follows the aforementioned Weibull distribution, the jump will occur in the interval $[\underline{h},\ \bar{h}]$ with probability greater than 0.99, i.e. let $h_j$ denote the jump time, then $\Pr\{\underline{h} \leq h_j \leq \bar{h}\} > 0.99$. Note that the Weibull distribution has been widely used in the reliability engineering to model fault tolerant systems [75].

According to Corollary 2.2, if $M$ is set to 2, i.e. the sojourn-time $h$ is divided into two sections by $h = 0.8326$. Therefore, when $h < 0.8326$, the state feedback control law is $K(1,1)$ for mode 1 and $K(2,1)$ for mode 2; when $h \geq 0.8326$, the state feedback control law is $K(1,2)$ for mode 1 and $K(2,2)$ for mode 2. The computation time is 0.0749 s on a PC (3.0 GHz, 2.0 GB of RAM memory). The state feedback control law designed using Corollary 2.2 is obtained as follows:

$$\begin{aligned} K(1,1) &= \begin{bmatrix} -22.1292 & 14.1944 \end{bmatrix}, \quad K(2,1) = \begin{bmatrix} -4.7141 & 6.3067 \end{bmatrix}, \\ K(1,2) &= \begin{bmatrix} -11.0213 & 7.1232 \end{bmatrix}, \quad K(2,2) = \begin{bmatrix} -4.0094 & 3.3051 \end{bmatrix}. \end{aligned} \tag{2.27}$$

Implementing the control law, and starting from the initial state $x_0 = [5\ -4]^{\mathrm{T}}$, $r_0 = 1$, the state trajectories of the controlled system are shown in Figure 2.2a. It is obvious that the designed controller is feasible and guarantees the stochastic stability of the closed-loop system despite the time-varying transition rates.

**Controller design based on different interval partitions:** It is noticed that, by applying Theorem 2.4, the condition in (2.20) is not feasible. By further dividing the sojourn-time $h$ into 2 sections, the controller (2.27) is obtained. In addition, for certain systems, $m = 4$ yields a feasible solution, while $m = 2$ does not. Therefore, using Corollary 2.2, a larger $M$ is more likely to yield a feasible controller. The problem on how to appropriately divide the sojourn-time into several sections still deserves further research.

**Comparisons to [1, 2]:** The proposed controller by using the techniques in [1, 2] is $K_1 = [-3.7949\ 2.2244]$, $K_2 = [-1.7292\ 1.2225]$ for each operating mode, respectively. In the simulation, the same initial condition $x_0 = [5\ -4]^{\mathrm{T}}$ and the same switching time are applied, and the state trajectories are also shown in Figure 2.2a. For the proposed controller, it takes 2.95s for the two states converge to 0, while it takes more than 10s for the controller designed in [1, 2]. Theoretically, the controller obtained from [1, 2] has relatively smaller feedback gains, so the transient response is slower. Therefore, the proposed control design technique outperforms the existing methodologies.

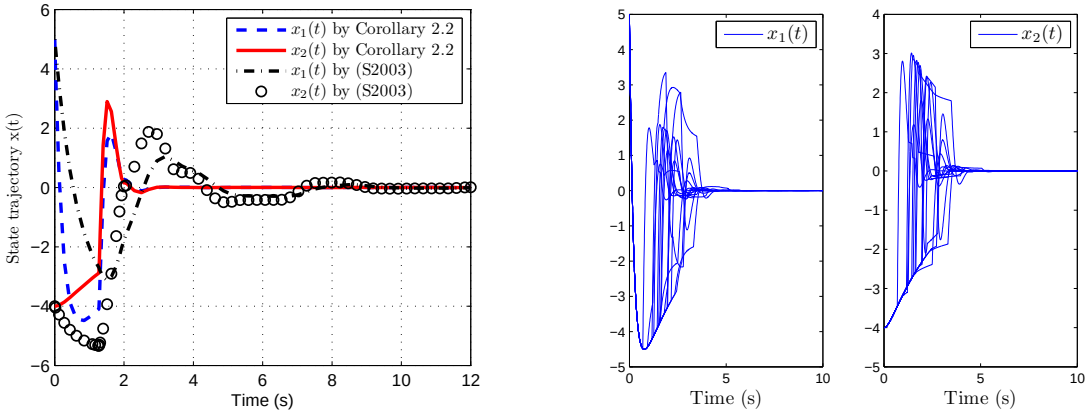


(a) Comparison by using Corollary 2.2 and techniques in [1, 2] (S2003).

(b) Monte Carlo simulation with different semi-Markov processes for 20 runs by using Corollary 2.2.

Figure 2.2: One run simulation and Monte Carlo simulation.

To further illustrate the effectiveness of the proposed technique, we perform the Monte Carlo simulation. In Figure 2.2b, the trajectories of controlled system states $x_1(t)$ and $x_2(t)$ for 20 runs are shown, respectively. The semi-Markov processes are unique in each run and are generated by utilizing (2.26). It can be seen that the system is stochastically stabilized for every run of simulation. In addition, the average states $x(t) = [x_1(t)\ x_2(t)]^{\mathrm{T}}$ by 10000 Monte Carlo simulation runs are shown in Figure 2.4a. Obviously, by using the proposed controller, the states converge with less overshoot and small settling time. Statistically, the settling time for 10000 runs is summarized in Figure 2.4b. In the simulation, we denote the settling time as $T_s$ which is given by

$$|x(t)|_2 \leq 1.5\%|x(0)|_2, \text{ for all } t > T_s. \tag{2.28}$$

The mean values of the settling time by using two different controllers are 3.5741 s

and 9.9100 s, respectively. Therefore, in the stochastic sense, the control scheme proposed in this chapter generates faster transient response. Other than the mean value of the settling time, the standard deviation (Std) is also crucial to describe the system performance. The standard deviation of the settling time for 10000 runs are 0.8849 and 2.1895, respectively. Figure 2.4 shows the convergence of the mean valve and the standard deviation of the settling time for different number of simulation runs. The ± one, two, and three standard deviations are listed in Table 2.1.

Table 2.1: ± Standard deviation.

| ± standard deviation | ± 1 | ± 2 | ± 3 |
|---|---|---|---|
| Seconds (s) | 0.87 | 1.75 | 3.03 |

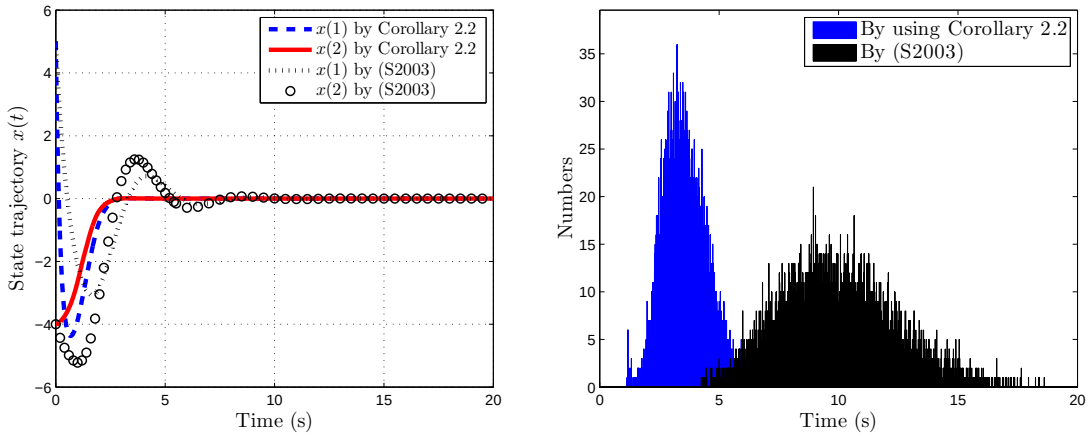


(a) Average system trajectories by using Monte Carlo simulation (10000 runs).

(b) Statistics of the settling time by using two methods (10000 runs).

Figure 2.3: Average results and statistics of the Monte Carlo simulation (10000 runs).

## 2.6 Conclusion

In this chapter, we have investigated the stochastic stability and robust stabilization problems for S-MJLSs. First, the infinitesimal generator for the quadratic Lyapunov function $V(\cdot)$ of the S-MJLS was derived. Then the sufficient stochastic stability condition for S-MJLSs with norm-bounded uncertainties was established. The sufficient condition is further relaxed by solving a set of LMIs. By partitioning the

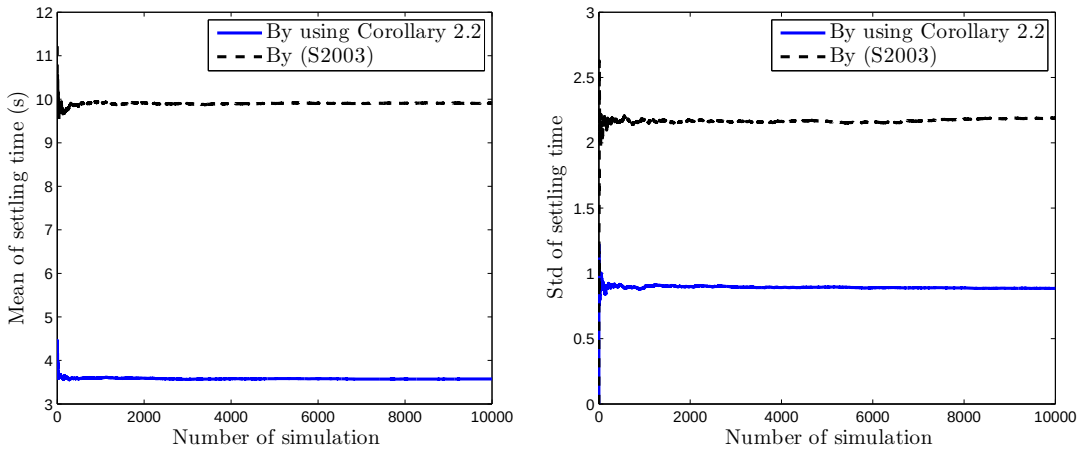


(a) Convergence of Monte Carlo simulation (Mean).

(b) Convergence of Monte Carlo simulation (Std).

Figure 2.4: Convergence of Monte Carlo simulation.

sojourn-time $h$ into sub-sections, the conservativeness of the sufficient condition can be effectively reduced. Different sojourn-time partitioning methods were presented in Remark 2.2; the effects on the stochastic stability and control performance by using different methods deserve further studies. Lastly, the robust state feedback controller design method was proposed. Numerical examples and comparisons illustrate the effectiveness of the proposed methods.

# Chapter 3

# $H_\infty$ State-Feedback Control for Semi-Markov Jump Linear Systems with Time-Varying Delays

## 3.1 Introduction

The study of jump linear systems is motivated by many real-world technical problems involving abrupt changes and switches [89, 90]. The evolution of system parameters can be modeled within a stochastic framework, where each set of the system parameters describes one linear system. In the jump linear system, the **sojourn-time** $h$ is the duration between two consecutive jumps/switches. In general, $h$ is a random variable following certain probability distributions. For example, in a continuous-time jump linear system, if $h$ is governed by an exponential distribution, then the jump linear system is reduced to the well-known Markov jump linear system (MJLS) which has attracted much research attention. Applications of MJLS cover several research areas, such as NCSs [56], fault tolerant systems [91], aerospace systems [92], and so on. Because the MJLS model is suitable for characterizing and representing system changes and switches, for example, system failures, random events, and unexpected configuration changes.

In a more general framework, the sojourn-time follows any probability distribution which may not always take the exponential distribution. In such cases, the jump linear system is termed as a semi-Markov jump linear system [1]. Therefore, the set of MJLSs is a subset of the set of S-MJLSs. The relationship among MJLS and

S-MJLS as well as jump linear system can be shown in Figure 3.1. Compared to the rich literature on MJLSs, relatively less research attention has been paid to S-MJLSs. In [1] and [2], a stochastic stability condition was established and a controller was designed based on the proposed stability condition. The designed controller was tested on a bunch-train cavity interaction system which can be formulated as an S-MJLS. However, the probability distributions of the sojourn-time in [1] and [2] were chosen as "nearly exponential", which indicates that the S-MJLS behaves similarly as an MJLS. In [88], we proposed a numerically testable condition for ensuring the stability of the S-MJLS. To further reduce the conservativeness of the method, the sojourn-time partitioning technique was developed. For other results on S-MJLSs, please refer to [88] and the references therein.

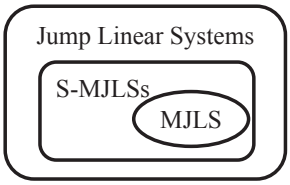


Figure 3.1: The relationship among the jump linear systems, S-MJLSs, and MJLSs.

On the other hand, the $H_\infty$ control has been proved to be a useful tool for attenuating the effect of disturbances/noises in dynamic systems [28, 93]. $H_\infty$ control stems from the robust stability problem in the frequency domain, and it is now commonly used to solve the optimal control problems which attenuates the $L_2$ gain from the disturbance/noise to the output of interest in the time domain. The $H_\infty$ controller can be effectively and conveniently designed by solving a set of linear matrix inequalities (LMIs) [23]. The $H_\infty$ controller design for MJLS with and without delays has been reported in the past decades; see, e.g. [94, 95, 96]. Compared to the aforementioned work, in this chapter, we consider a more general and practical scenario: The switching tendencies/trends from one state to another are not constant any more; in this case, if the well-developed MJLS methods are applied, 1) the time-varying information of the transition rate will be missed, and accordingly the control performance will be deteriorated; 2) the proposed controller or filter may malfunction due the evaluation failure of potential state jumps.

Besides the stochastic behavior of practical systems, the existence of time-delays is ubiquitous in many applications, and it has been studied extensively over the past years [97]. The time delay is an inherent feature of many control processes in mechanical plants, chemistry processes, and automation systems [98]. On one

hand, it is well recognized that time delays can lead to divergence, oscillation, or instability [99]. On the other hand, considerable efforts have been devoted to the analysis and synthesis problems for MJLSs with constant delays as well as time-varying delays. Especially, the time delay effect on MJLSs with partially known transition rates has been considered in [16]. In this chapter, we move one step further, where transition rates are not partially known, but are time-varying. However, until now, no result has been reported for the $H_\infty$ optimal control for the S-MJLS with time-varying delays, which motivates this research.

The remainder of this chapter is organized as follows. The $H_\infty$ state-feedback control design problem for the delayed S-MJLS is formulated in Section 3.2. In Section 3.3, the sufficient conditions for ensuring the stochastic stability of S-MJLSs with time-varying delays are established and the $H_\infty$ control design method is developed. To validate the proposed theorem and corollaries, simulation studies are provided in Section 3.4. Finally, the concluding remarks are given in Section 3.5.

## 3.2 Problem Formulation

Consider the switching system $\mathfrak{S}$ with semi-Markov jumping parameters and time-varying state delays

$$\begin{aligned}\mathfrak{S}: \dot{x}(t) =& A(r(t))x(t) + A_d(r(t))x(t-\tau(t,(r(t))) + B(r(t))u(t),\\ z(t) =& C(r(t))x(t),\\ x(s) =& \phi(s),\ s\in[-d,\ 0], \quad r(0)=r_0,\end{aligned} \tag{3.1}$$

where $x(t)\in\mathbb{R}^n$, $u(t)\in\mathbb{R}^p$, and $z(t)\in\mathbb{R}^q$ are the system state, control input, and system output, respectively. $A(r(t))$, $A_d(r(t))$, $B(r(t))$, and $C(r(t))$ are the system matrices depending on the semi-Markov process $\{r(t), t>0\}$, where $r(t)$ is a continuous-time discrete-state semi-Markov process taking values in the finite set $\mathcal{S}=\{1,2,\cdots,N\}$. In the following, $r(t)$ is denoted as $r_t$ for the purpose of simplicity. Similarly, $A(r(t))$, $A_d(r(t))$, $B(r(t))$, $C(r(t))$, and $\tau(t,r(t))$ are denoted as $A_i$, $A_{di}$, $B_i$, $C_i$, and $\tau_i(t)$, respectively, when $r(t)=i$. Here, $\tau_i(t)$ is the time-varying state delay in the system, and

$$\dot{\tau}_i(t)\le h_i<1. \tag{3.2}$$

Furthermore, we assume that the maximum allowable time delay is $\bar{\tau}$, i.e., $\tau_i(t) \leq \bar{\tau}$, for all $i \in \mathcal{S}$. $\phi(s)$ is the initial state and $r(0)$ is the initial mode of the semi-Markov process. For system $\mathfrak{S}$, if the control input is 0, i.e., $u(t) \equiv 0$, then we have the following unforced system $\mathfrak{S}_u$

$$\begin{aligned}\mathfrak{S}_u : \dot{x}(t) =& A(r_t)x(t) + A_d(r_t)x(t - \tau(t, r_t)),\\ z(t) =& C(r_t)x(t),\\ x(s) =& \phi(s),\ s \in [-d,\ 0], \quad r(0) = r_0.\end{aligned} \tag{3.3}$$

The semi-Markov process is given as follows [100]

$$\Pr\{r(t+h) = j | r(t) = i\} = \begin{cases}\lambda_{ij}(h)h + o(h), & r(t)\,\text{jumps from } i \text{ to } j,\\ 1 + \lambda_{ii}(h)h + o(h), & r(t) \text{ stays at mode } i.\end{cases} \tag{3.4}$$

Here, $o(h)$ is the little-$o$ notation defined as $\lim_{h\to 0} o(h)/h = 0$. From the transition property, $\sum_{j\in\mathcal{S}} \lambda_{ij}(h) = 0$, i.e.,

$$\lambda_{ii}(h) = -\sum_{j\in\mathcal{S}, j\neq i} \lambda_{ij}(h).$$

For the stochastic stability, we adopt the definition from [101].

**Definition 3.1.** *The unforced system $\mathfrak{S}_u$ is said to be mean square stochastically exponential stable if for all possible finite initial function $\phi(s) \in \mathbb{R}^n$ and all possible initial mode $r_0 \in \mathcal{S}$, such that the following inequality holds:*

$$\mathbb{E}\left\{\|x(t)\|^2\right\} \leq \sigma e^{-\lambda t}\|\phi\|^2, \tag{3.5}$$

*where $\lambda$ and $\sigma$ are called the decay rate and the decay coefficient, respectively.*

The objectives of this chapter are mainly two-fold.

**O1:** To establish the stochastic stability criteria for the delayed S-MJLS $\mathfrak{S}$ in (3.1) where the transition rates are time-varying.

**O2:** To design an $H_\infty$ state-feedback controller such that the closed-loop system is stochastically stable with prescribed noise attenuation level $\gamma$. The state feedback controller to be designed is mode-dependent and sojourn-time dependent

of the following form

$$u(r_t) = K(r_t, h)x(t). \tag{3.6}$$

It is worth mentioning that the control gain $K$ not only depends on the semi-Markov process $r_t$ but also depends on the sojourn-time $h$.

## 3.3 Main Results

In this section, the stochastic stability condition for the unforced delayed S-MJLS $\mathfrak{G}_u$ in (3.3) will be firstly addressed. Based on the stochastic stability definition in (3.5), the controller design method will be presented via solving a set of LMIs.

### 3.3.1 Stochastic Stability Condition for Delayed S-MJLS

The following proposition gives the stochastic stability condition for the system in (3.3).

**Proposition 1.** *The unforced S-MJLS $\mathfrak{S}_u$ with time-varying state delays in (3.3) achieves mean-square stochastically exponential stability if there exist matrices $P_i > 0$, $i \in \mathcal{S}$, and $Q > 0$ such that the following inequalities hold for all $i \in \mathcal{S}$ and $h > 0$*

$$\begin{bmatrix} \sum_{j\in\mathcal{S}} \lambda_{ij}(h)P_j + \mathrm{sym}\{P_iA_i\} & * \\ +(1+\eta(h)\bar{\tau})Q & \\ A_{di}^{\mathrm{T}}P_i & -(1-h_i)Q \end{bmatrix} < 0, \tag{3.7}$$

*where $\eta(h) = -\min\{\lambda_{ii}(h), i \in \mathcal{S}\}$ for all possible $h$.*

*Proof.* Consider the unforced system $\mathfrak{S}_u$ in (3.3) and the following Lyapunov functional

$$V(x(t), r_t) = V_1(x(t), r_t) + V_2(x(t), r_t) + V_3(x(t), r_t), \tag{3.8}$$

where

$$V_1(x(t), r_t) = x(t)^{\mathrm{T}}P(r_t)x(t), \tag{3.9}$$

$$V_2(x(t), r_t) = \int_{t-\tau_{r_t}(t)}^{t} x(s)^{\mathrm{T}}Qx(s)ds, \tag{3.10}$$

$$V_3(x(t), r_t) = \eta(h)\int_{-\bar{\tau}}^{0}\int_{t+\theta}^{t} x(s)^{\mathrm{T}}Qx(s)dsd\theta. \tag{3.11}$$

Let $\tilde{A}$ be the infinitesimal generator which can be regarded as the time derivative of the Lyapunov function (3.8). It can be verified that

$$\begin{aligned}
&\tilde{A}\left[e^{\beta t}V_1(x(t),i)\right]\\
=&e^{\beta t}x(t)^{\mathrm{T}}\left[\sum_{j\in\mathcal{S}}\lambda_{ij}(t)P_j\right]x(t)+\beta e^{\beta t}V_1(x(t),i)\\
&+2e^{\beta t}x(t)^{\mathrm{T}}P_i\left[A_ix(t)+A_{di}x(t)+A_{di}x(t-\tau_i(t))\right],\\
&\tilde{A}\left[e^{\beta t}V_2(x(t),i)\right]\\
=&e^{\beta t}x(t)^{\mathrm{T}}Qx(t)-e^{\beta t}[1-\dot{\tau}_i(t)]x(t-\tau_i(t))^{\mathrm{T}}Qx(t-\tau_i(t))\\
&+\beta e^{\beta t}V_2(x(t),i)+e^{\beta t}\sum_{j\in\mathcal{S}}\lambda_{ij}(h)\int_{t-\tau_j(t)}^{t}x(s)^{\mathrm{T}}Qx(s)ds,\\
&\tilde{A}\left[e^{\beta t}V_3(x(t),i)\right]\\
=&e^{\beta t}\eta(h)\bar{\tau}x(t)^{\mathrm{T}}Qx(t)-e^{\beta t}\eta(h)\int_{t-\bar{\tau}}^{t}x(s)^{\mathrm{T}}Qx(s)ds+\beta e^{\beta t}V_3(x(t),i).
\end{aligned}\tag{3.12}$$

Noting that $\lambda_{ij}(h)\geq 0$, for $i\neq j$ and $\lambda_{ii}(h)\leq 0$, we have

$$\begin{aligned}
\sum_{j\in\mathcal{S}}\lambda_{ij}(h)V_2(x(t),j)\leq&\sum_{j\in\mathcal{S},j\neq i}\lambda_{ij}(h)\int_{t-\bar{\tau}_j}^{t}x(s)^{\mathrm{T}}Qx(s)ds\\
\leq&\sum_{j\in\mathcal{S},j\neq i}\lambda_{ij}(h)\int_{t-\bar{\tau}}^{t}x(s)^{\mathrm{T}}Qx(s)ds\\
=&-\lambda_{ii}(h)\int_{t-\bar{\tau}}^{t}x(s)^{\mathrm{T}}Qx(s)ds\\
\leq&\eta(h)\int_{t-\bar{\tau}}^{t}x(s)^{\mathrm{T}}Qx(s)ds.
\end{aligned}$$

Applying the Schur complement formula to (3.7), we have

$$\sum_{j\in\mathcal{S}}\lambda_{ij}(h)P_j+A_i^{\mathrm{T}}P_i+P_iA_i+(1+\eta(h)\bar{\tau})Q+(1-h_i)^{-1}P_iA_{di}Q^{-1}A_{di}^{\mathrm{T}}P_i<0.\tag{3.13}$$

Then it can be shown that

$$\begin{aligned}
\tilde{A}\left[e^{\beta t}V(x(t),i)\right]\leq&\beta e^{\beta t}V(x(t),i)+e^{\beta t}x(t)^{\mathrm{T}}\left[\sum_{j\in\mathcal{S}}\lambda_{ij}(h)P_j+A_i^{\mathrm{T}}P_i+P_iA_i\right.\\
&\left.+(1+\eta(h)\bar{\tau})Q+(1-h_i)^{-1}P_iA_{di}Q^{-1}A_{di}^{\mathrm{T}}P_i\right]x(t).
\end{aligned}\tag{3.14}$$

For each $i$ and any scaler $\beta > 0$, we get

$$\begin{aligned}\tilde{A}\left[e^{\beta t}V(x(t),i)\right] <& -\alpha e^{\beta t}|x(t)|^2 + \beta e^{\beta t}V(x(t),i)\\ <& -\alpha e^{\beta t}|x(t)|^2 + \beta e^{\beta t}\Bigg[\alpha_1|x(t)|^2 + \lambda_{\max}(Q)\int_{t-\bar{\tau}}^{t}|x(s)|^2 ds\\ &+\eta(h)\lambda_{\max}(Q)\int_{-\bar{\tau}}^{0}\int_{t+\theta}^{t}|x(s)|^2 ds d\theta\Bigg]. \end{aligned} \tag{3.15}$$

Notice that

$$\int_{-\bar{\tau}}^{0}\int_{t+\theta}^{t}|x(s)|^2 ds d\theta \le \bar{\tau}\int_{t-\bar{\tau}}^{t}|x(s)|^2 ds, \tag{3.16}$$

which implies

$$\begin{aligned}&\tilde{A}\left[e^{\beta t}V(x(t),i)\right]\\ <&(-\alpha+\alpha_1\beta)e^{\beta t}|x(t)|^2 + \beta e^{\beta t}(\bar{\tau}\eta(h)+1)\lambda_{\max}(Q)\int_{t-\bar{\tau}}^{t}|x(s)|^2 ds. \end{aligned} \tag{3.17}$$

Applying the generalized Dynkin's formula [87], we have

$$\begin{aligned}&\mathbb{E}\left\{e^{\beta T}V(x(T),i)\right\} - V(x_0,r_0)\\ =&\mathbb{E}\left\{\int_0^T \tilde{A}\left[e^{\beta t}V(x_s,i)\right]ds\Big|(x_0,r_0)\right\}\\ <&(-\alpha+\alpha_1\beta)\int_0^T e^{\beta t}|x(t)|^2 dt + \beta e^{\beta t}(\bar{\tau}\eta(h)+1)\lambda_{\max}(Q)\int_0^T e^{\beta t}\int_{t-\bar{\tau}}^{t}|x(s)|^2 ds dt. \end{aligned} \tag{3.18}$$

Denote $\alpha_2(h) = (\bar{\tau}\eta(h)+1)\lambda_{\max}(Q)$, and also notice that

$$\int_0^T e^{\beta t}\int_{t-\bar{\tau}}^{t}|x(t)|^2 ds dt \le \bar{\tau}\int_{-\bar{\tau}}^{T} e^{\beta(t+\bar{\tau})}|x(t)|^2 dt. \tag{3.19}$$

So, for each $i \in \mathcal{S}$ and any scaler $\beta > 0$ we have

$$\begin{aligned}&\mathbb{E}\{e^{\beta T}V(x(T),i)\}\\ <&V(x_0,r_0) + (-\alpha+\alpha_1\beta)\int_0^T e^{\beta t}|x(t)|^2 dt + \alpha_2(h)\beta\int_{-\bar{\tau}}^{T} e^{\beta(t+\bar{\tau})}|x(t)|^2 dt \end{aligned}$$

$$\leq V(x_0, r_0) + \left(-\alpha + \alpha_1\beta + \alpha_2(h)\beta e^{\beta\bar{\tau}}\right) \int_0^T e^{\beta t}|x(t)|^2 dt + \alpha_2(h)\beta e^{\beta\bar{\tau}} \int_{-\bar{\tau}}^0 |x(t)|^2 dt.$$

Choose $\beta > 0$ to be the solution of the following equation

$$-\alpha + \alpha_1\beta + \alpha_2(h)\beta e^{\beta\bar{\tau}} = 0. \tag{3.20}$$

Next we will show that a positive solution $\beta$ always exists. (3.20) can be written as

$$f_\beta^{(1)} = f_\beta^{(2)}, \tag{3.21}$$

where

$$f_\beta^{(1)}(\beta) = \frac{\alpha}{\beta} - \alpha_p, \quad f_\beta^{(2)}(\beta) = \alpha_2(h)e^{\beta\bar{\tau}}.$$

With $Q > 0$, $\eta(h) > 0$ and $\bar{\tau} > 0$, $\alpha_2(h)$ is positive. It can be shown that for $\forall h > 0$, $\exists\beta > 0$ satisfying (3.21). Therefore, we can always find $\beta > 0$ such that (3.20) is satisfied. Therefore, we have

$$\mathbb{E}\left\{e^{\beta T}V(x(T), i)\right\} < V(x_0, r_0) + \alpha_2(h)\beta e^{\beta\bar{\tau}} \int_{-\bar{\tau}}^0 |x(t)|^2 dt \tag{3.22}$$

and hence, the system achieves mean-square stochastically exponential stability. This ends the proof. □

### 3.3.2 $H_\infty$ Controller Design for Delayed S-MJLS

Considering the external disturbance $\omega(t)$, and by using the feedback control law $u(r_t) = K(r_t, h)x(t)$ in (3.6), the closed-loop system becomes

$$\begin{aligned}
\mathfrak{G}_c : \dot{x}(t) =& A_c(r_t)x(t) + A_d(r_t)x(t - \tau(t, r_t)) + B(r_t)\omega(t), \\
z(t) =& C(r_t)x(t), \\
x(s) =& \phi(s), \quad s \in [-d,\ 0), \quad r(0) = r_0,
\end{aligned} \tag{3.23}$$

where $\omega(t) \in \mathcal{L}_2[0, \infty)$ is the external noise, and $A_c(r_t)$ is given as follows

$$A_c(r_t) = A(r_t) + B(r_t)K(r_t, h). \tag{3.24}$$

The objective is to design the control signal $u(t)$ such that the delayed system in (3.23) achieves mean-square stochastically exponential stability and

$$\|z\|_{E_2} < \gamma \|\omega\|_2 \tag{3.25}$$

under zero initial condition for any nonzero $\omega(t) \in \mathcal{L}_2[0,\, \infty)$, where $\|\cdot\|_2$ denotes the $\mathcal{L}_2[0,\, \infty)$ norm, and

$$\|z\|_{E_2} = \left[\mathbb{E}\left\{\int_0^\infty |z(t)|^2 dt\right\}\right]^{\frac{1}{2}}, \tag{3.26}$$

where $|\cdot|$ is the Euclidean vector norm.

The controller design technique is summarized in the following theorem.

**Theorem 3.1.** *If there exist symmetric matrices $\bar{P}_i > 0$, $\bar{Q} > 0$, and matrices $U_i(h)$, $i \in \mathcal{S}$, with appropriate dimensions such that the following matrix inequalities hold for all $i \in \mathcal{S}$ and $h > 0$*

$$\begin{bmatrix} \mathrm{sym}\{A_i\bar{P}_i\} + \mathrm{sym}\{B_iU_i(h)\} & * & * & * & * \\ +\lambda_{ii}(h)\bar{P}_i + C_i^{\mathrm{T}}C_i & & & & \\ \bar{Q}A_{di}^{\mathrm{T}} & -(1-h_i)\bar{Q} & * & * & * \\ \sqrt{1+\eta(h)\bar{\tau}}\bar{P}_i & 0 & -\bar{Q} & * & * \\ B_i^{\mathrm{T}}\bar{P}_i & 0 & 0 & -\gamma^2 I & * \\ \mathfrak{I}_i(h)^{\mathrm{T}}\bar{P}_i & 0 & 0 & 0 & \mathfrak{P}_i \end{bmatrix} < 0, \tag{3.27}$$

*where*

$$\mathfrak{P}_i = -\mathrm{diag}\{\bar{P}_1, \cdots, \bar{P}_{i-1}, \bar{P}_{i+1}, \cdots, \bar{P}_N\}, \tag{3.28}$$

$$\mathfrak{I}_i(h) = \left[\lambda_{i1}^{\frac{1}{2}}(h)I, \cdots, \lambda_{i,i-1}^{\frac{1}{2}}(h)I, \lambda_{i,i+1}^{\frac{1}{2}}(h)I, \cdots, \lambda_{iN}^{\frac{1}{2}}(h)I\right]. \tag{3.29}$$

*Then the closed-loop system $\mathfrak{G}_c$ in (3.23) is mean square stochastically exponential stable with $\gamma$-disturbance attenuation level.*

*Proof.* First, we will establish the stochastic stability condition. Based on the stability condition proposed in Proposition 1, the system will be stable if the following set of inequalities are satisfied

$$\begin{bmatrix} \sum_{j\in\mathcal{S}} \lambda_{ij}(h)P_j + \mathrm{sym}\{P_iA_{ci}\} & * \\ +(1+\eta(h)\bar{\tau})Q & \\ A_{di}^{\mathrm{T}}P_i & -(1-h_i)Q \end{bmatrix} < 0. \tag{3.30}$$

Plugging $A_{ci}$ in (3.24) into (3.30) gives rise to

$$\begin{bmatrix} \sum_{j\in\mathcal{S}} \lambda_{ij}(h)P_j + (1+\eta(h)\bar{\tau})Q & * \\ +\text{sym}\{P_i[A_i + B_iK(i,h)]\} & \\ A_{di}^{\mathrm{T}}P_i & -(1-h_i)Q \end{bmatrix} < 0. \tag{3.31}$$

Since $P_i > 0$ and $Q > 0$, denote $\bar{P}_i = P_i^{-1}$ and $\bar{Q} = Q^{-1}$. The last inequality can be written as

$$\begin{bmatrix} \text{sym}\{P_i[A_i + B_iK(i,h)]\} & & \\ +(1+\eta(h)\bar{\tau})Q + \lambda_{ii}(h)P_i & * & * \\ A_{di}^{\mathrm{T}}P_i & -(1-h_i)Q & * \\ \mathfrak{I}_i^{\mathrm{T}} & 0 & \mathfrak{P}_i \end{bmatrix} < 0. \tag{3.32}$$

By pre- and post-multiplying the last inequality by $\text{diag}\{\bar{P}_i, \bar{Q}, \underbrace{I, \ldots, I}_{N-1}\}$, we obtain

$$\begin{bmatrix} \text{sym}\{[A_i + B_iK(i,h)]\bar{P}_i\} & & \\ +(1+\eta(h)\bar{\tau})\bar{P}_iQ\bar{P}_i + \lambda_{ii}(h)\bar{P}_i & * & * \\ \bar{Q}A_{di}^{\mathrm{T}} & -(1-h_i)\bar{Q} & * \\ \mathfrak{I}_i^{\mathrm{T}}\bar{P}_i & 0 & \mathfrak{P}_i \end{bmatrix} < 0.$$

Applying the Schur complement again, we have

$$\begin{bmatrix} \text{sym}\{[A_i + B_iK(i,h)]\bar{P}_i\} & & & \\ +\lambda_{ii}(h)\bar{P}_i & * & * & * \\ \bar{Q}A_{di}^{\mathrm{T}} & -(1-h_i)\bar{Q} & * & * \\ \sqrt{1+\eta(h)\bar{\tau}}\bar{P}_i & 0 & -\bar{Q} & * \\ \mathfrak{I}_i^{\mathrm{T}}\bar{P}_i & 0 & 0 & \mathfrak{P}_i \end{bmatrix} < 0.$$

Denoting $U_i(h) = K(i,h)\bar{P}_i$ and considering the condition in (3.27), the last inequality is equivalent to

$$\begin{bmatrix} \text{sym}\{A_i\bar{P}_i\} + \text{sym}\{B_iU_i(h)\} & & & \\ +\lambda_{ii}(h)\bar{P}_i & * & * & * \\ \bar{Q}A_{di}^{\mathrm{T}} & -(1-h_i)\bar{Q} & * & * \\ \sqrt{1+\eta(h)\bar{\tau}}\bar{P}_i & 0 & -\bar{Q} & * \\ \mathfrak{I}_i^{\mathrm{T}}\bar{P}_i & 0 & 0 & \mathfrak{P}_i \end{bmatrix} < 0.$$

By noting (3.27) and the above inequality, the condition in (3.5) is satisfied, so the system is proven to be mean square stochastically exponential stable.

Next, we will show that (3.25) is satisfied. Consider the following function

$$J(T) = \int_0^T \left[z(t)^{\mathrm{T}} z(t) - \gamma^2 \omega(t)^{\mathrm{T}} \omega(t)\right] dt.$$

It is obvious that (3.25) is equivalent to $\mathbb{E}\{J(T)\} < 0$, when $T \to \infty$.

$$\begin{aligned}
&\mathbb{E}\{J(T)\} \\
&= \int_0^T \left[z(t)^{\mathrm{T}} z(t) - \gamma^2 \omega(t)^{\mathrm{T}} \omega(t) + \tilde{A}V(x(t), i)\right] dt - \int_0^T \left[\tilde{A}V(x(t), i)\right] dt \\
&\leq \int_0^T \hat{x}(t)^{\mathrm{T}} \Xi \hat{x}(t) dt,
\end{aligned}$$

where

$$\begin{aligned}
\hat{x}(t) &= \begin{bmatrix} x(t)^{\mathrm{T}} & x(t - \tau(t, r_t)^{\mathrm{T}} & \omega(t)^{\mathrm{T}} \end{bmatrix}^{\mathrm{T}}, \\
\Xi &= \begin{bmatrix} \mathrm{sym}\{[A_i + B_i K(i,h)]\bar{P}_i\} + C_i^{\mathrm{T}} C_i & * & * \\ \bar{Q} A_{di}^{\mathrm{T}} & -(1 - h_i)\bar{Q} & * \\ B_i^{\mathrm{T}} \bar{P}_i & 0 & -\gamma^2 I \end{bmatrix}.
\end{aligned} \tag{3.33}$$

Pre- and post-multiplying (3.27) by the following transformation matrices $\mathcal{T}$ and $\mathcal{T}^{\mathrm{T}}$, where the dimension of $\mathcal{T}$ is $3n \times (N+3)n$.

$$\mathcal{T} = \begin{bmatrix} I & 0 & 0 & 0 & \mathbf{0}_{n,(N-1)n} \\ 0 & I & 0 & 0 & \mathbf{0}_{n,(N-1)n} \\ 0 & 0 & 0 & I & \mathbf{0}_{n,(N-1)n} \end{bmatrix},$$

where $I$ is an $n \times n$ identity matrix and $\mathbf{0}_{n,(N-1)n}$ is the zero matrix with dimension $n \times (N-1)n$, then we can show that $\Xi < 0$. Therefore, the $H_\infty$ noise attenuation level is achieved. This completes the proof. □

**Remark 3.1** By observing the condition in (3.27), the involvement of $\lambda_{ij}(h)$ and $\eta(h)$ jeopardizes the design procedure on solving the linear matrix inequalities. Generally, $\lambda_{ij}(h)$ and $\eta(h)$ are time-varying. As a result, solving the conditions in Proposition 1 and Theorem 3.1 involves testing infinitely many LMIs, which is numerically impos-

sible. This poses the main difficulties on the stochastic stability analysis and the controller design method. Normally, $\lambda_{ij}(h)$ is lower and upper bounded, i.e.,

$$\underline{\lambda}_{ij} \leq \lambda_{ij}(h) \leq \bar{\lambda}_{ij}, \text{ for all possible } h. \tag{3.34}$$

Therefore, $\eta(h)$ is bounded, i.e.,

$$\underline{\eta} \leq \eta(h) \leq \bar{\eta}. \tag{3.35}$$

Here, $\underline{\eta} = \min\left\{\bar{\lambda}_{ij}\right\}$ and $\bar{\eta} = \max\left\{\bar{\lambda}_{ij}\right\}$.

**Remark 3.2** In Proposition 1, the remaining parameters where the sojourn-time $h$ gets involved are $U_i(h)$, which are unknown matrices to be determined. Here, we seek to find uniform $U_i$ which are able to satisfy the infinite number of LMIs.

To overcome the numerical difficulties, we propose Corollary 3.1. Before proceeding, we present the following lemmas which will facilitate the derivation of Corollary 3.1.

**Lemma 3.1.** *Given symmetric matrix $A_{n\times n} = [a_{ij}]$, $a_{ij} \in \tilde{\Omega}_{ij} = [\underline{a}_{ij}, \bar{a}_{ij}]$, $i \neq j$, define the following sets: $\Omega_{ij} = \{\underline{a}_{ij}, \bar{a}_{ij}\}$. If for all possible*

$$\begin{aligned}&(a_{12}, \ldots, a_{1n}, a_{23}, \ldots, a_{2n}, \ldots, a_{i,i+1}, \ldots, a_{i,n}, \ldots, a_{n-1,n})\\ \in&\Omega_{12} \times \ldots \times \Omega_{1n} \times \Omega_{23} \times \ldots \times \Omega_{2n} \times \ldots \times \Omega_{i,i+1} \times \ldots \times \Omega_{i,n} \times \ldots \times \Omega_{n-1,n}\end{aligned} \tag{3.36}$$

*such that $A < 0$, then for all possible*

$$\begin{aligned}&(a_{12}, \ldots, a_{1n}, a_{23}, \ldots, a_{2n}, \ldots, a_{i,i+1}, \ldots, a_{i,n}, \ldots, a_{n-1,n})\\ \in&\tilde{\Omega}_{12} \times \ldots \times \tilde{\Omega}_{1n} \times \tilde{\Omega}_{23} \times \ldots \times \tilde{\Omega}_{2n} \times \ldots \times \tilde{\Omega}_{i,i+1} \times \ldots \times \tilde{\Omega}_{i,n} \times \ldots \times \tilde{\Omega}_{n-1,n}\end{aligned} \tag{3.37}$$

$A < 0$.

*Proof.* The lemma can be proved by using the inductive method.

**(1).** If there is only one pair of symmetric entries with uncertainty in $A_{n\times n}$, without loss of generality, $a_{ij} = a_{ji} \in [\underline{a}_{ij}, \bar{a}_{ij}]$, then from (3.36) we have, for $\forall x = [x_1, \ldots, x_i, \ldots, x_n]^{\mathrm{T}} \in \mathbb{R}^n$,

$$x^{\mathrm{T}} A(\underline{a}_{ij}) x < 0, \quad x^{\mathrm{T}} A(\bar{a}_{ij}) x < 0,$$

where $A(\underline{a}_{ij})$ and $A(\bar{a}_{ij})$ are matrices with $\underline{a}_{ij}$ and $\bar{a}_{ij}$ at the $(i,j)$ and $(j,i)$ entries. The last set of inequalities is equivalent to

$$2x_i\underline{a}_{ij}x_j + \alpha < 0, \tag{3.38}$$

$$2x_i\bar{a}_{ij}x_j + \alpha < 0, \tag{3.39}$$

where $\alpha$ is a constant. Conditioning on $\theta_1+\theta_2 = 1$ and $\theta_1 \geq 0$, $\theta_2 \geq 0$, and multiplying $\theta_1$ to (3.38) and $\theta_2$ to (3.39), the summation of the two inequalities yields (3.37).

**(2).** Suppose there are $p$ entries with uncertainties in $A$, and (3.37) is satisfied. Now, we introduce uncertainty to the $(p+1)^{\text{th}}$ entry $a_{rs}$ and $a_{sr}$. From (3.36) we have, for $\forall x \in \mathbb{R}^n$,

$$x^{\mathrm{T}}A(\underline{a}_{rs})x < 0, \quad x^{\mathrm{T}}A(\bar{a}_{rs})x < 0,$$

which is equivalent to

$$2x_i\underline{a}_{rs}x_j + \beta < 0, \quad 2x_i\bar{a}_{rs}x_j + \beta < 0.$$

Here, $\beta$ is independent of $a_{rs}$ ($a_{sr}$). Similar to the first step, (3.37) can be obtained. The proof of the lemma is now complete. □

**Lemma 3.2.** *Lemma 3.1 will still hold if $a_{ij} = a_{ji}$, and there exists a scalar $\theta$ such that*

$$\underline{a}_{ij} = \theta\bar{a}_{ij}.$$

*Proof.* By using the inductive method, and follow a similar technique in the proof of Lemma 3.1, Lemma 3.2 can be readily obtained. □

**Corollary 3.1.** *If there exist symmetric matrices $\bar{P}_i > 0$, $i \in \mathcal{S}$, $\bar{Q} > 0$, and matrices $U_i$, $i \in \mathcal{S}$, with appropriate dimensions such that the following matrix inequalities*

*hold for all* $i \in \mathcal{S}$, $\underline{\mathfrak{I}}_i^{(2)}$ *and* $\eta^{(2)}$

$$\begin{bmatrix} \mathrm{sym}\{A_i\bar{P}_i\} + \underline{\lambda}_{ii}\bar{P}_i \\ +\mathrm{sym}\{B_iU_i\} + C_i^{\mathrm{T}}C_i & * & * & * & * \\ \bar{Q}A_{di}^{\mathrm{T}} & (h_i-1)\bar{Q} & * & * & * \\ (1+\eta^{(2)}\bar{\tau})\bar{P}_i & 0 & -(1+\underline{\eta}\bar{\tau})\bar{Q} & * & * \\ B_i^{\mathrm{T}}\bar{P}_i & 0 & 0 & -\gamma^2 I & * \\ \mathfrak{I}_i^{(2)\mathrm{T}}\bar{P}_i & 0 & 0 & 0 & \underline{\mathfrak{P}}_i^{(2)} \end{bmatrix} < 0, \quad (3.40)$$

*where*

$$\mathfrak{I}_i^{(2)} \in (\Gamma_{i1} \ \ldots \ \Gamma_{i,i-1} \ \Gamma_{i,i+1} \ \ldots \ \Gamma_{i,N}), \quad \Gamma_{ij} = \left\{\underline{\lambda}_{ij}I, \ \bar{\lambda}_{ij}I\right\}, \quad \eta^{(2)} \in \left\{\underline{\eta}, \ \bar{\eta}\right\},$$
$$\underline{\mathfrak{P}}_i^{(2)} = \mathrm{diag}\left\{\underline{\mathfrak{I}}_i^{(2)}\right\}\mathfrak{P}_i, \quad \underline{\mathfrak{I}}_i^{(2)} = \left[\underline{\lambda}_{i1}I, \ldots, \underline{\lambda}_{i,i-1}I, \underline{\lambda}_{i,i+1}I, \ldots, \underline{\lambda}_{iN}I\right]$$

*and* $\mathfrak{P}_i$ *is given in (3.28). Then the closed-loop system in (3.23) is mean square stochastically exponential stable with* $\gamma$*-disturbance attenuation level, i.e.,* $\|z\|_{E_2}/\|\omega\|_2 < \gamma$.

*Proof.* To prove this corollary, we firstly define the following congruent transformation matrix $\mathcal{J} = \mathrm{diag}\{I, \ I, \sqrt{1+\eta(h)\bar{\tau}}I, I, \mathrm{diag}(\mathfrak{I}_i(h))\}$. After making congruent transformation by using $\mathcal{J}$ on inequality (3.27), we have

$$\begin{bmatrix} \mathrm{sym}\{A_i\bar{P}_i\} + \lambda_{ii}(h)\bar{P}_i \\ +\mathrm{sym}\{B_iU_i\} + C_i^{\mathrm{T}}C_i & * & * & * & * \\ \bar{Q}A_{di}^{\mathrm{T}} & (h_i-1)\bar{Q} & * & * & * \\ (1+\eta(h)\bar{\tau})\bar{P}_i & 0 & -(1+\eta(h)\bar{\tau})\bar{Q} & * & * \\ B_i^{\mathrm{T}}\bar{P}_i & 0 & 0 & -\gamma^2 I & * \\ \mathfrak{I}_i^{(2)}(h)^{\mathrm{T}}\bar{P}_i & 0 & 0 & 0 & \mathfrak{P}_i^{(2)}(h) \end{bmatrix} < 0, \quad (3.41)$$

where,

$$\mathfrak{I}_i^{(2)}(h) = [\lambda_{i1}(h)I, \cdots, \lambda_{i,i-1}(h)I, \ \lambda_{i,i+1}(h)I, \ \cdots, \lambda_{iN}(h)I],$$
$$\mathfrak{P}_i^{(2)}(h) = \mathrm{diag}\left\{\mathfrak{I}_i^{(2)}(h)\right\}\mathfrak{P}_i.$$

Denote $A_{\mathrm{left}}$ as the left hand side of (3.41). Define the lower and upper bounds of $\eta(h)$ and $\lambda_{ij}(h)$ $(i \neq j)$ by $\underline{\eta}$, $\bar{\eta}$, $\underline{\lambda}_{ij}$ $(i \neq j)$, and $\bar{\lambda}_{ij}$ $(i \neq j)$, respectively, and further

define $\underline{\lambda}_{ii} = \sum_{j=1,j\neq i}^{N} \underline{\lambda}_{ij}$ $(i \in \mathcal{S})$, so we have the following fact

$$A_{\text{left}} < \begin{bmatrix} \text{sym}\{A_i\bar{P}_i\} + \underline{\lambda}_{ii}\bar{P}_i & * & * & * & * \\ +\text{sym}\{B_iU_i\} + C_i^{\mathrm{T}}C_i & & & & \\ \bar{Q}A_{di}^{\mathrm{T}} & (h_i-1)\bar{Q} & * & * & * \\ (1+\eta(h)\bar{\tau})\bar{P}_i & 0 & -(1+\underline{\eta}\bar{\tau})\bar{Q} & * & * \\ B_i^{\mathrm{T}}\bar{P}_i & 0 & 0 & -\gamma^2 I & * \\ \mathfrak{I}_i^{(2)}(h)^{\mathrm{T}}\bar{P}_i & 0 & 0 & 0 & \underline{\mathfrak{P}}_i^{(2)} \end{bmatrix}.$$

By using Lemma 3.2, then the condition in (3.40) is readily obtained. This completes the proof. □

### 3.3.3 Conservativeness Reduction

It is worth noting that the condition in Corollary 3.1 is conservative due to the fact that the common variables $\bar{P}_i$, $U_i$, and $\bar{Q}$ are able to satisfy infinitely many LMIs shown in Theorem 3.1. The idea of reducing the conservativeness is to solve the feasibility by introducing more sets of design variables, instead of using one set of matrices of $\bar{P}_i$, $U_i$, and $\bar{Q}$ [88]. By partitioning the range of the sojourn-time $h$, the transition rate $\lambda_{ij}(h)$ and $\eta(h)$ can be grouped into different intervals, which are termed as partitions. The following corollary demonstrates how the partitions can be utilized to reduce the conservativeness on the $H_\infty$ controller design by partitioning on the sojourn-time $h$ into $M$ partitions.

**Corollary 3.2.** *In each partition $m$, if there exist symmetric matrices $\bar{P}_{i,m} > 0$, $i \in \mathcal{S}$, $\bar{Q}_m > 0$, and matrices $U_{i,m}$ with appropriate dimensions such that the following matrix inequalities hold for all $i \in \mathcal{S}$ and $m \in \mathcal{M} = \{1, 2, \ldots, M\}$*

$$\begin{bmatrix} \text{sym}\{A_i\bar{P}_{i,m}\} + \underline{\lambda}_{ii,m}\bar{P}_{i,m} & * & * & * & * \\ +\text{sym}\{B_iU_{i,m}\} + C_i^{\mathrm{T}}C_i & & & & \\ \bar{Q}_m A_{di}^{\mathrm{T}} & (h_i-1)\bar{Q}_m & * & * & * \\ (1+\eta_m^{(2)}\bar{\tau})\bar{P}_{i,m} & 0 & -(1+\underline{\eta}_m\bar{\tau})\bar{Q}_m & * & * \\ B_i^{\mathrm{T}}\bar{P}_{i,m} & 0 & 0 & -\gamma^2 I & * \\ \mathfrak{I}_{i,m}^{(2)\mathrm{T}}\bar{P}_{i,m} & 0 & 0 & 0 & \underline{\mathfrak{P}}_{i,m}^{(2)} \end{bmatrix} < 0, \tag{3.42}$$

*where*

$$\begin{aligned}
\mathfrak{I}_{i,m}^{(2)} &\in (\Gamma_{i1,m} \ \dots \ \Gamma_{i,i-1,m} \ \Gamma_{i,i+1,m} \ \dots \ \Gamma_{i,N,m}), \quad \Gamma_{ij,m} = \left\{\underline{\lambda}_{ij,m} I, \ \bar{\lambda}_{ij,m} I\right\}, \\
\eta_m^{(2)} &\in \left\{\underline{\eta}_m, \ \bar{\eta}_m\right\}, \quad \mathfrak{P}_{i,m} = -\mathrm{diag}\{\bar{P}_{i1,m}, \dots, \bar{P}_{i,i-1,m}, \bar{P}_{i,i+1,m}, \dots, \bar{P}_{iN,m}\}, \\
\underline{\mathfrak{P}}_{i,m}^{(2)} &= \mathrm{diag}\left\{\underline{\mathfrak{I}}_{i,m}^{(2)}\right\} \mathfrak{P}_{i,m}, \quad \underline{\mathfrak{I}}_{i,m}^{(2)} = \left[\underline{\lambda}_{i1,m}, \dots, \underline{\lambda}_{i,i-1,m}, \underline{\lambda}_{i,i+1,m}, \dots, \underline{\lambda}_{iN,m}\right].
\end{aligned}$$

*Then the closed-loop system $\mathfrak{G}_c$ in (3.23) is mean square stochastically exponential stable with $\gamma$-disturbance attenuation level.*

*Proof.* The proof of Corollary 3.2 is similar to Corollary 3.1 and hence omitted here. □

## 3.4 Numerical Example

In this chapter, we consider a vertical take-off and landing (VTOL) vehicle example [102, 103]. The system dynamics can be written as

$$\begin{aligned}
\dot{x}(t) =& A(r_t)x(t) + A_d(r_t)x(t - \tau(t, r_t)) + B(r_t)u(t) + B(r_t)\omega(t), \\
z(t) =& C(r_t)x(t),
\end{aligned}$$

where

$$A(r_t) = \begin{bmatrix} -0.0366 & 0.0271 & 0.0188 & -0.4555 \\ 0.0482 & -1.01 & 0.0024 & -4.0208 \\ 0.1002 & a_{32}(r_t) & -0.707 & a_{34}(r_t) \\ 0 & 0 & 1 & 0 \end{bmatrix}, B(r_t) = \begin{bmatrix} 0.4422 & 0.1761 \\ b_{21}(r_t) & -7.5922 \\ -5.5200 & 4.4900 \\ 0 & 0 \end{bmatrix},$$

$$A_d(r_t) = 0.1A(r_t), \quad C(r_t) \equiv \begin{bmatrix} 0 & 0.1 & 0 & 0 \end{bmatrix}.$$

$x(t)$ indicates the state variables, where $x_1(t)$ is the horizontal velocity, $x_2(t)$ is the vertical velocity, $x_3(t)$ is the pitch rate, and $x_4(t)$ is the pitch angle.

For the simulation purpose, the maximum delay $\bar{\tau}$ is set as 0.3s. $h_1$, $h_2$, and $h_3$ in (3.2) are set as 0.5, 0.6, and 0.3, respectively. The time-varying delay $\tau(r_t)$ are characterized by

$$\tau(t, i) = 0.5\bar{\tau}\left[\sin\left(\frac{2h_i t}{\bar{\tau}}\right) + 1\right], t \geq 0. \tag{3.43}$$

Table 3.1: VTOL parameters depending on the speed.

| Airspeed (knot) | $a_{32}$ | $a_{34}$ | $b_{21}$ |
|---|---|---|---|
| 135 | 0.3681 | 1.4200 | 3.5446 |
| 60 | 0.0664 | 0.1198 | 0.9775 |
| 170 | 0.5047 | 2.5460 | 5.1120 |

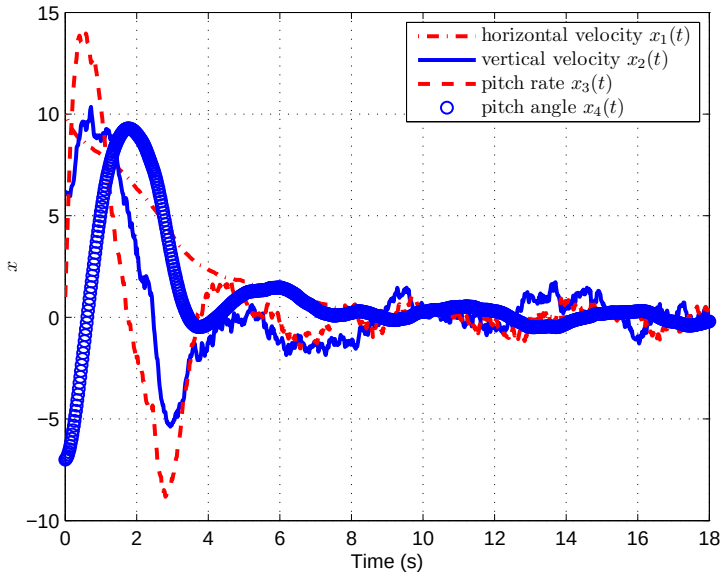


Figure 3.2: The state trajectories of the closed-loop S-MJLS using the proposed controller in (3.27).

The external disturbance is $\omega(t) = [\omega_1(t)\ \omega_2(t)]^{\mathrm{T}}$, where $\omega_1(t)$ and $\omega_2(t)$ are zero mean, uncorrelated Gaussian white noise with unity variances.

The system dynamics depends on the airspeeds, which are characterized by the modes of the governing semi-Markov process. The dependant parameters are listed in table 3.1. Without any control input, the unforced VTOL system is unstable. By using Corollary 3.2, and setting two partitions, i.e., $M = 2$, for the sojourn-time. When $h \leq 1.8$s, the S-MJLS is in partition 1, otherwise, it is running in partition 2. For each partition, the lower and upper bounds of transition rates are

$$\underline{\Lambda}_1 = \underline{\lambda}_{ij,1} = \begin{bmatrix} -0.3 & 0.1 & 0.2 \\ 0.2 & -0.5 & 0.3 \\ 0.3 & 0.3 & -0.6 \end{bmatrix}, \quad \bar{\Lambda}_1 = \bar{\lambda}_{ij,1} = \begin{bmatrix} -1.2 & 0.5 & 0.7 \\ 0.7 & -1.7 & 1.0 \\ 1.0 & 1.1 & -2.1 \end{bmatrix},$$

$$\underline{\Lambda}_2 = \underline{\lambda}_{ij,2} = \begin{bmatrix} -1.2 & 0.5 & 0.7 \\ 0.7 & -1.7 & 1.0 \\ 1.0 & 1.1 & -2.1 \end{bmatrix}, \quad \bar{\Lambda}_2 = \bar{\lambda}_{ij,2} = \begin{bmatrix} -2.0 & 0.8 & 1.2 \\ 0.9 & -2.4 & 1.5 \\ 1.8 & 2.2 & -4.0 \end{bmatrix}.$$

The designed mode and sojourn-time dependent state feedback controller is

$$K(1,1) = \begin{bmatrix} -1.3653 & -0.5117 & 0.4511 & 2.6099 \\ -0.4102 & -0.0651 & -0.0271 & 0.2903 \end{bmatrix},$$
$$K(2,1) = \begin{bmatrix} -1.3254 & -0.4512 & 0.4183 & 2.4012 \\ 0.1892 & 0.1996 & -0.1840 & -0.8173 \end{bmatrix},$$
$$K(3,1) = \begin{bmatrix} -1.2800 & -0.4908 & 0.5168 & 2.6215 \\ -0.4687 & -0.0820 & 0.0778 & 0.5266 \end{bmatrix},$$
$$K(1,2) = \begin{bmatrix} -2.7621 & -0.6190 & 0.5728 & 3.4891 \\ -0.8064 & -0.0701 & 0.0010 & 0.4413 \end{bmatrix},$$
$$K(2,2) = \begin{bmatrix} -2.6281 & -0.5833 & 0.5576 & 3.2410 \\ 1.4161 & 0.5205 & -0.3996 & -2.3219 \end{bmatrix},$$
$$K(3,2) = \begin{bmatrix} -2.9429 & -0.6438 & 0.6372 & 3.6782 \\ -0.6803 & 0.0019 & 0.0156 & 0.2481 \end{bmatrix}.$$

In the numerical analysis, the initial state of the simulation is $x(0) = [10 \;\; 6 \;\; 1 \;\; -7]^{\mathrm{T}}$. In Figure 3.2, all state variables of the helicopter are stabilized, i.e., the hover of the helicopter is achieved. Nevertheless, $x(t)$ does not converge to 0 due to the persistent external disturbance $\omega(t)$. In this example, the state variable of interest is the vertical velocity, i.e., $x_2(t)$. As can be seen from Figure 3.2, the magnitude of the vertical velocity is attenuated from 6m/s to less than 1m/s under disturbance and system delays. In the controller design, the $H_\infty$ attenuation level is set as $\gamma = 0.93$ and from the simulation results, $\|z\|_{E_2}/\|\omega\|_2 = 0.2320 < \gamma$.

## 3.5 Conclusion

The stochastic stability analysis and $H_\infty$ control design problem for a class of continuous-time S-MJLSs with time-varying delays are investigated in this chapter. The considered time-varying transition rates are more general and practicable than MJLSs. With the designed mode and sojourn-time dependent state feedback controller, the

closed-loop system is stochastically stable with prescribed disturbance attenuation level. It is worth expecting that the idea of sojourn-time partition for the S-MJLS in this chapter could be utilized to solve related problems for delayed S-MJLSs, e.g. $H_\infty$ output control, optimal dynamic controller design, and robust filtering. In real world scenarios, it is a challenging task to obtain exact transition rate matrices of stochastic processes, so the study on the S-MJLS with uncertain transition rates deserves further research and will greatly facilitate the applicability.

# Chapter 4

# Active Fault Tolerant Control Systems by the Semi-Markov Model Approach

## 4.1 Introduction

The fault detection and fault tolerant control problems have received increasing attention due to their broad applicability [104]. In order to achieve a higher reliability level and better control performance, modern control systems relying on sophisticated control algorithms have been developed to meet these critical requirements [105]. The designed fault tolerant control systems can achieve the system stability and maintain the acceptable control performance, even when they are subject to failure events. Generally speaking, fault tolerant control strategies can be categorized into two main categories: Passive control and active control [106]. In passive fault tolerant control systems, no reconfiguration of the controller is needed, so essentially it has limited fault tolerant capacities. On the contrary, active fault tolerant control configuration reacts to the system failure actively by adjusting control actions to achieve the stability and required performance of the closed-loop system [107]. Besides the classification of the control schemes, the system faults can also be classified into several groups, such as actuator faults, sensor faults, component faults, and a combination of the above [108]. In this chapter, we seek to design an active control method to accommodate a combination of the above faults.

Active fault tolerant control systems are feedback control systems that reconfigure

the control law in real time. The abrupt occurrence of faults in the system can be practically characterized as being governed by stochastic processes. The class of systems governed by stochastic processes is termed as the jump linear system [70]. In this class of systems, a stochastic process is defined to represent the random variations of the system parameters. Normally, continuous-time finite state Markov processes are used in continuous-time systems where the system may jump at any time instant; while in discrete-time systems, discrete-time finite state Markov processes are applied; to be precise, only Markov process kernels are used. Sometimes, finite state processes are also called discrete-state processes, or countable state processes. To practically formulate active fault tolerant control problems, two stochastic processes are involved in the system model: One is used to model the system faults, and the other one is used to represent the fault detection and identification (FDI) process [109]. The rationale behind the two-process model is that the FDI process brings random variations into the control law. In other words, the FDI process modifies the system dynamics by the control strategy reconfiguration [110]. The two-process model was proposed in [111], where necessary and sufficient conditions were provided for systems with single component failures. For the system with multiple failure occurrences, the stochastic stability analysis was presented in [112]. Further, considering the system uncertainties, detection delays, and noise/disturbances, results have been reported in [113]. Besides the results on the stability issue, optimal controller design problems have been studied for fault tolerant control systems modeled by Markov processes; see [114] and the references therein.

For all the aforementioned work, most of them deploys continuous-time or discrete-time Markov processes to model the system failure. To satisfy the requirements of Markov processes, the life time of the system components should be assumed to be exponentially distributed. However, such an assumption may not be appropriate in practice for two reasons. Firstly, in the reliability engineering, a typical transition/failure rate function is in a bathtub shape instead of a constant value [75, 76]. With such shapes of transition/failure rates, the system components would be more likely to fail in the "infant" or "senior" stages. For a more comprehensive literature review on time-varying and even random transition rates; see [115] and the references therein. In this chapter, for simplicity, we adopt the terminology "transition rate" from switching system theory, and it is mathematically equivalent to the "failure rate" in the reliability engineering. Secondly, suppose that the continuous-time probability distribution function (PDF) is an exponential distribution, i.e., the transition

rates are constant, which is a widely used assumption in reliability engineering [116]. Since the redundancy design finds wide applications in practice, for example, in the fly-by-wire aircraft system design [117, 118], the overall life time probability distribution function will not be exponential (red and blue curves in Figure 4.1) and the corresponding transition rates are not constant values (red and blue curves in Figure 4.2). Therefore, in this chapter, we investigate the fault tolerant control system

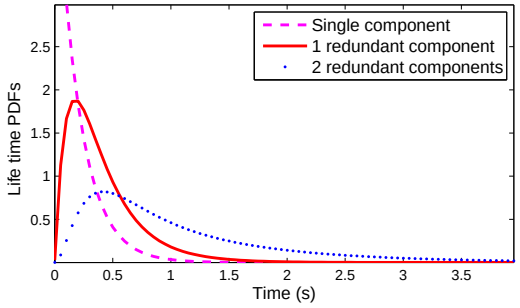


Figure 4.1: Life time PDFs with different number of redundant components.

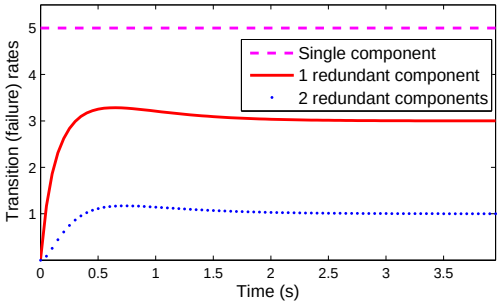


Figure 4.2: Transition rates with different number of redundant components.

where the life time of the components is not necessarily exponentially distributed. Therefore, the semi-Markov process is more appropriate for modeling the random changes/jumps in the system. Some related results have been reported; for example, in [119], a continuous-time countable (discrete) state semi-Markov process was used to characterize the failure phenomenon of an object. In the field of jump linear system research, semi-Markov processes have been deployed and studied [2, 78, 88, 120].

The remainder of this chapter is organized as follows. In Section 4.2, we formulate the fault detection problem by using semi-Markov processes. Next, we present the main results for the stochastic stability analysis and the controller design technique for the formulated fault tolerant control system in Section 4.3. In Section 4.4, a vertical take-off and landing (VTOL) vehicle simulation example is presented. Finally, we conclude this chapter in Section 4.5.

## 4.2 Problem Formulation

In this chapter, we consider the linear systems, where both system faults and active fault tolerant control strategies are simultaneously governed by independent semi-

Markov processes. The system model is given as follows:

$$\begin{aligned}\dot{x}(t) =& A(\eta_t)x(t) + B(\eta_t)u(r_t, t) + E(\eta_t)\omega(t),\\ y(t) =& C(\eta_t)x(t),\end{aligned} \tag{4.1}$$

where $x(t) \in \mathbb{R}^n$ is the state; $y(t) \in \mathbb{R}^{n_p}$ is the system output; $u(r_t, t) \in \mathbb{R}^{n_u}$ is the control input; and $\omega(t) \in \mathbb{R}^{n_\omega}$ is the external disturbance. $A(\eta_t)$, $B(\eta_t)$, $C(\eta_t)$, and $E(\eta_t)$ are system matrices of compatible dimensions. $\eta_t$ and $r_t$ are semi-Markov processes which will be addressed in the following context. For the convenience of notations, $A(\eta_t)$ is denoted as $A_i$, when $\eta_t = i$; and similar notations are applied to $B(\eta_t)$, $C(\eta_t)$, and $E(\eta_t)$. Also, $x(t)$, $y(t)$, and $\omega(t)$ are written as $x_t$, $y_t$, and $\omega_t$, respectively.

**Remark 4.1** System faults are represented by system matrices. For example, in the normal working condition, system matrices are $A_1$, $B_1$, $C_1$, and $E_1$. If, for example, one sensor works improperly, then the elements in $C(\eta_t)$ may vary, or even be set to 0 in the total failure case. In such a fault scenario, the operating system matrices would be $A_2(= A_1)$, $B_2(= B_1)$, $C_2(\neq C_1)$, and $E_2(= E_1)$. Another often encountered fault is the so-called actuation fault. Under such circumstances, the operating system matrices are $A_3(= A_1)$, $B_3(\neq B_1)$, $C_3(= C_1)$, and $E_3(= E_1)$. Similarly, by tuning $E(\eta_t)$ the faults caused by the external disturbance can be appropriately modeled. Therefore, the switching system model can accommodate different types of fault scenarios.

Let $\{r_t,\ t \geq 0\}$ denote the FDI process; it monitors the state of $\{\eta_t,\ t \geq 0\}$ which describes the failures [110]. The FDI process induces random switchings to the control actions, therefore the closed-loop system dynamics will accordingly vary along time through the control reconfiguration when the controller is used to close the open-loop system. Here, we assume that $r_t$ and $\eta_t$ are continuous-time discrete-state semi-Markov processes, which take values in the finite sets $\mathcal{S}_r = \{1, 2, \ldots, \bar{r}\}$ and $\mathcal{S}_\eta = \{1, 2, \ldots, \bar{\eta}\}$, respectively. "Continuous-time" indicates that the system could switch from one state to another at any time; "discrete-state" means that the sets $\mathcal{S}_r$ and $\mathcal{S}_\eta$ are discrete sets. It is realistic since a component could fail at any time during the operation in the continuous-time system configuration. Therefore, the system description depends on the true failure state $\eta_t$; meanwhile, the input signal $u$ depends on the control strategy after detecting and identifying the system failure.

For the semi-Markov failure process $\eta_t$, the time-varying transition rate is given by

$$\Pr\{\eta(t+h)=j|\eta(t)=i\}=\begin{cases}\lambda_{ij}(h)h+o(h), & \eta(t) \text{ jumps from } i \text{ to } j,\\ 1+\lambda_{ii}(h)h+o(h), & \text{otherwise.}\end{cases}$$

Here, $\lambda_{ii}(h)=-\sum_{j=1,j\neq i}^{\mathcal{S}_\eta}\lambda_{ij}(h)$. $\lambda_{ij}(h)$ is directly related with system component failure rates. $o(h)$ is the little-$o$ notation defined by $\lim_{h\to 0} o(h)/h=0$.

Because $r_t$ is the decision and control process, the transition rate intuitively depends on $\eta_t$, and is defined as

$$\Pr\{r(t+h)=l|r(t)=k,\eta(t)=i\}=\begin{cases}\pi_{kl}^{(i)}(h)h+o(h), & r(t) \text{ jumps from } k \text{ to } l,\\ 1+\pi_{kk}^{(i)}(h)h+o(h), & \text{otherwise,}\end{cases}$$

when the system is operating on mode $i$, i.e., $\eta_t=i$. Here, $\pi_{kk}^{(i)}(h)=-\sum_{l=1,l\neq k}^{\mathcal{S}_r}\pi_{kl}^{(i)}(h)$. The transition rate matrices are defined as $\Lambda(h)=[\lambda_{ij}(h)]$ and $\Pi^{(i)}(h)=[\pi_{ij}^{(i)}(h)]$, respectively. In this chapter, we assume that the transition rates are all upper and lower bounded [121]. In the case when the FDI process is difficult to examine, a simplified version of the semi-Markov process, i.e., a Markov process could be implemented in the controller. By using the Markov process, the controller loses the time-varying transition rate information in computing control signals. In order to obtain the transition rates, an experimental test of the system should be conducted before determining the transition rate matrix. Xie *et al.* stated two approaches to determine the parameters of transition rates: 1) conventional statistical estimation techniques and 2) graphical approaches [76]. When the parameter number of the stochastic process is small, the conventional statistical estimation method is suggested; while the graphical technical is preferred when the parameter number increases.

**Remark 4.2** The *sojourn-time* is an important concept in this chapter. In the jump linear system, the duration $h$ between two consecutive jumps is termed as sojourn-time which is usually a random variable. For example, in the continuous-time jump linear system, $h$ is a random variable characterized by a continuous probability distribution $F$. Especially, in the continuous-time Markov jump linear systems, $F$ is an exponential distribution. However, in the current semi-Markov framework, $F$ can be any continuous probability distribution, rendering the corresponding description being more general and practical. Therefore, the Markov jump linear system approach

for dealing with active fault tolerant control problems can be regarded as a special case of the proposed method in this chapter.

**Remark 4.3** It is noticed that the memoryless property, being one of the key properties in the Markov process, does not hold for the semi-Markov process. According to the stochastic process theory, in the Markov process the transition rate does not depend on the past, i.e., $\Pr\{\eta(t+h)=j|\eta(t)=i\}=\Pr\{\eta(h)=j|\eta(0)=i\}$ [72]. But in our current design framework, with a non-exponential sojourn-time distribution, the above equality does not hold any more, which inherently leads to some challenges in the following design procedure.

The main objective of this chapter is to design the state feedback controller $u_t = K(r_t,h)x_t$, under any possible type of faults stated in Remark 4.1, such that the following closed-loop system

$$\dot{x}_t = A_c(\eta_t, r_t)x_t \tag{4.2}$$

is stochastically stable, when there is no external disturbance i.e., $\omega_t \equiv 0$; also, the prescribed $H_\infty$ performance should be simultaneously guaranteed. Here,

$$A_c(\eta_t, r_t) = A(\eta_t) + B(\eta_t)K(r_t,h). \tag{4.3}$$

When $\eta_t = i$ and $r_t = k$, $A_c(\eta_t, r_t)$ is denoted as $A_{c,ik}$. We now recall the stochastic stability definition established in [53] for the stochastic closed-loop system with semi-Markov jumps.

**Definition 4.1.** *The system in (4.2) is stochastically stable if for all possible initial conditions $x_0 = x(0) \in \mathbb{R}^n$, and initial modes $\eta_0 = \eta(0) \in \mathcal{S}_\eta$ and $r_0 = r(0) \in \mathcal{S}_r$, there exists a finite matrix $W > 0$ such that the following inequality holds*

$$\mathbb{E}\left\{\int_0^\infty \|x_t\|^2 dt \middle| x_0, \eta_0, r_0\right\} \le x_0^{\mathrm{T}} W x_0. \tag{4.4}$$

The $H_\infty$ control performance is defined as follows: Given a scalar $\gamma > 0$, with the proposed state feedback controller $K$, it is expected that the closed-loop system is stochastically stable and the following condition holds for any non-zero $\omega_t \in l_2[0,\ \infty)$

$$\mathbb{E}\left\{\int_0^\infty y_t^{\mathrm{T}} y_t dt\right\} < \gamma^2 \int_0^\infty \omega_t^{\mathrm{T}} \omega_t dt. \tag{4.5}$$

For the sake of a more general setup and wider applications, we adopt the stochastic integral quadratic constraint (SIQC) [122].

**Definition 4.2.** *The SIQC for the output signal $y_t$ and the disturbance $\omega_t$ is satisfied if the following inequality holds*

$$\mathbb{E}\left\{\int_0^T \begin{bmatrix} y_t^{\mathrm{T}} & \omega_t^{\mathrm{T}} \end{bmatrix} \begin{bmatrix} \Gamma_{11} & \Gamma_{12} \\ \Gamma_{21} & \Gamma_{22} \end{bmatrix} \begin{bmatrix} y_t \\ \omega_t \end{bmatrix} dt\right\} < 0, \tag{4.6}$$

*where, $\Gamma_{11}$ is symmetric and positive definite, and $\Gamma_{22}$ is symmetric and negative definite. Moreover, it is assumed that $\Gamma_{12} = \Gamma_{21}^{\mathrm{T}}$, and the time $T$ is finite.*

**Remark 4.4** The four involved matrices in the SIQC are supposed to have compatible dimensions. By tuning these matrices, different control performance can be achieved by using the correspondingly proposed controller. For example, if $\Gamma_{11} = I$ and $\Gamma_{22} = -\gamma^2 I$, then the SIQC constraint reduces to the standard $H_\infty$ performance. Therefore, in this chapter, the control design technique is more general than the conventional $H_\infty$ control method.

Before presenting the main results, the following fact to be frequently referred to in the following derivation, is presented as follows.

**Fact 1.** *For matrix $A = A^{\mathrm{T}}$, which can be partitioned as $A = \begin{bmatrix} A_{11} & A_{12} \\ A_{21} & A_{22} \end{bmatrix}$, if there exist a matrix $P = P^{\mathrm{T}} > 0$, and a scalar $\alpha > 0$ such that $\begin{bmatrix} A_{11} & A_{12} \\ A_{21} & A_{22} + \alpha P \end{bmatrix} < 0$, then $A < 0$.*

## 4.3 Main Results

The stabilization problem and the $H_\infty$ control problem are addressed in this section. First of all, we deal with the stochastic stability problem in Section 4.3.1. The following theorem provides the sufficient conditions such that the system in (4.1) with $\omega_t \equiv 0$ achieves the conditions in Definition 4.1. The proof follows a similar line of the proof in [110], but considers the more general model using semi-Markov process model.

### 4.3.1 Stochastic Stability

**Theorem 4.1.** *The closed-loop system in (4.2) is stochastically stable if there exist a set of matrices $X_{ik} > 0$ and $R_{ik}$, for all $i \in \mathcal{S}_\eta$ and $k \in \mathcal{S}_r$, such that*

$$\begin{bmatrix} A_iX_{ik} + X_{ik}A_i^{\mathrm{T}} + B_iR_{ik} + R_{ik}^{\mathrm{T}}B_i^{\mathrm{T}} & * & * \\ +\lambda_{ii}(h)X_{ik} + \pi_{kk}^{(i)}(h)X_{ik} & & \\ \mathbf{1}_{\bar{\eta}-1,1} \otimes X_{ik} & -\Xi_{ik}(h) & * \\ \mathbf{1}_{\bar{r}-1,1} \otimes X_{ik} & 0 & -\Omega_{ik}^{(i)}(h) \end{bmatrix} < 0, \tag{4.7}$$

*where*

$$\Xi_{ik}(h) = \mathrm{diag}\left\{ \frac{1}{\lambda_{i1}(h)}X_{1k}, \ldots, \frac{1}{\lambda_{i,i-1}(h)}X_{i-1,k}, \frac{1}{\lambda_{i,i+1}(h)}X_{i+1,k}, \ldots, \frac{1}{\lambda_{i\bar{\eta}}(h)}X_{\bar{\eta}k} \right\}, \tag{4.8}$$

$$\Omega_{ik}^{(i)}(h) = \mathrm{diag}\left\{ \frac{1}{\pi_{k1}^{(i)}(h)}X_{i1}, \ldots, \frac{1}{\pi_{k,k-1}^{(i)}(h)}X_{i,k-1}, \frac{1}{\pi_{k,k+1}^{(i)}(h)}X_{i,k+1}, \ldots, \frac{1}{\pi_{k\bar{r}}^{(i)}(h)}X_{i\bar{r}} \right\}. \tag{4.9}$$

*Proof.* When the closed-loop system operates on modes $(i, k)$, i.e., $\eta_t = i$ and $r_t = k$ at $t$, consider the following Lyapunov functional candidate

$$V(x_t, \eta_t, r_t) = x_t^{\mathrm{T}} P_{ik} x_t. \tag{4.10}$$

Here, $P_{ik} > 0$, therefore $V(x_t, \eta_t, r_t) > 0$, for all $x_t \neq 0$. The infinitesimal generator $\tilde{A}$ of the Lyapunov function is

$$\tilde{A}V = \lim_{\Delta \to 0} \frac{1}{\Delta} \left[ \mathbb{E}\{V(x_{t+\Delta}, \eta_{t+\Delta}, r_{t+\Delta}) | x_t, \eta_t, r_t\} - V(x_t, \eta_t, r_t) \right] \tag{4.11}$$

$$= \lim_{\Delta \to 0} \frac{1}{\Delta} \left[ \mathbb{E}\{x_{t+\Delta}^{\mathrm{T}} P_{ik} x_{t+\Delta} | x_t, \eta_t, r_t\} - x_t^{\mathrm{T}} P_{ik} x_t \right], \tag{4.12}$$

where $\Delta > 0$ is a small positive number. The $1^{\mathrm{st}}$ order expansion of $x_{t+\Delta}$ is

$$x_{t+\Delta} = \left[ A_i\Delta + B_iK(k,h)\Delta + I \right] x_t + o(\Delta^2) \approx \left[ A_i\Delta + B_iK(k,h)\Delta + I \right] x_t.$$

Given that $\Delta$ is small, we have

$$\begin{aligned}\tilde{A}V =& 2\dot{x}_t^{\mathrm{T}}\frac{\partial V}{\partial x_t} + \sum_{j=1}^{\bar{\eta}}\lambda_{ij}(h)V(x,j,k) + \sum_{l=1}^{\bar{r}}\pi_{kl}^{(i)}(h)V(x,i,l)\\ =& x_t^{\mathrm{T}}\left[P_{ik}A_{c,ik} + A_{c,ik}^{\mathrm{T}}P_{ik}\right]x_t + \sum_{j=1}^{\bar{\eta}}\lambda_{ij}(h)x_t^{\mathrm{T}}P_{jk}x_t + \sum_{l=1}^{\bar{r}}\pi_{kl}^{(i)}(h)x_t^{\mathrm{T}}P_{il}x_t\\ =& x_t^{\mathrm{T}}\left[P_{ik}A_{c,ik} + A_{c,ik}^{\mathrm{T}}P_{ik} + \sum_{j=1}^{\bar{\eta}}\lambda_{ij}(h)P_{jk} + \sum_{l=1}^{\bar{r}}\pi_{kl}^{(i)}(h)P_{il}\right]x_t. \end{aligned} \tag{4.13}$$

Therefore, from the property of the quadratic form, if the following inequality holds, then the system is stochastically stable

$$P_{ik}A_{c,ik} + A_{c,ik}^{\mathrm{T}}P_{ik} + \sum_{j=1}^{\bar{\eta}}\lambda_{ij}(h)P_{jk} + \sum_{l=1}^{\bar{r}}\pi_{kl}^{(i)}(h)P_{il} < 0. \tag{4.14}$$

To facilitate the following derivation, further define $X_{ik} = P_{ik}^{-1}$, then pre- and post-multiply the last inequality by $X_{ik}$; we have

$$\begin{aligned}&A_{c,ik}X_{ik} + X_{ik}A_{c,ik}^{\mathrm{T}} + X_{ik}\left[\sum_{j=1}^{\bar{\eta}}\lambda_{ij}(h)P_{jk} + \sum_{l=1}^{\bar{r}}\pi_{kl}^{(i)}(h)P_{il}\right]X_{ik} =\\ &A_{c,ik}X_{ik} + X_{ik}A_{c,ik}^{\mathrm{T}} + \sum_{j=1}^{\bar{\eta}}\lambda_{ij}(h)X_{ik}P_{jk}X_{ik} + \sum_{l=1}^{\bar{r}}\pi_{kl}^{(i)}(h)X_{ik}P_{il}X_{ik} < 0. \end{aligned} \tag{4.15}$$

By applying the Schur complement, the last inequality becomes

$$\begin{bmatrix} A_{c,ik}X_{ik} + X_{ik}A_{c,ik}^{\mathrm{T}} & * & * \\ +\lambda_{ii}(h)X_{ik} + \pi_{kk}^{(i)}(h)X_{ik} & & \\ \mathbf{1}_{\bar{\eta}-1,1}\otimes X_{ik} & -\Xi_{ik}(h) & * \\ \mathbf{1}_{\bar{r}-1,1}\otimes X_{ik} & 0 & -\Omega_{ik}^{(i)}(h) \end{bmatrix} < 0, \tag{4.16}$$

where $\Xi_{ik}(h)$ and $\Omega_{ik}^{(i)}(h)$ are defined in (4.8) and (4.9). Further define $R_{ik} = K_{ik}X_{ik}$ and plug $A_{c,ik}$ in (4.3) into the last inequality, then this theorem can be readily proved. □

The condition in Theorem 4.1 is not convenient to check due to the involvements of $\lambda_{ij}(h)$ and $\pi_{kl}^{(i)}(h)$. It is noticed that both $\lambda_{ij}(h)$ and $\pi_{kl}^{(i)}(h)$ are lower and upper

bounded, so the condition in Theorem 4.1 could be further relaxed, then we have the following corollary.

**Corollary 4.1.** *The closed-loop system in (4.2) is stochastically stable if there exists a set of matrices $X_{ik} > 0$ and $R_{ik}$, for $i \in \mathcal{S}_\eta$ and $k \in \mathcal{S}_r$, such that*

$$\begin{bmatrix} A_i X_{ik} + X_{ik} A_i^{\mathrm{T}} + B_i R_{ik} + R_{ik}^{\mathrm{T}} B_i^{\mathrm{T}} & * & * \\ +\bar{\lambda}_{ii} X_{ik} + \bar{\pi}_{kk}^{(i)} X_{ik} & & \\ \mathbf{1}_{\bar{\eta}-1,1} \otimes X_{ik} & -\bar{\Xi}_{ik} & * \\ \mathbf{1}_{\bar{r}-1,1} \otimes X_{ik} & 0 & -\bar{\Omega}_{ik}^{(i)} \end{bmatrix} < 0, \tag{4.17}$$

*where*

$$\bar{\Xi}_{ik} = \mathrm{diag}\left\{ \frac{1}{\bar{\lambda}_{i1}} X_{1k}, \ldots, \frac{1}{\bar{\lambda}_{i,i-1}} X_{i-1,k}, \frac{1}{\bar{\lambda}_{i,i+1}} X_{i+1,k}, \ldots, \frac{1}{\bar{\lambda}_{i\bar{\eta}}} X_{\bar{\eta}k} \right\}, \tag{4.18}$$

$$\bar{\Omega}_{ik}^{(i)} = \mathrm{diag}\left\{ \frac{1}{\bar{\pi}_{k1}^{(i)}} X_{i1}, \ldots, \frac{1}{\bar{\pi}_{k,k-1}^{(i)}} X_{i,k-1}, \frac{1}{\bar{\pi}_{k,k+1}^{(i)}} X_{i,k+1}, \ldots, \frac{1}{\bar{\pi}_{k\bar{r}}^{(i)}} X_{i\bar{r}} \right\}. \tag{4.19}$$

*Here, $\bar{\lambda}_{ij}$ and $\bar{\pi}_{kl}^{(i)}$ are the upper bounds of $\lambda_{ij}(h)$ and $\pi_{kl}^{(i)}(h)$, respectively. Similarly, $\underline{\lambda}_{ij}$ and $\underline{\pi}_{kl}^{(i)}$ are the lower bounds of $\lambda_{ij}(h)$ and $\pi_{kl}^{(i)}(h)$, respectively. Since $\bar{\lambda}_{ii} < 0$ and $\bar{\pi}_{kk}^{(i)} < 0$, it is worth noting that*

$$\bar{\lambda}_{ii} = -\sum_{j=1, j\neq i}^{\bar{\eta}} \underline{\lambda}_{ij}, \quad \bar{\pi}_{kk}^{(i)} = -\sum_{l=1, l\neq k}^{\bar{r}} \underline{\pi}_{kl}^{(i)}. \tag{4.20}$$

*Proof.* Considering the Fact 1, the corollary can be readily proved. □

### 4.3.2 Control Performance

In this sub-section, we will propose the control design technique to ensure a prescribed disturbance attenuation level. The following theorem gives the sufficient condition.

**Theorem 4.2.** *If there exist a set of matrices $X_{ik} > 0$ and $R_{ik}$, for all $i \in \mathcal{S}_\eta$ and*

*$k \in \mathcal{S}_r$, such that the following matrix inequality holds*

$$\begin{bmatrix} A_iX_{ik} + X_{ik}A_i^{\mathrm{T}} + B_iR_{ik} + R_{ik}^{\mathrm{T}}B_i^{\mathrm{T}} \\ +\lambda_{ii}(h)X_{ik} + \pi_{kk}^{(i)}(h)X_{ik} & * & * & * & * \\ \Gamma_{21}C_iX_{ik} + E_i^{\mathrm{T}} & \Gamma_{22} & * & * & * \\ \mathbf{1}_{\bar{\eta}-1,1} \otimes X_{ik} & 0 & -\Xi_{ik}(h) & * & * \\ \mathbf{1}_{\bar{r}-1,1} \otimes X_{ik} & 0 & 0 & -\Omega_{ik}^{(i)}(h) & * \\ C_iX_{ik} & 0 & 0 & 0 & -\Gamma_{11}^{-1} \end{bmatrix} < 0, \tag{4.21}$$

*then the system in (4.2) is stochastically stable with a prescribed disturbance attenuation level. Here, $\Xi_{ik}(h)$ and $\Omega_{ik}^{(i)}(h)$ are given in Theorem 4.1.*

*Proof.* When the closed-loop system operates on modes ($i$, $k$), we deploy the same Lyapunov function $V(\cdot)$ in the proof of Theorem 4.1. Define the following index

$$\begin{aligned} &\mathbb{E}\left\{\int_0^T \begin{bmatrix} y_t^{\mathrm{T}} & \omega_t^{\mathrm{T}} \end{bmatrix} \begin{bmatrix} \Gamma_{11} & \Gamma_{12} \\ \Gamma_{21} & \Gamma_{22} \end{bmatrix} \begin{bmatrix} y_t \\ \omega_t \end{bmatrix} + \tilde{A}V dt\right\} \\ =&\mathbb{E}\left\{\int_0^T \begin{bmatrix} x_t^{\mathrm{T}} & \omega_t^{\mathrm{T}} \end{bmatrix} \begin{bmatrix} C_i^{\mathrm{T}}\Gamma_{11}C_i & C_i^{\mathrm{T}}\Gamma_{12} \\ \Gamma_{21}C_i & \Gamma_{22} \end{bmatrix} \begin{bmatrix} x_t \\ \omega_t \end{bmatrix} + \tilde{A}V dt\right\} \\ =&\mathbb{E}\left\{\int_0^T \begin{bmatrix} x_t^{\mathrm{T}} & \omega_t^{\mathrm{T}} \end{bmatrix} \begin{bmatrix} C_i^{\mathrm{T}}\Gamma_{11}C_i + P_{ik}A_{c,ik} + A_{c,ik}^{\mathrm{T}}P_{ik} & * \\ +\sum_{j=1}^{\bar{\eta}} \lambda_{ij}(h)P_{jk} + \sum_{l=1}^{\bar{r}} \pi_{kl}^{(i)}(h)P_{il} & \\ \Gamma_{21}C_i + E_i^{\mathrm{T}}P_{ik} & \Gamma_{22} \end{bmatrix} \begin{bmatrix} x_t \\ \omega_t \end{bmatrix} dt\right\}. \end{aligned} \tag{4.22}$$

Therefore, if the following inequality holds, then the stability can be established and the control performance can be simultaneously guaranteed.

$$\begin{bmatrix} C_i^{\mathrm{T}}\Gamma_{11}C_i + P_{ik}A_{c,ik} + A_{c,ik}^{\mathrm{T}}P_{ik} & * \\ +\sum_{j=1}^{\bar{\eta}} \lambda_{ij}(h)P_{jk} + \sum_{l=1}^{\bar{r}} \pi_{kl}^{(i)}(h)P_{il} & \\ \Gamma_{21}C_i + E_i^{\mathrm{T}}P_{ik} & \Gamma_{22} \end{bmatrix} < 0. \tag{4.23}$$

Plugging the closed-loop system in (4.2) into the last inequality yields

$$\begin{bmatrix} C_i^{\mathrm{T}}\Gamma_{11}C_i + P_{ik}A_i + A_i^{\mathrm{T}}P_{ik} + P_{ik}B_iK_{ik} + K_{ik}^{\mathrm{T}}B_i^{\mathrm{T}}P_{ik} & * \\ +\sum_{j=1}^{\bar{\eta}} \lambda_{ij}(h)P_{jk} + \sum_{l=1}^{\bar{r}} \pi_{kl}^{(i)}(h)P_{il} & \\ \Gamma_{21}C_i + E_i^{\mathrm{T}}P_{ik} & \Gamma_{22} \end{bmatrix} < 0. \tag{4.24}$$

Pre- and post-multiply (4.24) by $\mathrm{diag}\{X_{ik}, I\}$, then we have

$$\begin{bmatrix} X_{ik}C_i^{\mathrm{T}}\Gamma_{11}C_iX_{ik} + A_iX_{ik} + X_{ik}A_i^{\mathrm{T}} + B_iX_{ik} + R_{ik}^{\mathrm{T}}B_i^{\mathrm{T}} & * \\ +\sum_{j=1}^{\bar{\eta}}\lambda_{ij}(h)X_{ik}P_{jk}X_{ik} + \sum_{l=1}^{\bar{r}}\pi_{kl}^{(i)}(h)X_{ik}P_{il}X_{ik} & \\ \Gamma_{21}C_iX_{ik} + E_i^{\mathrm{T}} & \Gamma_{22} \end{bmatrix} < 0. \tag{4.25}$$

Applying the Schur complement, and letting $T$ approach $\infty$, the condition in (4.6) can be satisfied. Then the proof is completed. □

The above condition is not in linear forms due to the existence of $\lambda_{ij}(h)$ and $\pi_{kl}^{(i)}(h)$. Since both $\lambda_{ij}(h)$ and $\pi_{kl}^{(i)}(h)$ are lower and upper bounded, the condition in Theorem 4.2 could be relaxed. Then we have the following corollary.

**Corollary 4.2.** *The system is stochastically stable with a prescribed disturbance attenuation level, if there exist a set of matrices $X_{ik} > 0$ and $R_{ik}$, for all $i \in \mathcal{S}_\eta$ and $k \in \mathcal{S}_r$, such that*

$$\begin{bmatrix} A_iX_{ik} + X_{ik}A_i^{\mathrm{T}} + B_iR_{ik} + R_{ik}^{\mathrm{T}}B_i^{\mathrm{T}} & * & * & * & * \\ +\bar{\lambda}_{ii}X_{ik} + \bar{\pi}_{kk}^{(i)}X_{ik} & & & & \\ \Gamma_{21}C_iX_{ik} + E_i^{\mathrm{T}} & \Gamma_{22} & * & * & * \\ \mathbf{1}_{\bar{\eta}-1,1} \otimes X_{ik} & 0 & -\bar{\Xi}_{ik} & * & * \\ \mathbf{1}_{\bar{r}-1,1} \otimes X_{ik} & 0 & 0 & -\bar{\Omega}_{ik}^{(i)} & * \\ C_iX_{ik} & 0 & 0 & 0 & -\Gamma_{11}^{-1} \end{bmatrix} < 0, \tag{4.26}$$

*where $\bar{\Xi}_{ik}$ and $\bar{\Omega}_{ik}^{(i)}$ are defined in (4.18) and (4.19), respectively; and $\bar{\lambda}_{ii}$ and $\bar{\pi}_{kk}^{(i)}$ are defined in (4.20).*

The sojourn-time partition technique has been proved to be an effective approach to further reduce the conservativeness in the controller synthesis [88]. By applying this technique, we have the following corollary.

**Corollary 4.3.** *The system is stochastically stable with a prescribed disturbance attenuation level, if there exist a set of matrices $X_{ik,m} > 0$ and $R_{ik,m}$, for all $i \in \mathcal{S}_\eta$ and*

*$k \in \mathcal{S}_r$, such that*

$$\begin{bmatrix} A_iX_{ik,m} + X_{ik,m}A_i^{\mathrm{T}} + B_iR_{ik,m} + R_{ik,m}^{\mathrm{T}}B_i^{\mathrm{T}} \\ \quad +\bar{\lambda}_{ii,m}X_{ik,m} + \bar{\pi}_{kk,m}^{(i)}X_{ik,m} & * & * & * & * \\ \Gamma_{21}C_iX_{ik,m} + E_i^{\mathrm{T}} & \Gamma_{22} & * & * & * \\ \mathbf{1}_{\bar{\eta}-1,1} \otimes X_{ik,m} & 0 & -\bar{\Xi}_{ik,m} & * & * \\ \mathbf{1}_{\bar{r}-1,1} \otimes X_{ik,m} & 0 & 0 & -\bar{\Omega}_{ik,m}^{(i)} & * \\ C_iX_{ik,m} & 0 & 0 & 0 & -\Gamma_{11}^{-1} \end{bmatrix} < 0,$$

for $m \in \mathcal{M}$, (4.27)

*where $m$ is the partition index and $\bar{\Xi}_{ik,m}$, $\bar{\Omega}_{ik,m}^{(i)}$, $\bar{\lambda}_{ii,m}$, and $\bar{\pi}_{kk,m}^{(i)}$ are given as follows*

$$\bar{\Xi}_{ik,m} = \mathrm{diag}\left\{ \frac{1}{\bar{\lambda}_{i1,m}}X_{1k,m}, \ldots, \frac{1}{\bar{\lambda}_{i,i-1,m}}X_{i-1,k,m}, \frac{1}{\bar{\lambda}_{i,i+1,m}}X_{i+1,k,m}, \ldots, \frac{1}{\bar{\lambda}_{i\bar{\eta},m}}X_{\bar{\eta}k,m} \right\},$$

$$\bar{\Omega}_{ik,m}^{(i)} = \mathrm{diag}\left\{ \frac{1}{\bar{\pi}_{k1,m}^{(i)}}X_{i1,m}, \ldots, \frac{1}{\bar{\pi}_{k,k-1,m}^{(i)}}X_{i,k-1,m}, \frac{1}{\bar{\pi}_{k,k+1,m}^{(i)}}X_{i,k+1,m}, \ldots, \frac{1}{\bar{\pi}_{k\bar{r},m}^{(i)}}X_{i\bar{r},m} \right\},$$

$$\bar{\lambda}_{ii,m} = -\sum_{j=1,j\neq i}^{\bar{\eta}} \underline{\lambda}_{ij,m}, \quad \bar{\pi}_{kk,m}^{(i)} = -\sum_{l=1,l\neq k}^{\bar{r}} \underline{\pi}_{kl,m}^{(i)}.$$

*Proof.* By using Fact 1, the conditions in the two corollaries can be easily obtained. □

**Remark 4.5** The basic principle behind the partition technique is to avoid the common matrix variables $X_{ik}$ and $R_{ik}$ in the matrix inequality. By separating the transition rates $\lambda_{ij}(h)$ and $\pi_{kl}^{(i)}(h)$ into several sections according to the sojourn-time $h$, $X_{ik}$ and $R_{ik}$ are not necessarily the same for all sections. In other words, the non-partition technique can be viewed as the partition technique with extra constraints: $X_{ik,m_i} = \cdots = X_{ik,m_j}$ and $R_{ik,m_i} = \cdots = R_{ik,m_j}$, for all $m_i \in \mathcal{M}$ and $m_j \in \mathcal{M}$.

## 4.4 Numerical Examples

In this section, to demonstrate the validity of the results obtained previously, we consider a vertical take-off and landing (VTOL) vehicle example taken from [102, 123]. The system state is $x = [x_1\ x_2\ x_3\ x_4]^{\mathrm{T}}$, where $x_1$ is the horizontal velocity in knot; $x_2$ is the vertical velocity in knot; $x_3$ is the pitch rate in degree per second; and $x_4$ is the pitch angle in degree. To save space, only one type of fault is considered in the

numerical example, so $\bar{\eta} = \bar{r} = 2$. The system state-space model has the following system matrices:

$$A_1 = A_2 = \begin{bmatrix} -0.0366 & 0.0271 & 0.0188 & -0.4555 \\ 0.0482 & -1.0100 & 0.0024 & -4.0208 \\ 0.1002 & 0.3681 & -0.707 & 1.4200 \\ 0 & 0 & 1 & 0 \end{bmatrix}, B_1 = \begin{bmatrix} 0.4422 & 0.1761 \\ 3.5446 & -7.5922 \\ -5.5200 & 4.4900 \\ 0 & 0 \end{bmatrix},$$

$$B_2 = \begin{bmatrix} 0.4422 & 0.1761 \\ 1.7723 & -7.5922 \\ -5.5200 & 4.4900 \\ 0 & 0 \end{bmatrix}, E_1 = E_2 = \begin{bmatrix} 0 & 0.1 \\ 0.1 & 0 \\ 0 & 0 \\ 0 & 0 \end{bmatrix}, C_1 = C_2 = \begin{bmatrix} 0 & 1 & 0 & 0 \end{bmatrix}.$$

The signal of interest is the vertical velocity $x_2(t)$, and suppose that no fault happens to the sensors associated with the output, so $C_1 = C_2 = [0\ 1\ 0\ 0]$, i.e., $y(t) = x_2(t)$. Here, $A_1$, $B_1$, $C_1$, and $E_1$ are system parameters in the normal working condition, while $A_2$, $B_2$, $C_2$, and $E_2$ are system matrices when a fault happens. The fault scenario is the lost effectiveness from the collective pitch control input $u_1(t)$ to the vertical velocity $x_2(t)$ by 50%, i.e., $B_1(2,1) = 2B_2(2,1)$. Since $\bar{\eta} = \bar{r} = 2$, the two governing stochastic processes $\eta_t$ and $r_t$ take values in $\mathcal{S}_\eta = \{1, 2\}$ and $\mathcal{S}_r = \{1, 2\}$. The transition rate matrix of $\eta_t$ is time-varying, and it is lower and upper bounded by $\underline{\Lambda}_1$ and $\bar{\Lambda}_2$, respectively. Similarly, the time-varying transition rate matrix of $r_t$ is lower and upper bounded by $\underline{\Pi}_1^{(\eta_t)}$ and $\bar{\Pi}_2^{(\eta_t)}$ ($\eta_t = 1, 2$), respectively. We separate the transition rates into two sections by the mid-points of their upper and lower bounds, so $\bar{\Lambda}_1 = \underline{\Lambda}_2$, $\bar{\Pi}_1^{(1)} = \underline{\Pi}_2^{(1)}$, and $\bar{\Pi}_1^{(2)} = \underline{\Pi}_2^{(2)}$. The resulting closed-loop system switches according to the states of the two stochastic processes: $\eta_t$ and $r_t$. For example, in the first section, the control strategy switching scheme is governed by $\underline{\Pi}_1^{(1)}$ and $\bar{\Pi}_1^{(1)}$ when the VTOL is running on the normal condition, and it is governed by $\underline{\Pi}_1^{(2)}$ and $\bar{\Pi}_1^{(2)}$ when the VTOL is running with the aforementioned fault: effectiveness loss. Here, we assume that the *a prior* transition rates for the fault process have been determined and known before the controller design. All the upper and lower bounds are listed as follows:

$$\underline{\Lambda}_1 = \begin{bmatrix} -0.333 & 0.333 \\ 0.1 & -0.1 \end{bmatrix}, \bar{\Lambda}_1 = \underline{\Lambda}_2 = \begin{bmatrix} -0.5 & 0.5 \\ 0.118 & -0.118 \end{bmatrix}, \bar{\Lambda}_2 = \begin{bmatrix} -1 & 1 \\ 0.143 & -0.143 \end{bmatrix},$$

$$\underline{\Pi}_1^{(1)} = \begin{bmatrix} -1 & 1 \\ 1.429 & -1.429 \end{bmatrix}, \bar{\Pi}_1^{(1)} = \underline{\Pi}_2^{(1)} = \begin{bmatrix} -1.538 & 1.538 \\ 2.128 & -2.128 \end{bmatrix},$$
$$\bar{\Pi}_2^{(1)} = \begin{bmatrix} -3.333 & 3.333 \\ 4.167 & -4.167 \end{bmatrix}, \underline{\Pi}_1^{(2)} = \begin{bmatrix} -0.833 & 0.833 \\ 2 & -2 \end{bmatrix},$$
$$\bar{\Pi}_1^{(2)} = \underline{\Pi}_2^{(2)} = \begin{bmatrix} -1.176 & 1.176 \\ 2.857 & -2.857 \end{bmatrix}, \bar{\Pi}_2^{(2)} = \begin{bmatrix} -2 & 2 \\ 5 & -5 \end{bmatrix}. \tag{4.28}$$

The system is in continuous-time domain, and from $\mathcal{S}_\eta = \{1, 2\}$ and $\mathcal{S}_r = \{1, 2\}$, there are two possible states of $\eta_t$ and $r_t$. Therefore the "continuous-time discrete-state conditions" for the stochastic processes are satisfied in this VTOL example.

In the $H_\infty$ controller design, $\gamma$ is set to be 1.5, so the parameters in the SIQC are

$$\Gamma = \begin{bmatrix} \Gamma_{11} & \Gamma_{12} \\ \Gamma_{21} & \Gamma_{22} \end{bmatrix} = \begin{bmatrix} I & 0 \\ 0 & -\gamma^2 I \end{bmatrix} = \begin{bmatrix} I & 0 \\ 0 & -1.5^2 I \end{bmatrix}. \tag{4.29}$$

To compare the results by using different corollaries, both controllers without partition ($\mathcal{M} = \{1\}$) and with partition ($\mathcal{M} = \{1, 2\}$) are proposed. And the state feedback control gains are given as follows:

$$K_{11} = \begin{bmatrix} -29.0476 & -21.4139 & 1.0877 & 15.8314 \\ -28.8441 & -10.1142 & 1.0381 & 15.0394 \end{bmatrix},$$
$$K_{12} = \begin{bmatrix} -4.6499 & 8.6516 & 0.0341 & 2.3851 \\ 2.3578 & 6.0641 & -0.1738 & -1.8877 \end{bmatrix},$$
$$K_{21} = \begin{bmatrix} -12.0394 & -2.4476 & 0.2371 & 6.6857 \\ -4.3991 & 0.7927 & 0.3011 & 2.1268 \end{bmatrix},$$
$$K_{22} = \begin{bmatrix} -11.3574 & -2.6805 & 0.2439 & 6.3312 \\ -4.2524 & 0.7151 & 0.2960 & 2.0400 \end{bmatrix}; \tag{4.30}$$

$$K_{11,1} = \begin{bmatrix} -0.6338 & 5.9167 & 0.0186 & 0.5508 \\ 0.7768 & 3.9104 & -0.5256 & -1.3280 \end{bmatrix},$$
$$K_{11,2} = \begin{bmatrix} 7.2148 & 26.4389 & -3.2662 & -6.9366 \\ 11.3268 & 14.2303 & -4.6697 & -11.1112 \end{bmatrix},$$
$$K_{12,1} = \begin{bmatrix} -2.4914 & -0.2779 & 0.8977 & 2.3757 \\ -1.5215 & 0.8716 & 0.5774 & 0.9304 \end{bmatrix},$$

$$
\begin{aligned}
K_{12,2} &= \begin{bmatrix} -0.5740 & 6.4361 & -0.0222 & 0.4278 \\ 1.2802 & 4.2206 & -0.6182 & -1.7637 \end{bmatrix}, \\
K_{21,1} &= \begin{bmatrix} -2.9476 & -4.8933 & 1.0848 & 3.0509 \\ -1.9784 & -0.4680 & 1.1723 & 1.5120 \end{bmatrix}, \\
K_{21,2} &= \begin{bmatrix} -5.8887 & -8.7909 & 2.0822 & 5.5006 \\ -4.7633 & -1.4625 & 2.1654 & 4.0147 \end{bmatrix}, \\
K_{22,1} &= \begin{bmatrix} -1.9209 & 0.0587 & 0.4517 & 1.8868 \\ -0.6037 & 0.9049 & 0.2209 & 0.0931 \end{bmatrix}, \\
K_{22,2} &= \begin{bmatrix} -3.3354 & -2.6980 & 0.9347 & 3.0805 \\ -1.8901 & 0.1669 & 0.7811 & 1.2869 \end{bmatrix}.
\end{aligned} \tag{4.31}
$$

In the simulation, the initial states are given as $x_0 = [0.1\ 1\ -0.2\ -0.5]^{\mathrm{T}}$, $\eta_0 = 1$, and $r_0 = 1$. The external disturbance $\omega_t$ is a white noise process with zero mean and variance 1. The fault occurrence sequence is generated by the above transition matrices. For the purpose of a clear view, the first 19 seconds, instead of 3 seconds in the simulation, of the fault sequence $\eta_t$ is displayed (Figure 4.3). When $\eta_t = 1$, the closed-loop system operates on the normal condition; when $\eta_t = 2$, actuation fault happens. The state trajectories $x_t$ by using the controller in (4.30) are shown in Figure 4.4. From the simulation results, $\|y_t\|/\|\omega_t\| = 0.4606$. As a comparison, the state trajectories $x_t$ by using the controller in (4.31) are shown in Figure 4.5 and $\|y_t\|/\|\omega_t\| = 0.3093$. So the $H_\infty$ control performance with the disturbance attenuation level $\gamma = 1.5$ is achieved.

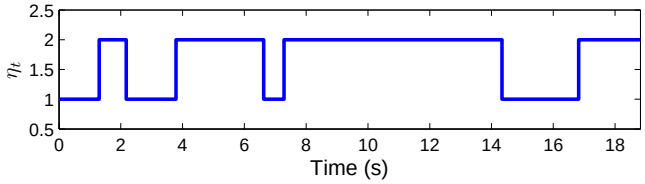


Figure 4.3: Fault occurrence trajectory.

To perform the Monte Carlo simulation, 100 runs of simulation by using the computed two controllers are performed. For each round of simulation, the semi-Markov processes $\eta_t$ and $r_t$ are randomly generated according to the transition rate matrices in (4.28). From the Monte Carlo simulation, it is obvious that the overshoot is greatly reduced by using the sojourn-time partition technique. For the 100 simulations, the ratio from the disturbance $\omega_t$ to the output $y_t$ are summarized in Figure 4.8.

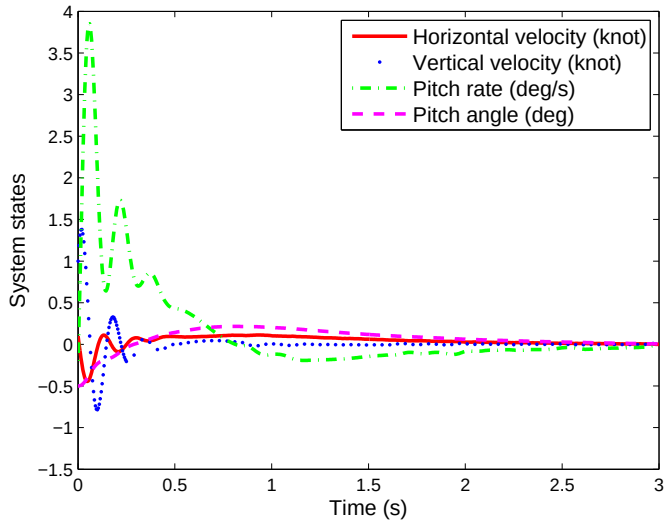


Figure 4.4: State trajectories by using the proposed controller (4.30).

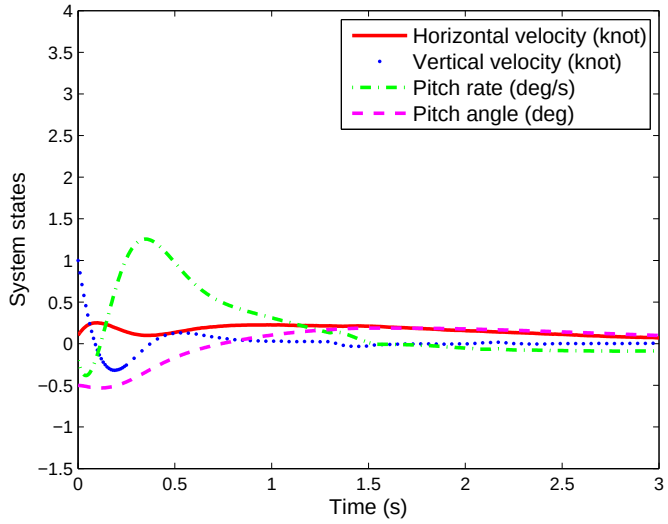


Figure 4.5: State trajectories by using the proposed controller (4.31).

Quantitatively, the disturbance attenuation level is suppressed using the proposed controller.

**Remark 4.6** Quantitatively, it is observed that the overshoot of the state by using the partition technique can be significantly reduced, especially for the output signal $y_t$, i.e., the vertical velocity. The norm of the output signal $y_t$ is reduced as well conditioning on the same disturbance $\omega_t$. It is also worth noting that the improved

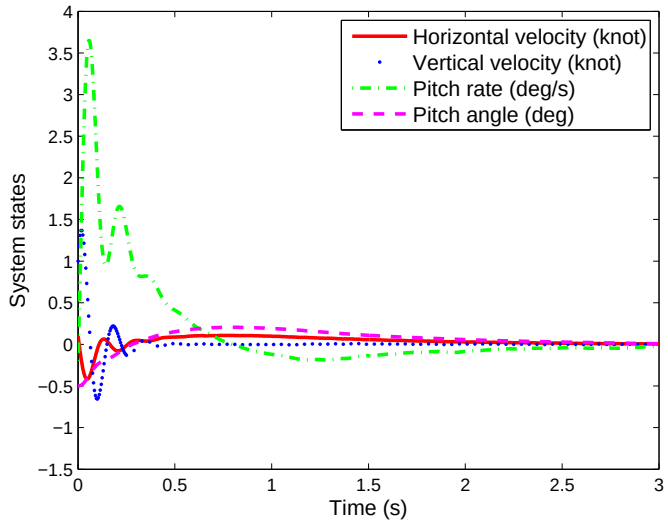


Figure 4.6: Average system trajectories (Monte Carlo simulation (100 runs)) by using the proposed controller (4.30).

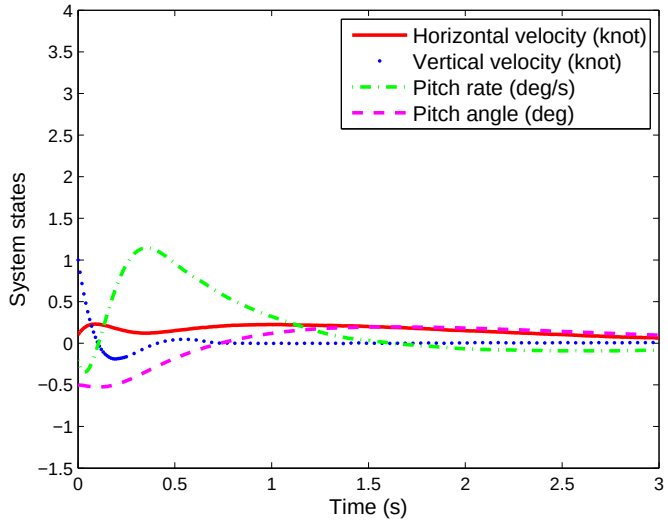


Figure 4.7: Average system trajectories (Monte Carlo simulation (100 runs)) by using the proposed controller (4.31).

transient performance is not achieved by the cost of increasing the control gains (e.g., $\|K_{11}\| > \|K_{11,1}\|$, $\|K_{11}\| > \|K_{11,2}\|$), which would potentially saturate the actuator. Instead, it is achieved by adding more freedom in manipulating control signals.

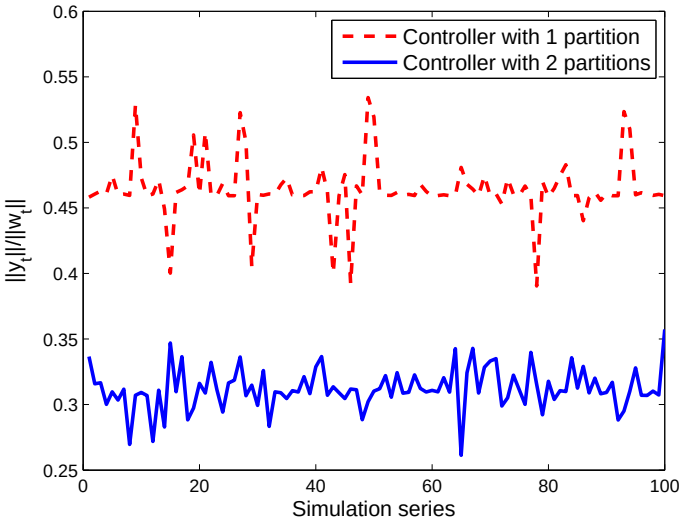


Figure 4.8: $\|y_t\|/\|\omega_t\|$ for the 100 simulations.

## 4.5 Conclusions

In this paper, a novel fault tolerant control strategy for linear systems subject to abrupt changes in their structure characterized by semi-Markov processes has been developed. Based on the stability analysis and the $H_\infty$ performance analysis, a reliable active fault tolerant state feedback controller has been designed. The designing process could be completed offline; once the control gains are determined, no online calculation for the control parameters will be required during the operation. By measuring the sojourn-time, the controller could determine which partition that the system is operating on and select appropriate control gains accordingly. This method has been applied to a VTOL vehicle model. Simulations with different controller parameters have been performed, and the effectiveness of the proposed method is demonstrated. In addition, from the Monte Carlo simulations with randomly generated stochastic processes in each run, it could be concluded that the proposed controller is reliable and the disturbance attenuation level can be significantly reduced (Figure 4.8).

Future work will focus on improving the control performance on the current system and systems with possible uncertainties. Firstly, state-space models in (4.1) may be subject to model uncertainties in practise, e.g., norm-bounded uncertainties or polytopic uncertainties. As a result, $A(\eta_t) = A_0(\eta_t) + \Delta A(\eta_t)$, where $A_0$ represents the nominal system dynamics and $\Delta A(\eta_t)$ denotes the possible system uncertain-

ties. Secondly, optimal control strategies such as the $H_2$ control and the $H_\infty$ control may be implemented to improve the control performance and reduce the disturbance attenuation level. Lastly, other than a pure feedback gain used in this chapter, a higher order feedback controller, e.g., a dynamic controller, may potentially reduce the steady state error.

# Chapter 5

# Networked Control System Design Using Historical Data

## 5.1 Introduction

The modeling, control, and filtering problems for NCSs have been studied extensively over the last few years [33, 70, 124]. In the conventional NCSs, the sensors of the plant are located at the same place; as a result, the measurements of the plant can be sent to the controller within one data packet at the same time. Recently, with the fast development of the sensor technology, a significant research interest in the control society has been devoted to combining the data supplied by different sensors [125]. Especially, different communication protocols are being developed, which will be used in the next generation NCSs, such as WirelessHART [126], ZigBee [127], ISA100 [128]. The interested readers are referred to [129] and the references therein. In a modern NCS, it is common to have distributed sensors for the measurements [130]. Different from the conventional control system, the distributed sensor configuration enhances the reliability and robustness of the control system, improves the resolution of the measurement, and extends the coverage [131]. While enjoying these advantages, new problems arise. Take the intelligent building system as an example, the spatially distributed sensors detect the gas, noise, temperature and humidity of the building and transmit the information to the central controller by shared interface device [132]. Using the shared interface, the controller cannot accept the data from all sensors at the same time. Another example is the state estimation problem where the out of sequence of data occurs, and the central controller estimates the state of a complex

control system by using the information provided by physically distributed sensors through communication networks [133].

Despite the rich literature on the controller design problem that aims to stabilize the closed-loop NCS, in practical systems, it is always desirable to propose a controller that not only stabilizes the plant but also satisfies certain control performance. A widely used control strategy is the so-called guaranteed cost control [134]. The guaranteed cost control for the NCS is often referred to as the guaranteed cost networked control (GCNC) [135]. The GCNC seeks to stabilize the closed-loop system and simultaneously guarantees a prescribed system performance in terms of a cost function. For example, Wu *et al.* proposed the static state feedback controller for the discrete-time NCS which satisfied the specific control performance [136]. Also in [137], the authors considered the guaranteed cost control problem for a class of NCSs with uncertainties where an improved predictive controller was developed to compensate for the communication delays and packet dropouts in the communication links. Apart from linear systems, GCNC was also applied to the nonlinear NCSs where the time delays can be represented by T-S fuzzy models [138].

With the spatially distributed sensors, the connection between the sensor and the controller would be multi-channel links. In this chapter, we consider the NCSs in which each individual sensor measures one state information and transmits the measurement to the controller via separate communication channels. In [136], the data packet dropout and disorder problems for multi-channel NCS were studied where the guaranteed cost controller can be proposed by solving a set of linear matrix inequalities (LMIs). Chen *et al.* designed controller for the NCS where the communication delays were modeled by Markov processes [139]. In [139], after transforming the resulting closed-loop system into a Markov jump linear system, the controller can be readily computed. It is noticed that in the aforementioned works and more (see e.g. [63, 140, 141]), only the most updated/recent state information will be used to determine the control effort. Intuitively, the information behind the historical data is wasted when computing the control signal. In addition, with the fast developed compressive sensing theory [142, 143], the compressive sensor can transmit a substantial length of historical data of the system state to the controller with small network bandwidth. Therefore, in this chapter, motivated by making the most of the historical state information, the novel guaranteed cost state feedback controller will not only depend on the most updated state information, but also the historical data at the controller node.

The rest of the chapter is organized as follows. In Section 5.2, we present the structure of the NCS and the sensor scheduling scheme. Also, the cost function is given along the design objectives. In Section 5.3, the controller design procedure is provided and the equivalent LMI conditions with nonconvex constraints are developed. The numerical simulation and concluding remarks are given in Sections 5.4 and 5.5, respectively.

## 5.2 Problem Formulation

Consider the discrete-time plant with multiple state delays in Figure 5.1. The discrete-time state-space model is

$$x(k+1) = Ax(k) + \sum_{j=1}^{\tau} A_{d,j}x(k-j) + Bu(k), \tag{5.1}$$

where $x(k) = [x_1(k), x_2(k), \ldots, x_n(k)]^{\mathrm{T}} \in \mathbb{R}^n$ is the state vector, and $u(k) \in \mathbb{R}^p$ is the control input. $A$, $A_{d,j}$, and $B$ are system matrices with appropriate dimensions. $\tau$ is the number of delayed states. In Figure 5.1, $n$ sensors in the plant connect with the controller through communication networks. Sensor $i$ measures the system state variable $x_i$. The measurement is transmitted to the controller over the sensor-to-controller link. In such an NCS, one component (controller/sensor) can only transmit or receive the data from one channel at a time [144]. Therefore, the controller receives the measurement for one state at each time step $k$. In this chapter, we assume the control signal can reach the actuator immediately.

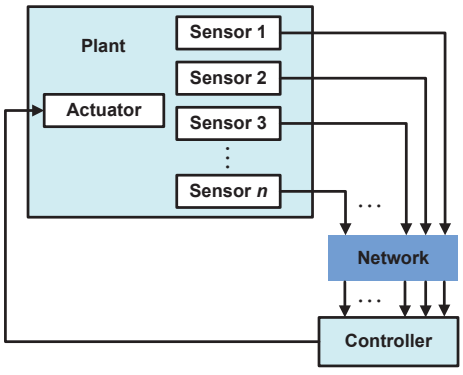


Figure 5.1: NCSs with multi-sensors.

To simplify the presentation, we define an indicator function $\mathcal{I}(k)$ for the sensor

scheduling scheme. $\mathcal{I}(k)$ takes values in a finite set $\mathcal{N} = \{1, 2, \ldots, n\}$. At time instant $k$, $\mathcal{I}(k) = i$ means that the controller receives the measurement information from sensor $i$. For the sensors used in the current NCS, a buffer is mounted on the sensor to record the historical data of length $m$ for the measurements. The data is packed within one packet and transmitted to the controller when the network is available [145]. It is noticed that some network protocols have a maximal length of data in one packet [146]. In such cases, a compressive sensor can be implemented to reduce the data size and further lessens the network transmission load when the sensor measurement is sparse or slowly time-varying [147]. We apply the following sensor scheduling scheme: When $\mathcal{I}(k) = i$

$$\mathcal{I}(k+1) = \begin{cases} i+1, & \text{if } i < n, \\ 1, & \text{if } i = n. \end{cases} \tag{5.2}$$

Under the proposed scheduling scheme in (5.2), $n$ sensors send the measurement of the plant one by one with equal priority, which is a fixed manner instead of a random fashion.

Associated with (5.1), we define the following cost function

$$J(u) = \sum_{k=0}^{\infty} x^{\mathrm{T}}(k) \Xi x(k). \tag{5.3}$$

Here, the symmetric positive definite matrix $\Xi$ is the weighting factor. By choosing different weighting factors, different levels of system performance will be achieved.

Since the controller receives one data packet from the sensor at each time step, the controller to be designed will depend on the indicator function $\mathcal{I}(k)$. The objective of this chapter is to design the sensor-dependent guaranteed cost state feedback controller of the following form

$$u(k) = \sum_{j=0}^{\tau} K(\mathcal{I}(k), j) x(k-j). \tag{5.4}$$

Here, we let $m = \tau - n + 2$. From (5.4), it is noted that the control signal is a linear combination of the current information $x(k)$ and the historical information $x(k-j)$. Depending on the current updating sensor, i.e., denoted by $\mathcal{I}(k)$, a set of specific control gains will be implemented to generate the control signal.

Closing the control system using the proposed state feedback controller, and after some manipulations, the closed-loop system becomes

$$x(k+1) = A_{c,0}(\mathcal{I}(k))x(k) + \sum_{j=1}^{\tau} A_{c,j}(\mathcal{I}(k))x(k-j), \tag{5.5}$$

where $A_{c,0}(\mathcal{I}(k))$ is given by

$$A_{c,0}(\mathcal{I}(k)) = A + BK(\mathcal{I}(k), 0), \tag{5.6}$$

and $A_{c,j}(\mathcal{I}(k))$, $j = 1, 2, \ldots, \tau$, are given by

$$A_{c,j}(\mathcal{I}(k)) = A_{d,j} + BK(\mathcal{I}(k), j). \tag{5.7}$$

**Remark 5.1** The parameters in the state feedback control gain $K(\mathcal{I}(k), j)$ cannot be freely designed; as a matter of fact, it should be designed with constraints. Taking

| | | | | | |
|---|---|---|---|---|---|
| $x_1(k-5)$ | $x_1(k-4)$ | $x_1(k-3)$ | $x_1(k-2)$ | $x_1(k-1)$ | $x_1(k)$ |
| $x_2(k-5)$ | $x_2(k-4)$ | $x_2(k-3)$ | $x_2(k-2)$ | $x_2(k-1)$ | $x_2(k)$ |
| $x_3(k-5)$ | $x_3(k-4)$ | $x_3(k-3)$ | $x_3(k-2)$ | $x_3(k-1)$ | $x_3(k)$ |
| $x_4(k-5)$ | $x_4(k-4)$ | $x_4(k-3)$ | $x_4(k-2)$ | $x_4(k-1)$ | $x_4(k)$ |

Figure 5.2: State information to be used by the controller.

Figure 5.2 as an example where $\mathcal{I}(k) = 3$, $n = 4$ and $m = 3$, the control effort $u(k)$ at time instant $k$ depends on the information in the shadowed areas. So the controller should follow the so-called zero element constraints:

$$\begin{aligned}
K(\mathcal{I}(k), 0) = K(3, 0) &= \begin{bmatrix} 0 & 0 & * & 0 \end{bmatrix}, \\
K(\mathcal{I}(k), 1) = K(3, 1) &= \begin{bmatrix} 0 & * & * & 0 \end{bmatrix}, \\
K(\mathcal{I}(k), 2) = K(3, 2) &= \begin{bmatrix} * & * & * & 0 \end{bmatrix}, \\
K(\mathcal{I}(k), 3) = K(3, 3) &= \begin{bmatrix} * & * & 0 & * \end{bmatrix}, \\
K(\mathcal{I}(k), 4) = K(3, 4) &= \begin{bmatrix} * & 0 & * & * \end{bmatrix}, \\
K(\mathcal{I}(k), 5) = K(3, 5) &= \begin{bmatrix} 0 & * & * & * \end{bmatrix}.
\end{aligned} \tag{5.8}$$

Here, $*$ represents the unknown control parameter to be designed. 0 means the corresponding state information of the plant is not available to the controller at

$k$. The zero element constraints of controller $K(\cdot,\cdot)$ come from two reasons: Either because the sensor measuring the corresponding state variable has not been scheduled to use the network (e.g., the 0 in $K(3,0)$, $K(3,1)$, and $K(3,2)$), or because the data length (history) of the state variable in the sensor buffer is not long enough (e.g., the 0 in $K(3,3)$, $K(3,4)$, and $K(3,5)$). It is worth mentioning that $x_2(k-5)$, $x_3(k-5)$, and $x_3(k-4)$ are accessible to the controller because they are included in the previous data packets, i.e., data from sensor 2 at $k-5$ and data from sensor 3 at $k-4$, respectively.

**Remark 5.2** By setting additional constraints on the sensor-dependent controller $K(\mathcal{I}(k), j)$, the constant network-induced delay in the sensor-to-controller link can be incorporated. For instance, by setting $K(\mathcal{I}(k), 0) \equiv 0_{n\times 1}$, the controller $u(k)$ in (5.4) is equivalent to the static state feedback controller when the sensor-to-controller delay is 1 where $x(k)$ is not available to the controller. In such a way, the guaranteed cost state feedback controller for the NCS with constant sensor-to-controller delays is obtained by putting additional constraint structures on the controller, which is a special case of this chapter.

## 5.3 Main Results

The objectives of the chapter are to design the guaranteed cost state feedback controller such that the closed-loop system in (5.5) is stable and the cost function $J$ in (5.3) is upper bounded by a finite constant value. In this section, we formulate the design problem into a set of LMIs with nonconvex constraints.

**Theorem 5.1.** *For the discrete-time NCS where the plant has multiple state delays, the sensor-dependent guaranteed cost state feedback controller can be designed if there exist positive definite matrices $P$ and $Q_j$, $j = 1, 2, \ldots, \tau$ of appropriate dimensions, such that*

$$\begin{bmatrix} -X & \bar{A}_c(\mathcal{I}(k)) \\ \bar{A}_c^{\mathrm{T}}(\mathcal{I}(k)) & -\bar{\Omega} \end{bmatrix} < 0 \tag{5.9}$$

*holds for all $\mathcal{I}(k) = 1, 2, \ldots, n$ subject to the nonconvex constraint $PX = I$, where*

$$\bar{A}_c(\mathcal{I}(k)) = \begin{bmatrix} A_{c,0}(\mathcal{I}(k)) & A_{c,1}(\mathcal{I}(k)) & \cdots & A_{c,\tau}(\mathcal{I}(k)) \end{bmatrix},$$

$$\bar{\Omega} = \text{diag}\{P - \sum_{j=1}^{\tau} Q_j - \Xi, Q_1, Q_2, \ldots, Q_\tau\}.$$

*Then the controller $u(k)$ in (5.4) stabilizes the NCS and the system performance in (5.3) will be satisfied.*

*Proof.* For the closed-loop networked system in (5.5), choose a Lyapunov function as follows

$$V(x(k)) = x^{\mathrm{T}}(k)Px(k) + \sum_{j=1}^{\tau} \sum_{h=j-\tau-1}^{-1} x^{\mathrm{T}}(k+h)Q_j x(k+h).$$

The difference of the Lyapunov function with the system in (5.5) is

$$\begin{aligned}\Delta V(x(k)) =& V(x(k+1)) - V(x(k)) \\ =& x^{\mathrm{T}}(k+1)Px(k+1) - x^{\mathrm{T}}(k)Px(k) + \sum_{j=1}^{\tau} \left[x^{\mathrm{T}}(k)Q_j x(k)\right. \\ & \left. - x^{\mathrm{T}}(k+j-\tau-1)Q_j x(k+j-\tau-1)\right].\end{aligned}$$

Substituting $x(k+1)$ from (5.5) into the last equation, we obtain

$$\begin{aligned}& \Delta V(x(k)) \\ =& \left[x^{\mathrm{T}}(k)A_{c,0}^{\mathrm{T}}(\mathcal{I}(k)) + \sum_{j=1}^{\tau} x^{\mathrm{T}}(k-j)A_{c,j}^{\mathrm{T}}(\mathcal{I}(k))\right] P \\ & \left[A_{c,0}(\mathcal{I}(k))x(k) + \sum_{j=1}^{\tau} A_{c,j}(\mathcal{I}(k))x(k-j)\right] - x^{\mathrm{T}}(k)Px(k) \\ & + \sum_{j=1}^{\tau} \left[x^{\mathrm{T}}(k)Q_j x(k) \; - x^{\mathrm{T}}(k+j-\tau-1)Q_j x(k+j-\tau-1)\right] \\ =& \eta^{\mathrm{T}}(k)\bar{A}_c^{\mathrm{T}}(\mathcal{I}(k))P\bar{A}_c(\mathcal{I}(k))\eta(k) - \eta^{\mathrm{T}}(k)\Omega(k)\eta(k),\end{aligned}$$

where

$$\begin{aligned}\Omega(k) =& \text{diag}\{P - \sum_{j=1}^{\tau} Q_j, Q_1, Q_2, \ldots, Q_\tau\}, \\ \eta(k) =& \left[\begin{array}{cccc} x^{\mathrm{T}}(k) & x^{\mathrm{T}}(k-1) & \cdots & x^{\mathrm{T}}(k-\tau) \end{array}\right]^{\mathrm{T}}.\end{aligned}$$

According to the Lyapunov theory, if $\Delta V(x(k)) < 0$ for all $k \geq 0$, then the closed-loop system in (5.5) is stable. Using the Schur complement, if

$$\begin{bmatrix} -P^{-1} & \bar{A}_c(\mathcal{I}(k)) \\ \bar{A}_c^{\mathrm{T}}(\mathcal{I}(k)) & -\Omega(k) \end{bmatrix} < 0 \tag{5.10}$$

holds, then

$$\Delta V(x(k)) = \eta^{\mathrm{T}}(k) \left[ \bar{A}_c^{\mathrm{T}}(\mathcal{I}(k)) P \bar{A}_c(\mathcal{I}(k)) - \Omega(k) \right] \eta(k) < 0. \tag{5.11}$$

Since $P > 0$, further define $X = P^{-1} > 0$, then the closed-loop system is stable if the following LMI holds

$$\begin{bmatrix} -X & \bar{A}_c(\mathcal{I}(k)) \\ \bar{A}_c^{\mathrm{T}}(\mathcal{I}(k)) & -\Omega \end{bmatrix} < 0, \tag{5.12}$$

for all $\mathcal{I}(k) = 1, 2, \ldots, n$, subject to the constraint $PX = I$.

In the following, we will show that the cost function in (5.3) is upper bounded by a finite constant. Considering the difference of the Lyapunov function $\Delta V(x(k)) < 0$, if the following inequality holds

$$\begin{bmatrix} -X & \bar{A}_c(\mathcal{I}(k)) \\ \bar{A}_c^{\mathrm{T}}(\mathcal{I}(k)) & -\bar{\Omega} \end{bmatrix} < 0 \tag{5.13}$$

for all $\mathcal{I}(k) = 1, 2, \ldots, n$, and by using

$$\eta^{\mathrm{T}}(k) \bar{\Omega} \eta(k) = \eta^{\mathrm{T}}(k) \Omega \eta(k) - x^{\mathrm{T}}(k) \Xi x(k),$$

and further considering (5.11), then we have

$$\Delta V(x(k)) + x^{\mathrm{T}}(k) \Xi x(k) < 0.$$

The last inequality implies

$$x^{\mathrm{T}}(k) \Xi x(k) < V(x(k)) - V(x(k+1)). \tag{5.14}$$

For $k = 0$, 1, until $\infty$, summing (5.14) on both sides yields

$$\begin{aligned} J =& \sum_{k=0}^{\infty} x^{\mathrm{T}}(k)\Xi x(k) \\ <& V(x(0)) - V(x(\infty)) \\ <& V(x(0)) \\ =& x^{\mathrm{T}}(0)Px(0) + \sum_{j=1}^{\tau} \sum_{h=j-\tau-1}^{-1} x^{\mathrm{T}}(h)Q_j x(h), \end{aligned} \tag{5.15}$$

where the right hand side is a positive constant. Thus the system performance is guaranteed. This ends the proof. □

The condition in Theorem 5.1 is a set of LMIs with nonconvex constraints. With the developed cone complement linearization (CCL) algorithm, which is an iterative LMI approach, the controller can be readily computed (see [55, 148] and [149] for detail).

**Remark 5.3** Different from the conventional state feedback controller, where a static feedback gain $K$ will be implemented when the system evolves, the feedback control gain proposed in this chapter depends on the indicator function $\mathcal{I}(k)$. The closed-loop NCS is essentially a switching system, where the transition probability of $\mathcal{I}(k)$ is

$$\Lambda = \begin{bmatrix} 0 & 1 & 0 & \cdots & 0 \\ 0 & 0 & 1 & \cdots & 0 \\ \vdots & \vdots & \vdots & \ddots & \vdots \\ 0 & 0 & 0 & \cdots & 1 \\ 1 & 0 & 0 & \cdots & 0 \end{bmatrix} = \begin{bmatrix} 0_{(n-1)\times 1} & I_{(n-1)\times(n-1)} \\ 1_{1\times 1} & 0_{1\times(n-1)} \end{bmatrix}.$$

Here, $\Lambda_{i,i+1} = 1$, $i = 1, 2, \ldots, n-1$ means the probability $\Pr\{\mathcal{I}(k+1) = i+1 | \mathcal{I}(k) = i\} = 1$. Similar meaning is applied for $\Lambda_{n,1} = 1$. With the fixed switching path, the closed-loop system is a deterministic switching system. Therefore, the condition that the difference of the Lyapunov function $\Delta V(x(k)) < 0$ should be tested for every possible path along the system evolution. So the LMIs in Theorem 5.1 need to be solved for all $\mathcal{I}(k) = 1, 2, \ldots, n$.

## 5.4 Numerical Examples

Consider a networked system with system parameters given as follows

$$A = \begin{bmatrix} 0.8 & 0.1 & -0.016 & -0.5 \\ 0 & 0.5 & -0.337 & -0.017 \\ 0 & 0 & 1.1 & 0.2 \\ 0 & 0 & 0.024 & 0.09 \end{bmatrix},$$

$$A_{d1} = \begin{bmatrix} -0.0044 & 0.0520 & -0.0356 & 0.1662 \\ -0.0806 & -0.1230 & 0.0276 & -0.1278 \\ 0.0932 & -0.0848 & 0.0194 & -0.0420 \\ -0.0632 & -0.1570 & 0.0290 & 0.0024 \end{bmatrix},$$

$$A_{d2} = \begin{bmatrix} -0.0440 & -0.0111 & -0.0380 & 0.0035 \\ -0.0122 & 0.0228 & -0.0411 & -0.0494 \\ 0.0547 & 0.0532 & -0.0769 & 0.0438 \\ 0 & 0.0185 & -0.0083 & -0.0243 \end{bmatrix},$$

$$A_{d3} = \begin{bmatrix} -0.0171 & 0.0435 & -0.0405 & 0.0230 \\ -0.0001 & 0.0061 & -0.0487 & 0.0059 \\ -0.0154 & 0.0398 & -0.0362 & 0.0050 \\ 0.0010 & -0.0439 & -0.0201 & -0.0359 \end{bmatrix},$$

$$A_{d4} = \begin{bmatrix} -0.0542 & -0.0265 & 0.0115 & -0.0217 \\ 0.0300 & -0.0113 & 0.0773 & 0.0064 \\ -0.0037 & -0.0119 & -0.0001 & -0.0033 \\ 0.0246 & 0.0241 & 0.0023 & -0.0351 \end{bmatrix},$$

$$A_{d5} = \begin{bmatrix} 0.0025 & 0.0032 & -0.0040 & 0.0017 \\ 0.0013 & -0.0006 & -0.0004 & 0.0067 \\ -0.0043 & 0.0011 & -0.0041 & -0.0011 \\ 0.0085 & -0.0032 & -0.0014 & -0.0012 \end{bmatrix},$$

$$B = \begin{bmatrix} 0.0045 & 0.0896 & -0.0068 & -0.1377 \end{bmatrix}^{\mathrm{T}}.$$

The dimensions of the state vector $x(k)$ and the control input vector $u(k)$ are $n = 4$ and $p = 1$, respectively. The length of the historical data for each state variable is $m = 3$. We choose the weighting matrix $\Xi$ in the cost function $J$ as $0.1I_{n\times n}$. The sensor-dependent controller to be designed has 24 $n \times 1$ matrices:

$$
\begin{aligned}
K(1,0) &= [\ 0.0077 \quad 0 \quad 0 \quad 0\ ],\\
K(1,1) &= [\ 0.0213 \quad 0 \quad 0 \quad 0.0102\ ],\\
K(1,2) &= [\ 0.0285 \quad 0 \quad -0.0008 \quad 0.0412\ ],\\
K(1,3) &= [\ 0 \quad -0.1363 \quad 0.0908 \quad -0.2066\ ],\\
K(1,4) &= [\ 0.0613 \quad 0.0929 \quad -0.1737 \quad 0\ ],\\
K(1,5) &= [\ 0.0264 \quad -0.0201 \quad 0 \quad -0.0329\ ],
\end{aligned}
$$

$$
\begin{aligned}
K(2,0) &= [\ 0 \quad -0.0955 \quad 0 \quad 0\ ],\\
K(2,1) &= [\ 0.0161 \quad -0.0366 \quad 0 \quad 0\ ],\\
K(2,2) &= [\ 0.0407 \quad 0.0467 \quad 0 \quad 0.0537\ ],\\
K(2,3) &= [\ 0.0060 \quad 0 \quad 0.0975 \quad -0.3191\ ],\\
K(2,4) &= [\ 0 \quad 0.1049 \quad -0.1654 \quad -0.1838\ ],\\
K(2,5) &= [\ 0.0240 \quad -0.0322 \quad -0.0087 \quad 0\ ],
\end{aligned}
$$

$$
\begin{aligned}
K(3,0) &= [\ 0 \quad 0 \quad 0.0044 \quad 0\ ],\\
K(3,1) &= [\ 0 \quad -0.0602 \quad 0.0819 \quad 0\ ],\\
K(3,2) &= [\ 0.0431 \quad 0.0482 \quad 0.0335 \quad 0\ ],\\
K(3,3) &= [\ -0.0199 \quad -0.1363 \quad 0 \quad -0.2093\ ],\\
K(3,4) &= [\ 0.0532 \quad 0 \quad -0.1446 \quad -0.1115\ ],\\
K(3,5) &= [\ 0 \quad -0.0235 \quad -0.0106 \quad -0.0113\ ],
\end{aligned}
$$

$$
\begin{aligned}
K(4,0) &= [\ 0 \quad 0 \quad 0 \quad 0.1798\ ],\\
K(4,1) &= [\ 0 \quad 0 \quad 0.0863 \quad -0.0107\ ],
\end{aligned}
$$

$$
\begin{aligned}
K(4,2) =&[\ 0 \quad 0.0168 \quad 0.0305 \quad 0.1038\ ],\\
K(4,3) =&[\ -0.0318 \quad -0.1771 \quad 0.0905 \quad 0\ ],\\
K(4,4) =&[\ 0.1151 \quad 0.1491 \quad 0 \quad -0.2225\ ],\\
K(4,5) =&[\ 0.0293 \quad 0 \quad -0.0018 \quad -0.0584\ ].
\end{aligned} \tag{5.16}
$$

As a comparison, a sensor-dependent controller without considering the historical data is also designed:

$$
\begin{aligned}
K(1,0) &= \begin{bmatrix} -0.7615 & 0 & 0 & 0 \end{bmatrix}, \quad K(2,0) = \begin{bmatrix} 0 & -1.1651 & 0 & 0 \end{bmatrix},\\
K(3,0) &= \begin{bmatrix} 0 & 0 & 1.6105 & 0 \end{bmatrix}, \quad K(4,0) = \begin{bmatrix} 0 & 0 & 0 & 0.7005 \end{bmatrix}.
\end{aligned} \tag{5.17}
$$

The initial values in the simulation are

$$
\begin{aligned}
x(k) &= \begin{bmatrix} 0 & 0 & 0 & 0 \end{bmatrix}^{\mathrm{T}}, \quad k = -5, -4, \ldots, -1,\\
x(0) &= \begin{bmatrix} -4 & 3 & -6 & 1 \end{bmatrix}^{\mathrm{T}}.
\end{aligned}
$$

Figure 5.3 and Figure 5.4 illustrate the trajectories of $x(k)$ by using the controller in (5.17) and the proposed controller, respectively. Shown from the figures, both controllers stabilize the networked plant. The proposed controller generates a smoother response compared to the results by using the controller in (5.17), especially for $x_2(k)$ and $x_4(k)$. Yet, the settling time by using the proposed controller is larger. It may be caused by the use of historical data which delays the system response.

According to the numerical results, the cost function and the upper bound $V(x(0))$ in (5.15) are found as

$$
\begin{aligned}
J &= \sum_{k=0}^{\infty} x^{\mathrm{T}}(k)\Xi x(k) = 220.2,\\
V(x(0)) &= x^{\mathrm{T}}(0)Px(0) + \sum_{j=1}^{\tau} \sum_{h=j-\tau-1}^{-1} x^{\mathrm{T}}(h)Q_j x(h) = 616.5,
\end{aligned}
$$

which means that the condition $J < V(x(0))$ is satisfied and the proposed controller is effective for the NCS.

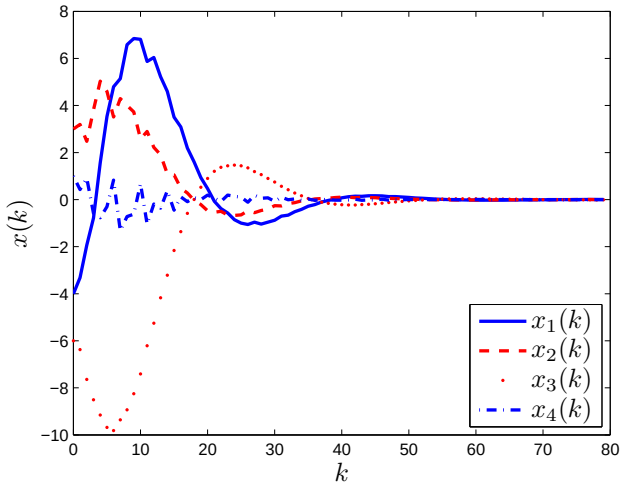


Figure 5.3: State trajectories by using controller without historical information.

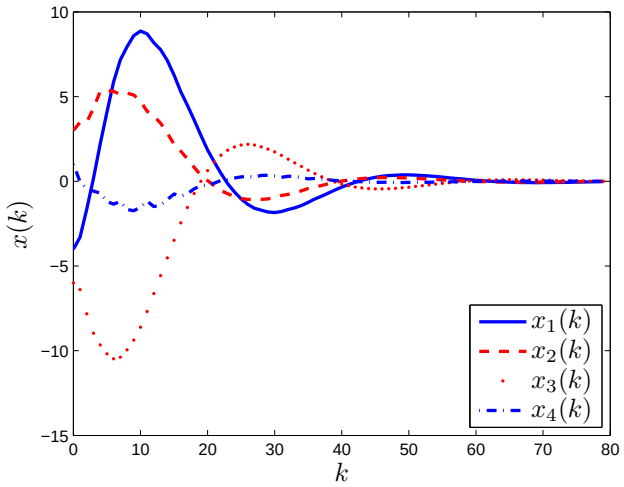


Figure 5.4: State trajectories by using the proposed controller.

## 5.5 Conclusions

In this chapter, the guaranteed cost state feedback controller is proposed for the discrete-time NCS where the plant is subject to multiple state delays. The NCS considered in this chapter has multiple channels from the sensors to the controller over which the sensors transmit the state measurement to the controller. Instead of only considering the most updated state information, the proposed controller incorporates historical data into the controller design. The simulation example shows that the proposed controller outperforms the conventional control technique.

Nevertheless, some issues deserve further research. Firstly, the inevitable measurement noise from the distributed sensors or the reconstruction errors from the

compressive sensors, if applied, will have negative effects on the control performance. Secondly, if the control signal $u$ is incorporated in the cost function, such as

$$J(u) = \sum_{k=0}^{\infty} \left[ x^{\mathrm{T}}(k) \Xi x(k) + u^{\mathrm{T}}(k) \Xi_u u(k) \right], \tag{5.18}$$

where $\Xi_u$ is the weighting factor for the control action, then the control effort can be regulated to avoid the potential actuator saturation. And lastly, if the sensor scheduling scheme is not deterministic, but stochastic, the controller to be designed should be able to guarantee that the system is stochastically stable.

# Chapter 6

# Networked Control System Design: A Haptic Example

## 6.1 Introduction

A haptic system allows the human operator to interact kinesthetically with the dynamics of a virtual environment through a motorized haptic device [150, 151]. Connecting the haptic device to the virtual environment, the virtual coupler seeks to let the haptic dynamics mimic the dynamics of the virtual environment. It is challenging to accurately render the dynamics of the virtual environment to the human operator, while simultaneously maintaining the system stability [152]. Both stability and transparency are essential for giving operators the sense of the virtual presence [153]. Although stability and transparency should be satisfied simultaneously, they are generally competing objectives [154]. On one hand, the system should be stable. Different from the traditional robot manipulators, the haptic device is interactively connected with an operator; therefore, any unexpected/unstable behavior of the device may cause oscillation of the manipulator or injuries of the human operator. Even minor oscillation can impair the realism to the user. On the other hand, transparency is required to ensure a realistic feeling of the surface properties such as the stiffness. Transparency quantifies the fidelity with which the virtual object properties are presented to the user [155]. For example, a virtual wall in the virtual environment should not be felt like materials with apparent deformation. On the contrary, a soft tissue in the virtual environment should not be touched like a wall either [156].

A meaningful transparency measurement will only exist unless all haptic dynam-

ics, including the virtual environment, the device, and the human operator interact to produce a stable system [155]. The stability issue in haptics has been studied by several authors, among which, Minsky *et al.* [157] firstly investigated it by approximating the sampling and hold effects to a delayed continuous-time model. This early study and several following work assumed a particular model of the human operator. However, the time-varying nature of the human body poses a challenge for the design of stable haptic systems. Later, the time domain passivity control approach was developed by designing the observer and controller separately to guarantee a stable haptic system. Miller *et al.* [158] attempted to avoid explicit modeling of human dynamics by establishing the passivity of the haptic components: The haptic device, the virtual coupler, and the virtual environment. Using the passivity theory, the concept of virtual coupler was proposed in [159]. The virtual coupler for one-dimensional interaction guaranteeing the stability and transparency was proposed by converting the design problem into an $H_\infty$ optimization problem in [160].

In traditional haptic systems, the control computer and the device are directly interconnected. However, with the fast development of the NCS [161, 162], there is a great trend to employ the wireless communication links in the control system; see, e.g., [163, 164, 165]. The wireless haptic systems have also been reported in [166], where a wireless controller is implemented to control the direction and the speed of a humanoid robot. In [167], the virtual environment and the haptic device are connected through wireless communication links. The measurement of the position, the velocity and the control signal are transmitted through wireless channels. The wireless haptic system has a great potential in many applications, for example, the remotely controlled robot can operate in locations where wired ones cannot reach, e.g., inside a nuclear power plant. However, the time delays introduced by the network can degrade the performance of the tele-operated devices [168]. In [168], it is suggested to alter the force reflected from the environment depending on the force applied by the human operator. In order to achieve stability of a tele-operated haptic system with time delays, several different approaches have been reported. Please refer to [169] and references therein.

In the virtual environment, multi-material parts have been increasingly employed in manufacturing as means for increasing the application as well as adding the functional capability [170]. In [170], the haptic rendering for the system where multiple virtual materials was presented. This multi-material virtual environment is called a mixed virtual environment. In mixed virtual environments, the virtual physical

property varies from place to place. Stiffness and damping are not constant throughout the mixed virtual environment. The digital object in the virtual environment which follows the operator movement through the haptic device is generally termed *avatar* [171]. Because the movement of the operator is generally not predictable, so the contact position in the virtual space between the avatar and the virtual environment is not predictable either. In other words, the change of the contact position inherently exhibits a stochastic pattern. In order to design the virtual coupler, the stochastic process as a mathematical tool can be used to characterize the trajectory of the avatar. We assume the movement of the human operator is independent of the past. Therefore, the Markov process is suitable for modeling the trajectory of the avatar due to its memoryless property. Until now, little research attention has been paid to the virtual coupler design for the mixed virtual environment, especially in a network environment, which is the main motivation of this chapter. The main contributions of the chapter are three-fold:

- The movement of the avatar in the *multi-material* virtual environment is modeled by a stochastic process to better characterize its practical feature.
- The stochastic stability condition is established for the networked haptic system considering the network-induced delay.
- By converting the design problem into a model matching problem to characterize the transparency requirement, the virtual coupler is designed for the networked haptic system.

The remainder of this chapter is organized as follows. Section 6.2 presents the system identification of the haptic device and constructs the stochastic model of the virtual environment. The virtual coupler design procedure is discussed in Sections 6.3 and 6.4 in which the stability and transparency issues are discussed, respectively. Finally, the simulation and experimental results and concluding remarks are given in Sections 6.5 and 6.6, respectively.

## 6.2 System Identification and the Stochastic Model

In order to design the virtual coupler, the mathematical description of the haptic device and the virtual environment should be obtained first [172]. In this Section,

the dynamics of the haptic device is firstly identified, and then a stochastic process is applied to model the movement of the avatar on the virtual wall.

### 6.2.1 System Identification

Since the dynamic model of the haptic device is highly involved in the design procedure, it is important to identify an accurate dynamic model. For the system used in this chapter, the input is the torque exerted by the motor while the output is the encoder measurement of the angular displacement/position of the haptic device. The Phantom Omni Haptic System used in this chapter is a 3-DOF nonlinear device, and the three degrees of freedom come from the three joints of the device. Each joint provides one rotational degree of freedom. The virtual wall considered in this chapter is in $y$-$z$ plane, as shown in Figure 6.1. So the one-dimensional penetration on the wall only depends on one joint, which makes the device rotate around axis-$z$. Considering the positions of the other two joints, the rotational inertia is configuration-dependent. Here, we derive the nominal device transfer function when $\angle P_1Ox = \angle OP_1P_2 = \pi/4$.

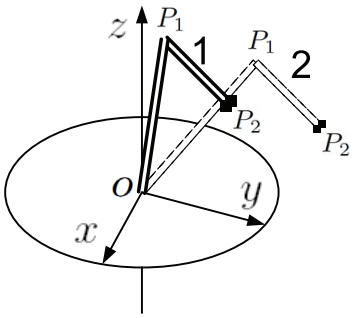


Figure 6.1: Phantom Omni device modeling.

Applying Newton's Second Law, the continuous-time transfer function from the torque (N·m) to the angular position (rad) is obtained as

$$M(s) = \frac{1}{s(ms+b)}. \tag{6.1}$$

Here, $m$ is the mass of the rod and $b$ is the axial rod damping. With one pole at the origin, the system by itself is unstable, i.e., the integrator makes the system bounded-input bounded-output (BIBO) unstable. The input-output system identification technique cannot be applied for this unstable plant directly. Therefore, a

proportional controller is used to perform the closed-loop identification experiment with the input signal as square wave with frequency of 0.4545 Hz and magnitude of 0.02 V. Using the least squares identification method, the identified parameters of the haptic device are $m = 0.7943$ kg and $b = 1.9857$ N·s/m, respectively. So the identified transfer function is

$$M(s) = \frac{1}{s(0.7943s + 1.9857)}. \tag{6.2}$$

### 6.2.2 Stochastic Model

The mixed virtual wall considered in this chapter consists of several materials. An example is shown in Figure 6.2. The mixed virtual wall consists of three distinct materials, 1, 2, and 3, with different physical properties. The avatar will contact the wall with one-dimensional penetration. Since the movement of human is not predictable or sometimes even random, it is very reasonable to characterize the stochastic behavior by its probability properties.

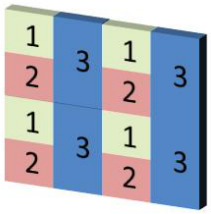


Figure 6.2: A part of the mixed virtual environment.

The contact point between the avatar and the virtual wall switches from one material to another. The stochastic switching behavior can be modeled as a Markov process ($r(k) \in \{1, 2, \ldots, N\}$, $k = 0, 1, 2, \ldots$), i.e., the Markov process is said to be in the mode $i$ when the avatar contacts with the material $i$ on the wall. Here, $N$ is the number of materials. The evolution of the Markov process can be described by the transition probability $\lambda_{ij}(\nu)$ $(i \neq j)$, where $\nu$ is the sliding speed of the avatar. Further denote the boundary length between material $i$ and material $j$ by $c_{ij}$ $(i \neq j)$. It is obvious that

$$\lambda_{ij}(\nu) \propto \frac{c_{ij}}{\sum_{j=1, j\neq i}^{N} c_{ij}} \nu. \tag{6.3}$$

A larger $c_{ij}$ leads to a larger probability for the avatar moving from mode $i$ to mode $j$. With a time-varying sliding speed $\nu$, $\lambda_{ij}(\nu)$ is time-varying, and the resulting Markov process is nonhomogeneous which is hard to tackle. In order to simplify

the problem formulation, we assume that the avatar is sliding (if contacting with the virtual wall) at a constant speed, i.e., $\nu$ is constant, then $\lambda_{ij}(\mu) \equiv \lambda_{ij}$. As a matter of fact, the constant speed traverse movement can be widely used in the industry applications, such as laser fabrication processes [173], abrasive machining processes [174], and friction stir processes [175]. The transition matrix $\Lambda$ of the discrete-time Markov process $r(k)$ is given by

$$\Lambda = [\lambda_{ij}] \in \mathbb{R}^{N\times N}, \quad \lambda_{ii} = 1 - \sum_{j=1, j\neq i}^{N} \lambda_{ij}.$$

Here, $\Lambda$ is a constant matrix and the transition probabilities of the homogeneous Markov process are given by

$$\Pr\{r(k+1) = j | r(k) = i\} = \lambda_{ij}.$$

With the identified system transfer function and the stochastic switching model, we are at a good position to present the virtual coupler design for the mixed virtual wall. About the patch patterns and the transition rates, we have the following remarks.

**Remark 6.1** The patches on the virtual wall align in a repeated pattern. In such a pattern, all patches with the same material have the identical shape and the same adjacent patches. Therefore, the transition rate $\lambda_{ij}$, $j = 1, \ldots, N$ on one patch $i$ can be applied to all patches with material $i$ all across the virtual wall.

**Remark 6.2** It is noticed that the avatar cannot jump **arbitrarily** between any two patches. For example, material $i$ is not adjacent to material $j$, i.e., $c_{ij} = 0$, then the avatar cannot move from $i$ to $j$, nor from $j$ to $i$. In such cases, some symmetric elements in the transition matrix $\Lambda$ will be 0 ($\lambda_{ij} = \lambda_{ji} = 0$), yet $\Lambda$ is still a valid transition matrix. The design procedure in this chapter allows 0 elements in $\Lambda$.

## 6.3 Stability Analysis

In this section, before the stability analysis of the haptic system, the role of the haptic controller will be firstly discussed. For the haptic system depicted in Figure 6.3, there are two torques imposed on the manipulator of the device. Through the wireless

communication channel, the motor in the device drives the manipulator with a torque $u$. The torque $u$ from the controller to the motor will be delayed when transmitting over the communication link, which is denoted by $\hat{u}$. Similarly, the haptic position $\hat{x}$ will be delayed through the communication link, where the delayed position is denoted by $x$. The delays of the position $\hat{x}$ and the torque $u$ are denoted by $\tau_1$ and $\tau_2$, respectively. The time delays considered in this chapter are assumed to be constant values. In fact, the constant delays can be used to model some types of networks with certain communication protocols. The virtual coupler and the virtual environment can be lumped together as $C_o$. Meanwhile, the human operator applies a torque $f$ on the manipulator. (All the variables are functions of the Laplace variable $s$ unless otherwise specifically indicated [152].) Using the identified transfer function $M$ in (6.2), the position of the manipulator $\hat{x}$ is given by

$$\hat{x} = M(f + \hat{u}), \tag{6.4}$$

while the control action $u$ is

$$u = -C_o x. \tag{6.5}$$

From the view of the human operator, if there is no communication delay, the closed-loop system from $f$ to $\hat{x}$ is

$$G = \frac{\hat{x}}{f} = \frac{M}{1 + MC_o}. \tag{6.6}$$

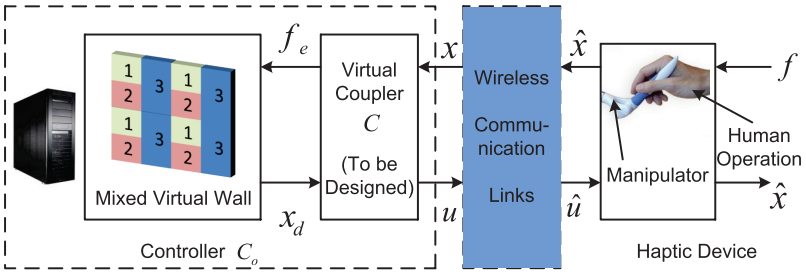


Figure 6.3: Schematic diagram of the haptic system.

In the haptic rendering, the objective is to shape the closed-loop response of the device position $\hat{x}$ to the human operator's input $f$. The desired position response is denoted by $x_d$. Therefore, the transparent environment dynamics is achieved by minimizing the error between the actual position response and the desired position response, i.e., $\hat{x} - x_d$. When the error is zero, the perfect haptic rendering is achieved.

Reconfigure the problem into the following minimization problem

$$\min_{\text{Virtual Coupler } C} |\hat{x} - x_d|, \tag{6.7}$$

which will be presented in Section 6.4.

Because the complex virtual environment can be decomposed to small planar pieces, we focus on the virtual wall problem in which the virtual environment is modeled as a linear spring-damper system [159]. When the mixed virtual wall is penetrated, the human should feel a reaction force that equals to

$$f_i = -K_i x - B_i \dot{x}, \tag{6.8}$$

where $K_i$ and $B_i$ are the stiffness and damping of material $i$. In fact, the wall can only be compressed, so the negative signs indicate that the force direction is opposite to the displacement and the velocity.

A sufficient stability condition of the virtual wall interaction in the haptic system is given by $b > K_i T/2 + |B_i|$ [176]. This condition reveals that for a haptic system without virtual coupler, the stability can not be guaranteed if the damping coefficient $B_i$ is large, or the stiffness $K_i$ is large, or the sampling period $T$ is large. This leads to the idea of introducing the virtual coupler block $C(z) \in \{C_i(z)\}$, $i = 1, 2, \ldots, N$, where $C_i(z)$ will be applied when the avatar interacts with material $i$. So $C(z)$ is a switching virtual coupler. The virtual coupler brings extra degrees of freedom to the system design with a larger sampling period and more flexible choices of $K_i$ and $B_i$.

**Theorem 6.1.** *If the human operator has a passive real rational transfer function and that*

$$\frac{z-1}{Tz}\left(C_i(z) - \frac{T}{2b}\right) \in \text{DPR}, \tag{6.9}$$

*where DPR denotes the set of all discrete positive real transfer functions, then the haptic system in Figure 6.4 is oscillation free.*

The proof of this result is inspired by the result in [177] where a deterministic case was presented.

*Proof.* Denote the networked parallel connection of $F(z)$ and $C_i(z)(z-1)/Tz$ in Figure 6.4 with input $f_k$ and output $v_k$ as $L_i(z)$, when the avatar contacts with the material $i$,

$$L_i(z) = \frac{z-1}{Tz} F(z) z^{-(\tau_1+\tau_2)} + \frac{z-1}{Tz} C_i(z),$$

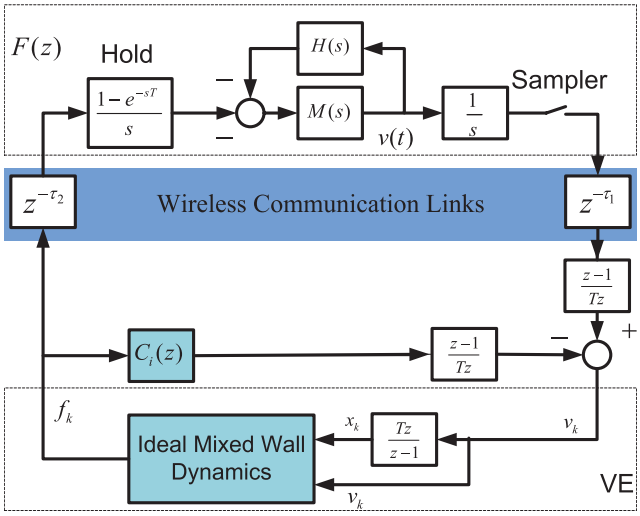


Figure 6.4: Block diagram of the haptic system.

where

$$F(z) = \mathcal{Z}\left\{\frac{1-e^{-sT}}{s^2}\cdot\frac{M(s)}{1+M(s)H(s)}\right\}.$$

Here, $H(s)$ represents the human operation, which is a positive real rational transfer function. It can be shown that [177]

$$\left(\frac{z-1}{Tz}F(z)+\frac{1}{2b}\frac{z-1}{z}\right)z^{-(\tau_1+\tau_2)}\in \text{DPR}. \tag{6.10}$$

If we choose $C_i(z)$ such that (6.9) holds, then the summation $L_i(z)$ is DPR.

To show that the virtual environment (VE) in Figure 6.4 is passive, we construct the following storage function

$$V_E(x_k)=\begin{cases}\frac{K}{2T}x_k^2, & x_k>0,\\ 0, & x_k\le 0.\end{cases} \tag{6.11}$$

$x_k$ and external force $f_k$ are

$$x_k = x_{k-1}+Tv_k,\quad f_k=\begin{cases}K_ix_k+B_iv_k, & x_k\ge 0,\\ 0, & x_k<0,\end{cases}$$

where $v_k$ is the velocity of the manipulator. The passive definition in the energy sense requires that the input energy into the system should not be less than the increment of

the storage function. In other words, $v_k f_k$ should not be less than $V_E(x_k) - V_E(x_{k-1})$. Then, in any time interval, from step $k$ to $k+p$ where $p$ is any positive integer, the following inequality holds [160]

$$\sum_{i=k}^{k+p} v_i f_i \geq V_E(x_{k+p}) - V_E(x_k).$$

By computing $V_E(x_k) - V_E(x_{k-1})$ in different cases, it can be seen that $v_k f_k \geq V_E(x_k) - V_E(x_{k-1})$. Therefore, the system is oscillation free. □

**Remark 6.3** The stochastic stability of the haptic system is established based on the passivity theory. By proving that the connected system among the virtual coupler, the haptic device and the human operator is passive as well as that the virtual environment is passive, the stability of the closed-loop system is achieved. Different from [177], the time delays and the stochastic switching of the closed-loop system are considered in this chapter.

In this section, the stability condition has been derived for the haptic system. In the following Section, the virtual coupler will be designed to maximize the transparency of the networked haptic system.

## 6.4 Transparent Virtual Coupler Design

The admittance of a haptic system is the transfer function from the position to the motor applied torque. To facilitate the derivation, we assume that the avatar is in contact with the virtual environment, then the system behaves as a switching system. For the haptic system shown in Figure 6.4, the ideal admittance is

$$G_i(z) = B_i \frac{z-1}{Tz} + K_i, \quad i = 1, 2, \ldots, N.$$

as this would be the discrete-time equivalence of the spring-damper virtual wall model in (6.8) without transmission delays. However, from the human operator's point of view, due to the virtual coupler and the transmission delays, the actual resulting admittance becomes

$$G_{v,i}(z) = \frac{G_i(z)}{1 + G_i(z)C_i(z)} z^{-(\tau_1+\tau_2)}, \quad i = 1, 2, \ldots, N.$$

The difference between the ideal admittance and the resulting admittance, $G_{v,i}(z) - G_i(z)$, is called haptic distortion. The minimization problem in (6.7) is equivalent to minimizing the haptic distortion. Usually, the human operators are more sensitive to a specific frequency range, for which they are more interested in preserving the transparency. It is more a physiological, psychophysical, and even neurological problem on how to determine the interesting frequency in the haptic rendering; the interested reader can refer to [178] and references therein. An appropriate weighting function could be selected according to the operator sensitivity over different frequencies [160]. So the weighting function $W(z)$ that allows to maximize transparency at different frequencies is introduced. Then the problem is converted to designing the virtual coupler $C(z)$ that minimizes the following transparency criteria

$$\left\| W(z) \left( \frac{G_i(z)}{1 + G_i(z)C_i(z)} z^{-(\tau_1+\tau_2)} - G_i(z) \right) \right\|_\infty^2, \quad i = 1, 2, \ldots, N. \tag{6.12}$$

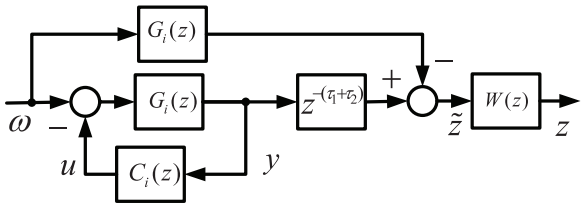


Figure 6.5: Block diagram representation of $W(z) \cdot \left( \frac{G_i(z)}{1+G_i(z)C_i(z)} z^{-(\tau_1+\tau_2)} - G_i(z) \right)$.

For simplicity and the ease of the following computation, the direct feedforward term is pulled out from $C_i(z)$, and we restrict the search among the virtual couplers of the form

$$C_i(z) = \bar{C}_i(z) + \frac{dz}{z-1} + D_{c_i},$$

where $\bar{C}_i$ is a strictly proper transfer function, so Theorem 6.1 is satisfied. The remaining terms in the above equation can be regarded as the feedback of $G_i(z)$. As a result, the inner closed-loop transfer function $\bar{G}_i$ is obtained as

$$\bar{G}_i(z) = \frac{G_i(z)}{1 + G_i(z)\left(\frac{dz}{z-1} + D_{c_i}\right)},$$

leaving the external feedback $\bar{C}_i$. With these two notations, Figure 6.5 can be redrawn as Figure 6.6. The realizations of $G_i(z)$ and $\bar{G}_i(z)$ in Figure 6.6 with inputs $\omega(k)$ and

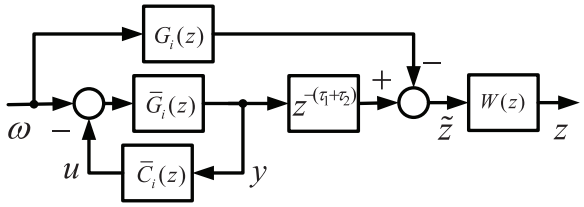


Figure 6.6: Block diagram representation of $W(z)\cdot\left(\frac{\bar{G}_i(z)}{1+\bar{G}_i(z)\bar{C}_i(z)}z^{-(\tau_1+\tau_2)}-G_i(z)\right)$.

output $y(k)$ are

$$\begin{aligned}\mathbb{G}: \quad x_g(k+1) &= A_{gi}x_g(k)+B_{gi}\omega(k),\\ y(k) &= C_{gi}x_g(k)+D_{gi}\omega(k),\end{aligned}$$

$$\begin{aligned}\bar{\mathbb{G}}: \quad x_{\bar{g}}(k+1) &= A_{\bar{g}i}x_{\bar{g}}(k)+B_{\bar{g}i}\omega(k),\\ y(k) &= C_{\bar{g}i}x_{\bar{g}}(k)+D_{\bar{g}i}\omega(k).\end{aligned}$$

The realization of the strictly proper transfer function $\bar{C}_i(z)$ is

$$\begin{aligned}\mathbb{C}: \quad x_c(k+1) &= A_{ci}x_c(k)+B_{ci}y(k),\\ u(k) &= C_{ci}x_c(k).\end{aligned}$$

The realization of the weighting function $W(z)$ is

$$\begin{aligned}\mathbb{W}: \quad x_w(k+1) &= A_w x_w(k)+B_w\tilde{z}(k),\\ z(k) &= C_w x_w(k)+D_w\tilde{z}(k).\end{aligned} \tag{6.13}$$

Connecting the systems $\mathbb{G}$, $\bar{\mathbb{G}}$, $\mathbb{C}$, and $\mathbb{W}$, the closed-loop system is given by

$$\begin{aligned}\mathbb{F}: \quad \tilde{x}(k+1) &= \tilde{A}_i\tilde{x}(k)+\tilde{B}_i\omega(k),\\ z(k) &= \tilde{C}_i\tilde{x}(k)+\tilde{C}_{di}\tilde{x}(k-\tau_1-\tau_2)+\tilde{E}_i\omega(k),\end{aligned}$$

where

$$\tilde{x}(k)=\begin{bmatrix}x_g(k)\\ x_{\bar{g}}(k)\\ x_c(k)\\ x_w(k)\end{bmatrix},\quad \tilde{B}_i=\begin{bmatrix}B_{gi}\\ B_{\bar{g}i}\\ B_{ci}D_{\bar{g}i}\\ 0\end{bmatrix},$$

$$\tilde{A}_i = \begin{bmatrix} A_{gi} & 0 & 0 & 0 \\ 0 & A_{\bar{g}i} & -B_{\bar{g}i}C_{ci} & 0 \\ 0 & B_{ci}C_{\bar{g}i} & A_{ci} - B_{ci}D_{\bar{g}i}C_{ci} & 0 \\ 0 & 0 & 0 & A_w \end{bmatrix}, \quad \tilde{E}_i = \begin{bmatrix} D_w D_{gi} \end{bmatrix},$$

$$\tilde{C}_i = \begin{bmatrix} D_w C_{gi} & 0 & 0 & C_w \end{bmatrix}, \quad \tilde{C}_{di} = \begin{bmatrix} 0 & -D_w C_{\bar{g}i} & D_w D_{\bar{g}i} C_{ci} & 0 \end{bmatrix}. \tag{6.14}$$

The goal is to determine $A_{ci}$, $B_{ci}$ and $C_{ci}$ such that the $H_\infty$ norm of the system $\mathbb{F}$ from the input $w$ to the output $z$ is minimized. Then the problem can be summarized as

$$\min_{A_{ci}, B_{ci}, C_{ci}} \|\mathbb{F}\|_\infty^2. \tag{6.15}$$

In the following, we analyze the $H_\infty$ disturbance attenuation performance of the haptic system. From Theorem 2 in [179], the system $\mathbb{F}$ is stochastically stable with the given disturbance attenuation level $\gamma$, i.e.,

$$\|z\|_2 < \gamma \|\omega\|_2, \tag{6.16}$$

if there exist matrices $P_i = P_i^{\mathrm{T}} > 0$, $i = 1, 2, \ldots, N$, and $Q = Q^{\mathrm{T}} > 0$ such that

$$\begin{bmatrix} \Xi_i & \tilde{C}_i^{\mathrm{T}} \tilde{C}_{di} & \tilde{A}_i^{\mathrm{T}} \tilde{P}_i \tilde{B}_i + \tilde{C}_i^{\mathrm{T}} \tilde{E}_i \\ * & -Q + \tilde{C}_{di}^{\mathrm{T}} \tilde{C}_{di} & \tilde{C}_{di} \tilde{E}_i \\ * & * & -\gamma^2 I + \tilde{B}_i^{\mathrm{T}} \tilde{P}_i \tilde{B}_i + \tilde{E}_i^{\mathrm{T}} \tilde{E}_i \end{bmatrix} < 0, \tag{6.17}$$

where

$$\Xi_i = \tilde{A}_i^{\mathrm{T}} \tilde{P}_i \tilde{A}_i - P_i + Q + \tilde{C}_i^{\mathrm{T}} \tilde{C}_i$$

holds for all $i = 1, 2, \ldots, N$. Here, $\gamma$ is a positive scalar and $\tilde{P}_i = \sum_{j=1}^{N} p_{ij} P_j$.

Due to the coupled terms in (6.17), the matrix inequality is not in a linear form. The algorithm from [180] and [181] is applied to solve the coupled matrix inequality. Define the following convex set $\Omega_\eta$, where $\eta \in \{1, 2, \ldots, N\}$. If a triple $\{A_c, B_c, C_c\}$ is selected from the set $\Omega_\eta$, then the matrix inequalities in (6.17) becomes linear matrix inequalities (LMIs). Then solve the minimization problem in (6.15) for each set, and choose the minimum disturbance attenuation level $\gamma$ as the approximation of the solution of (6.15). The virtual coupler is readily obtained.

## 6.5 Simulation and Experimental Results

We use the Phantom Omni Haptic System (Figure 6.7) as the test platform with sampling period of $T = 0.05$ s. For the mixed virtual wall illustrated in Figure 6.2, the stiffness and damping are given by $K_1 = 1000$ N/m, $B_1 = 2$ N·s/m, $K_2 = 800$ N/m, $B_2 = 2$ N·s/m, and $K_3 = 800$ N/m, $B_3 = 5$ N·s/m for materials 1, 2, and 3, respectively. Considering the patch pattern and (6.3), the transition matrix for

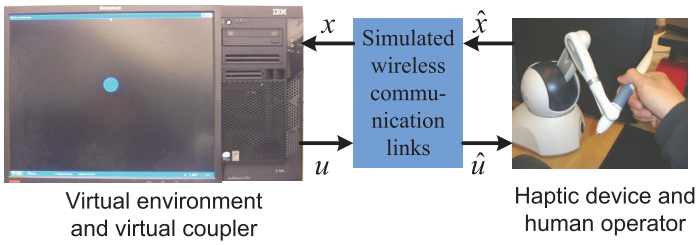


Figure 6.7: Configuration of the Phantom Omni Haptic System.

switching of the contact position between the avatar and the virtual wall is given by

$$\Lambda = \begin{bmatrix} 0.4 & 0.3 & 0.3 \\ 0.3 & 0.4 & 0.3 \\ 0.15 & 0.15 & 0.7 \end{bmatrix}.$$

### 6.5.1 Simulation

Before the experiments, the simulation studies are performed for each material. A constant force of 1 N is applied to the device towards the wall. The results of penetration depth on each material are shown in Figure 6.8. From this figure, it can be seen that with the virtual coupler presence, there is decayed oscillation at the beginning of the contact between the avatar and the wall. And then the end effector is stabilized at a constant depth. The final depths of the avatar penetration into materials 2 and 3 are the same, which comes with no surprise, because both materials have the same stiffness. Also, the delays of the three responses are caused by the simulated constant network-induced delays.

### 6.5.2 Experiment

In the experiment, the haptic device follows the movement of an arm. However, due to the randomness of the human behavior, the applied force onto the virtual wall will

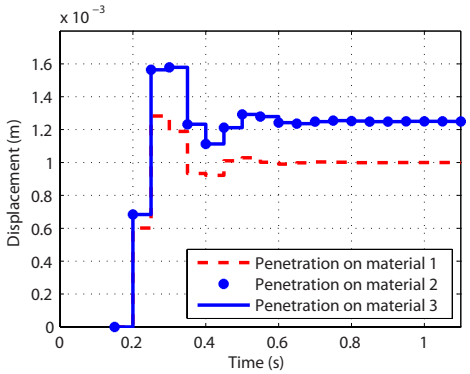


Figure 6.8: Penetration response by applying a constant force on each material.

not be constant. The simulated communication delays are set as $\tau_1 = \tau_2 = 3T = 0.15$ s. The positions of the device are measured by the mounted encoders on the device and transmitted to virtual environment. Depending on the relative positions between the device and the virtual wall, the control computer calculates the feedback force to the user. The trajectory of the end effector is an arc. The feedback force from the virtual environment/wall is felt by the user. In the experiment, it is clear that different parts of the wall have different stiffness; so the designed haptic system can provide a good haptic perception for the mixed virtual wall.

From Figure 6.2, the area of material 3 is larger than 1 and 2, so the avatar has less chance of moving from material 3 to 1 or 2, therefore $\lambda_{31}$ and $\lambda_{32}$ are smaller than the others. With the designed virtual coupler, the 3D trajectory of the avatar is shown in Figure 6.9 from different view points in order to obtain a clearer view. From this figure, the penetration is in $x$ direction and the avatar is sliding on the $y$-$z$ plane. The $x$ displacement is very small without oscillation, so the designed virtual coupler is effective for the haptic system. By comparing the simulation and experimental results, the penetration depths are in the same order, which shows good agreement of the results.

The switching among different materials on the virtual wall is shown in Figure 6.10. The red curve is the moving trajectory of the avatar on the wall which starts from the left and moves to the right. Comparing with Figure 6.2, the Markov modes evolution can be concluded from Figure 6.10: $\{2, 3, 2, 3, 2, 1\}$.

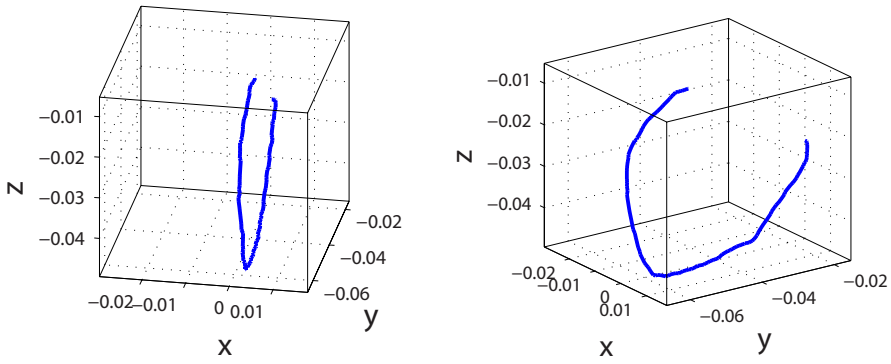


Figure 6.9: The 3D avatar trajectory at different view points.

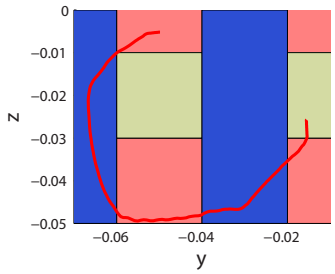


Figure 6.10: The trajectory of the avatar on the mixed virtual wall.

## 6.6 Conclusion and Future Work

In this chapter, the virtual coupler has been designed for the networked haptic system, in which the virtual environment is a mixed virtual wall consisting of multiple materials. The controller of the haptic system and the haptic device are connected via wireless communication links. The constant communication delays of the wireless connection were considered. The effectiveness of the proposed virtual coupler was validated and tested on the Phantom Omni Haptic System.

As our future work, the following technical issues will be further explored. Firstly, in this chapter, using the Markov process to characterize the stochastic behavior assumes that the avatar is sliding at a constant speed; yet in some applications, the speed is varying. In order to eliminate this assumption, a more general semi-Markov process will be investigated for this problem. Secondly, the designed virtual coupler depends on the damping ($b$) of the haptic device. This parameter may change when the haptic device moves in the workspace. Moreover, the damping can change drastically in $y$ and $z$ directions, because different motors in the device will be involved

in $y$ or $z$ penetration on the wall; for example, when the wall is not in the $y$-$z$ plane. Thirdly, the current work considers the constant delays. The cases of time-varying delays or random delays will deserve further research.

# Chapter 7

# Robust Tracking Control of Networked Control Systems: Application to a Networked DC Motor

## 7.1 Introduction

With the fast development of digital network technologies, there is a steadily increasing trend to integrate communication networks into the control system design. This kind of systems are called networked control systems (NCSs) [32, 33, 141, 182, 183]. NCSs have advantages in terms of cost reduction, easy system diagnosis and flexibility, relatively simple addition and replacement of individual elements, and so on. Hence, the industrial applications of NCSs are very wide, ranging from the large scale factory automation and plant monitoring [184, 185] to smaller yet complicated systems such as autonomous mobile robots [37]. The presence of wired and/or wireless networks, however, has also induced several challenging problems. These challenges involve the constraints on communication bandwidth, network-induced time delays, packet dropouts, jitter, and asynchronization [40, 186]. It is recognized that the network characteristics must be considered explicitly in the NCS design.

Among the challenges that communication networks bring, the time delays and packet dropouts are two major issues that may degrade system performance and, even worse, cause instability [99]. On the one hand, new internet transport proto-

cols were studied for teleoperation tasks regarding network characteristics [187, 188]. Some network protocols guarantee the synchronization among network nodes, such as WorldFIP, FlexRay, and Profibus-DP; other network protocols, for instance, Ethernet or WiFi, cannot guarantee the synchronization among the sensor, the controller, and the actuator [189]. In this chapter, we consider a scenario where the system components are connected and synchronized over networks with time-varying delays [71, 190]. Besides standard industrial networks such as Profibus and CAN, the general-purpose networks, such as Ethernet, are increasingly applied in NCSs due to its affordability, simplicity, widespread usage, and the connectivity to Internet; see [191] and references therein for more details. On the other hand, the control community has developed new methods regarding the stability conditions and the performance analysis for NCSs by taking network properties into account [54, 55, 125]. Compared to the constant delay model and the bounded random delay model, the stochastic process model cannot only characterize the stochastic property of the delay but also illustrate the correlation between the current time delay and the delay in next transmission [46]. The Bernoulli process and the discrete-time Markov chain were effectively employed to model time delays and packet dropouts in the literature [47, 55]. The resulting closed-loop system was formulated as a Markovian jump linear system (MJLS) [24, 48, 49, 50]. Further, the stabilization and control synthesis of NCSs have been considered in the existing literature under the framework of MJLSs. Xiao *et al.* [47] designed the delay dependent state feedback controller for NCSs with sensor-to-controller (S-C) delays modeled by Markov chains, and the delay independent output feedback controller for NCSs with both S-C and controller-to-actuator (C-A) delays. In [50], the authors considered a vehicle control problem over lossy communication links where the packet loss process was modeled as the Bernoulli process and the controller was co-located with the actuator, meaning that only the S-C packet loss was considered in this NCS; an $H_\infty$ mode dependent output feedback controller was designed. In [192], the authors considered the stabilization problem of NCSs with random communication delays both in the system state and in the S-C links. To consider both S-C and C-A delays in NCSs, and to make full use of the available delay information, Zhang and Shi *et al.* [53, 55] proposed a two-mode dependent controller that depends on both S-C and C-A delay information for NCSs with time delays modeled by Markov chains. It is noticed that the state feedback controller in [55] and the output feedback controller in [53] depend on the both current S-C delay ($\tau_k$) and previous C-A delay ($d_{k-1}$ or $d_{k-\tau_k-1}$). If the newest delay infor-

mation can be incorporated into the controller design, it is desirable to achieve better performance. Hence, a more effective delay dependent control scheme is expected to be dependent on both *current* S-C delays and *current* C-A delays. However, when control signals are generated, the current C-A delay is not known to the controller because the C-A delay will occur in the future when the control signal is transmitted through the C-A link. In this chapter, a "*send all, apply one*" scheme is developed to design the delay dependent controller that depends on not only the current S-C delay but also the current C-A delay.

It is well recognized that the tracking control problem is more challenging than stabilization and can find applications in various fields. While most of the existing work focused on the stabilization problem, only a few considered the tracking problem for NCSs [193, 194, 195, 196, 197]. In [193], the tracking control problem for NCSs with uncertain, time-varying sampling intervals and network delays was considered. Wu *et al.* [194] proposed an event-driven networked predictive tracking control method, where the control signal was selected according to the plant output. In [195], the $H_\infty$ output tracking control was studied for sampled-data systems; the time delays were assumed to have lower and upper bounds. In [196], the authors studied the $H_\infty$ control for NCSs with constant and time-varying sampling periods. Li *et al.* proposed an output tracking controller design method in [197]. Nevertheless, the step tracking control of NCSs with random delays modeled by Markov chains has not been fully investigated in the existing literature, which motivates the research in this chapter.

The contributions of this chapter are mainly three-fold.

- A "send all, apply one" scheme is applied to compensate for the C-A delays that can be modeled as Markov chains. For possible C-A delays, all the two-mode delay dependent control signals will be computed and sent to the actuator node; according to the actual C-A delay measured at the actuator node, the corresponding control signal will be picked up and applied. Since the random C-A delay is assumed to be governed by the Markov chain, the choice of a specific control signal is also governed by the Markov chain. The NCS with the "send all, apply one" scheme is then formulated as an MJLS to facilitate the controller design. Essentially, the "send all, apply one" scheme is originated from the prediction-based idea that has been applied in [198, 199, 200]. This work extends the scheme to NCSs subject to random delays governed by Markov chains.

- A delay dependent output feedback controller is developed. Such a controller depends on both current S-C and current C-A delays. Compared to the delay independent controller in [47], the proposed control scheme can reduce the conservativeness and it can include the delay independent controller as a special case. Compared to the delay dependent controller in [55], the proposed controller is more effective because it depends on the *current* C-A delay whereas the controller in [55] depends on the *previous* C-A delay.

- With the introduction of the ideal plant response, we develop the robust $H_2$ and $H_\infty$ control schemes to achieve the step tracking with disturbance rejection for NCSs with S-C and C-A delays modeled by Markov chains, which has not been studied in the literature.

The remainder of this chapter is organized as follows. The problem formulation of the NCS and the objective are given in Section 7.2. In Section 7.3, the closed-loop system is transformed to an MJLS and the robust $H_2$ and $H_\infty$ tracking problems are solved under the framework of MJLSs. Numerical simulations and experimental tests are presented in Section 7.4. Finally, concluding remarks are addressed in Section 7.5.

## 7.2 Problem Statement

Consider the NCS setup shown in Figure 7.1. The linear time-invariant plant can be described by

$$x(k+1) = Ax(k) + B\left[\tilde{u}(k) + \omega(k)\right], \tag{7.1a}$$

$$y(k) = Cx(k), \tag{7.1b}$$

where $x(k) \in \mathbb{R}^n$, $\tilde{u}(k) \in \mathbb{R}^m$, $y(k) \in \mathbb{R}^p$, and $\omega(k) \in \mathbb{R}^m$ are state, control, output, and disturbance vectors, respectively. $A$, $B$, and $C$ are known constant matrices with appropriate dimensions. Noting that, in Figure 7.1 the disturbance $\omega(k)$ affects the delayed control signal $\tilde{u}(k)$ directly, so it enters the system via the same $B$ matrix.

The controller node and the plant node are connected via S-C and C-A network links. Here, it is assumed that the sensor, controller and actuator are clock-driven and synchronized. $\tau_k$ stands for the S-C delays and $d_k$ represents the C-A delays, and

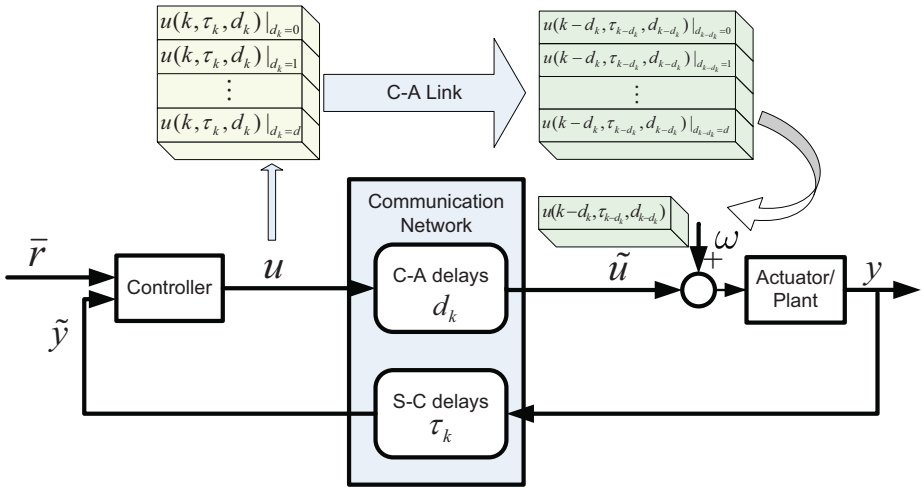


Figure 7.1: Diagram of a networked control system.

both $\tau_k$ and $d_k$ are bounded, that is

$$0 \leq \tau_k \leq \tau, \quad 0 \leq d_k \leq d. \tag{7.2}$$

To be precise, the random time delays from one component to another are continuous values. However, the clock-driven controller and actuator only accept data at discrete time instants. So $\tau_k$ and $d_k$ take values in discrete sets [71].

**Remark 7.1** The packet dropout and disorder can be incorporated naturally in the current problem formulation. If a packet is lost or a disorder occurs, the data from the most recently arrived packet will be applied. So the packet dropout and disorder can be treated in a similar way as tackling delays. Provided that the number of the successive/consecutive packet dropout is upper bounded, which is a commonly used assumption [197, 201, 202], the current problem formulation can accommodate packet dropouts and disorders.

The current delay is usually correlated with previous ones. For example, the network load which affects the transmission time is a time-varying factor [46]. So it is effective to model $\tau_k$ and $d_k$ as two homogeneous Markov chains that take values in $\mathcal{M} = \{0, 1, \cdots, \tau\}$ and $\mathcal{N} = \{0, 1, \cdots, d\}$, and their transition probability matrices are $\Lambda = [\lambda_{ij}]$ and $\Pi = [\pi_{rs}]$, respectively [47, 53, 55]. This implies that $\tau_k$ and $d_k$ jump from mode $i$ to $j$ and from mode $r$ to $s$, respectively, with probabilities $\lambda_{ij}$ and

$\pi_{rs}$, which are defined by

$$\lambda_{ij} = \Pr(\tau_{k+1} = j | \tau_k = i), \tag{7.3}$$

$$\pi_{rs} = \Pr(d_{k+1} = s | d_k = r) \tag{7.4}$$

with the constraints $\lambda_{ij}, \pi_{rs} \geq 0$ and

$$\sum_{j=0}^{\tau} \lambda_{ij} = 1, \qquad \sum_{s=0}^{d} \pi_{rs} = 1 \tag{7.5}$$

for all $i, j \in \mathcal{M}$ and $r, s \in \mathcal{N}$. More details on time delays modeled by Markov chains are presented in [47].

Now, the objective of this chapter is to achieve step tracking for the NCS shown in Figure 7.1, more specifically, to find a static output feedback control law that can guarantee the closed-loop stability and force the tracking error to be close to zero. Here, we choose the static output feedback control method because of the simplicity of its implementation.

In order to make the steady state tracking error zero, we introduce the *ideal plant response* for the system in (7.1) by following the ideas in [203, 204]. When the tracking error is zero for $k > 0$ (perfect tracking), the resulting plant state and the control signal are denoted as $x^* \in \mathbb{R}^n$ and $\tilde{u}^* \in \mathbb{R}^m$. Then, $x^*$ and $\tilde{u}^*$ can be derived from the following equations:

$$x^* = Ax^* + B\tilde{u}^*, \tag{7.6a}$$

$$\bar{r} = Cx^*, \tag{7.6b}$$

or

$$\begin{bmatrix} 0 \\ \bar{r} \end{bmatrix} = N \begin{bmatrix} x^* \\ \tilde{u}^* \end{bmatrix}, \tag{7.7}$$

where

$$N = \begin{bmatrix} A - I & B \\ C & 0 \end{bmatrix}.$$

It is assumed that $A$, $B$, and $C$ are of full rank. If $p > m$, in general, a solution does not exist. So we assume that $p \leq m$. If $p = m$, the unique solution can be obtained

by a standard matrix inversion of $N$. If $p < m$, there is no unique solution. One possible solution can be obtained by solving the following equation:

$$\begin{bmatrix} x^* \\ \tilde{u}^* \end{bmatrix} = N^{\mathrm{T}}(NN^{\mathrm{T}})^{-1} \begin{bmatrix} 0 \\ \bar{r} \end{bmatrix} \triangleq \begin{bmatrix} \Omega_{11} & \Omega_{12} \\ \Omega_{21} & \Omega_{22} \end{bmatrix} \begin{bmatrix} 0 \\ \bar{r} \end{bmatrix}.$$

Define $\hat{x}(k) = x(k) - x^*$, $\hat{u}(k) = \tilde{u}(k) - \tilde{u}^*$, and $\hat{y}(k) = y(k) - \bar{r}$, we have the following system:

$$\hat{x}(k+1) = A\hat{x}(k) + B\hat{u}(k) + B\omega(k), \tag{7.8a}$$

$$\hat{y}(k) = C\hat{x}(k). \tag{7.8b}$$

Now, we propose the *delay dependent output feedback controller*:

$$\hat{u}_1(k) = K(\tau_k, d_k)\hat{y}(k - \tau_k), \tag{7.9}$$

where $\hat{u}_1(k)$ is the control signal at the controller node and

$$\hat{u}_1(k) = u(k) - \tilde{u}^*, \quad \hat{u}(k) = \hat{u}_1(k - d_k). \tag{7.10}$$

Once $K(\tau_k, d_k)$ is designed, the control signal $u(k)$ can be obtained from (7.10)

$$u(k) = [\Omega_{22} - K(\tau_k, d_k)]\,\bar{r} + K(\tau_k, d_k)y(k - \tau_k). \tag{7.11}$$

It is important to note that the controller in (7.9) is dependent on both current S-C delay $\tau_k$ and current C-A delay $d_k$ at time instant $k$. However, a problem arises here: The S-C delay $\tau_k$ can be obtained by using the time-stamping technique at time instant $k$ whereas the current C-A delay $d_k$ cannot be known by the controller because it does not happen yet. To solve this problem, we need to utilize the advantage the network brings: A sequence of signals can be packed and transmitted simultaneously [125, 199]. Then, the "*send all, apply one*" scheme is proposed to solve the aforementioned problem. The scheme is described as follows. When the output information $\hat{y}(k - \tau_k)$ is received at the controller node, the controller calculates a series of control signals for all possible $d_k$ based on the known $\tau_k$ and sends them to the actuator node

in a packet. Hence, the control sequence packet is

$$\begin{bmatrix} u(k,\tau_k,d_k)|_{d_k=0} \\ u(k,\tau_k,d_k)|_{d_k=1} \\ \vdots \\ u(k,\tau_k,d_k)|_{d_k=d} \end{bmatrix}. \tag{7.12}$$

For example, $u(k,\tau_k,d_k)|_{d_k=0}$ means the control signal generated at time instant $k$ based on the known $\tau_k$, when $d_k = 0$. At time instant $k$, considering the C-A delay $d_k$, the control sequence packet at the actuator/plant node is

$$\begin{bmatrix} u(k-d_k,\tau_{k-d_k},d_{k-d_k})|_{d_{k-d_k}=0} \\ u(k-d_k,\tau_{k-d_k},d_{k-d_k})|_{d_{k-d_k}=1} \\ \vdots \\ u(k-d_k,\tau_{k-d_k},d_{k-d_k})|_{d_{k-d_k}=d} \end{bmatrix}. \tag{7.13}$$

For the ease of presentation, $u(k-d_k,\tau_{k-d_k},d_{k-d_k})|_{d_{k-d_k}=0}$ is written as $u(k-d_k,\tau_{k-d_k},0)$ for short. At the actuator/plant node, the current C-A delay $d_k$ can be obtained by the time-stamping technique, and the previous time delay can be stored and also known. As the control signal (7.13) is generated at time instant $k-d_k$, the control signal is chosen based on the value of $d_{k-d_k}$ which is known at the actuator/plant node. For example, at time instant $k$, if $d_{k-d_k}=1$, then among all $d+1$ signals in (7.13), $u(k-d_k,\tau_{k-d_k},1)$ will be picked up and implemented as the control signal. This way, the controller can be designed based on the *current* S-C and *current* C-A delays.

We remark that another potential method to obtain the current C-A delay $d_k$ is to estimate the state of the Markov chain, which is still under current studies.

**Remark 7.2** Many results on NCS research concern the design of a remote controller capable of stabilizing a plant with a known model in a network environment. Other than the important stability analysis, disturbance rejection and tracking control for systems with model uncertainties merit further studies. Though the stabilization problem of NCSs has received much attention, there are relatively less results on the study of the disturbance rejection control for NCSs [205], especially when the S-C and C-A delays are modeled as Markov chains.

**Remark 7.3** In [53], a two-mode dependent output feedback controller was pro-

posed; however, the controller depends on the current S-C delay and the most recent C-A delay. By applying the "send all, apply one" scheme, the controller is dependent on not only the current S-C delay but also the current C-A delay. This can be regarded as a more proactive way to compensate for the C-A delays.

## 7.3 Robust $H_2$ and $H_\infty$ Optimal Tracking

In this section, we first reformulate the system in (7.8) with delay dependent controller (7.9) as the MJLS using the augmentation technique. This further enables us to apply the results of MJLSs to solve the robust $H_2$ and $H_\infty$ tracking problems of such NCSs. The sufficient and necessary conditions for the tracking problems are given in terms of linear matrix inequalities (LMIs) with nonconvex constraints.

### 7.3.1 Reformulating the NCS as MJLS

Considering the system in (7.8) with delay dependent controller (7.9), if we augment the state variables as

$$\begin{aligned} X(k) = \Big[ \; & \hat{x}(k)^{\mathrm{T}} \quad \hat{x}(k-1)^{\mathrm{T}} \quad \cdots \quad \hat{x}(k-\tau)^{\mathrm{T}} \\ & \hat{u}_1(k-1)^{\mathrm{T}} \quad \hat{u}_1(k-2)^{\mathrm{T}} \quad \cdots \quad \hat{u}_1(k-d)^{\mathrm{T}} \; \Big]^{\mathrm{T}}, \end{aligned}$$

the following closed-loop system is obtained

$$X(k+1) = \bar{A}(\tau_k, d_k)X(k) + \bar{B}\omega(k), \tag{7.14a}$$

$$X(0) = 0, \; \tau(0) = \tau_0, \; d(0) = d_0, \tag{7.14b}$$

$$z(k) = \bar{C}X(k). \tag{7.14c}$$

Here,

$$\bar{A}(\tau_k, d_k) = \begin{bmatrix} A & [0 & \underbrace{BK(\tau_k, d_k)C}_{(1+\tau_k)th\ block} & 0] & 0 & 0 & \cdots & 0 \\ I & 0 & \cdots & 0 & 0 & 0 & \cdots & 0 \\ 0 & I & \ddots & 0 & 0 & 0 & \ddots & 0 \\ 0 & 0 & \ddots & 0 & 0 & 0 & \ddots & 0 \\ [0 & 0 & \underbrace{K(\tau_k, d_k)C}_{(1+\tau_k)th\ block} & 0] & 0 & 0 & 0 & 0 \\ 0 & 0 & \cdots & 0 & I & 0 & \cdots & 0 \\ 0 & 0 & \ddots & 0 & 0 & I & \ddots & 0 \\ 0 & 0 & \ddots & 0 & 0 & 0 & \ddots & 0 \end{bmatrix}, \text{ if } d_k = 0;$$

$$\bar{A}(\tau_k, d_k) = \begin{bmatrix} A & 0 & \cdots & 0 & [0 & 0 & \underbrace{B}_{(1+\tau+d_k)th\ block} & 0] \\ I & 0 & \cdots & 0 & 0 & 0 & \cdots & 0 \\ 0 & I & \ddots & 0 & 0 & 0 & \ddots & 0 \\ 0 & 0 & \ddots & 0 & 0 & 0 & \ddots & 0 \\ [0 & 0 & \underbrace{K(\tau_k, d_k)C}_{(1+\tau_k)th\ block} & 0] & 0 & 0 & 0 & 0 \\ 0 & 0 & \cdots & 0 & I & 0 & \cdots & 0 \\ 0 & 0 & \ddots & 0 & 0 & I & \ddots & 0 \\ 0 & 0 & \ddots & 0 & 0 & 0 & \ddots & 0 \end{bmatrix}, \text{ if } d_k > 0.$$

Here, $B$ is at the $(1 + \tau + d_k)^{\text{th}}$ block of the first row in $\bar{A}$ for $d_k > 0$, and $\bar{B}$, $\bar{C}$ are given as below

$$\bar{B} = \begin{bmatrix} B^{\mathrm{T}} & 0 & \cdots & 0 & 0 & 0 & \cdots & 0 \end{bmatrix}^{\mathrm{T}}, \tag{7.15}$$

$$\bar{C} = \begin{bmatrix} Q & 0 & \cdots & 0 & R & 0 & \cdots & 0 \end{bmatrix}. \tag{7.16}$$

Here, $z(k)$ is the augmented system output with $Q$ and $R$ being weighting matrices. In order to reduce the control input signal being fed to the plant, we incorporate $\hat{u}_1$ into the augmented system output $z(k)$ instead of using the original control signal before being transmitted over the C-A link.

**Remark 7.4** In (7.14), the extended system output $z(k) = Q\hat{x}(k) + R\hat{u}_1(k-1)$ is a weighted combination of both the state information $\hat{x}$ and the control signal $\hat{u}_1$. The introduction of $z(k)$ can facilitate the following controller design aiming at minimizing both the $\hat{x}$ and the control signal. By tuning the weighting factors $Q$ and $R$, certain tradeoff can be achieved between the resulting performance of $\hat{x}$ and $\hat{u}_1$. For example, a relatively larger $Q$ can be used to stabilize the state quickly [206], so fast positioning will be achieved at the cost of relatively large control signal. In practice, the choice of $Q$ and $R$ should be determined according to specific application requirements.

The closed-loop system in (7.14) is an MJLS involving two homogeneous modes $(\tau_k,\ d_k)$. The corresponding transition probability matrix is $\Lambda \otimes \Pi$, where $\otimes$ denotes the matrix Kronecker product. In the following, we recall the definition of the stochastic stability for this system.

**Definition 7.1.** *[49, 207] The system given by (7.14) with $\omega(k) \equiv 0$ is said to be stochastically stable if and only if for every initial state $X(0),\ \tau(0),\ d(0)$, there exists a finite $W > 0$ such that the following inequality holds:*

$$\mathcal{E}\left\{\sum_{k=0}^{\infty} \|X(k)\|_2^2 |_{X(0),\tau(0),d(0)}\right\} < X(0)^{\mathrm{T}} W X(0).$$

There are several other forms of stability for MJLSs, e.g., mean-square stability, exponential mean square stability, and almost sure stability [50, 207]. It was shown in [207] that the stochastic stability, mean-square stability, and exponential mean square stability are equivalent, and can be referred to as the second moment stability. Moreover, second moment stability is sufficient but not necessary for almost sure stability. In the remainder of this chapter, references to stability will be in the sense of stochastic stability, or equivalently second moment stability. The following theorem gives the sufficient and necessary conditions for ensuring stochastic stability.

**Theorem 7.1.** *Under the proposed control law in (7.9), the resulting closed-loop system in (7.14) is stochastically stable if and only if there exist symmetric matrices $P(i,r) > 0$ such that the following matrix inequality:*

$$-P(i,r) + \sum_{j=0}^{\tau} \sum_{s=0}^{d} \lambda_{ij}\pi_{rs} \bar{A}(i,r)^{\mathrm{T}} P(j,s) \bar{A}(i,r) \leq 0 \tag{7.17}$$

*holds for all $i \in \mathcal{M}$ and $r \in \mathcal{N}$.*

*Proof.* This theorem can be proved by following a similar line as in [49]. □

**Remark 7.5** It is worth noting that the monotonically decreasing behavior of the following function obtained from Theorem 7.1:

$$\Gamma(P) = \sum_{j=0}^{\tau}\sum_{s=0}^{d}\lambda_{ij}\pi_{rs}\bar{A}(i,r)^{\mathrm{T}}P(j,s)\bar{A}(i,r) - P(i,r), \tag{7.18}$$

where $P(i,r), \forall i \in \mathcal{M}, \forall r \in \mathcal{N}$, is the solution in Theorem 7.1. Suppose both $P_1(i,r)$ and $P_2(i,r)$ satisfy (7.17), and if $P_1(i,r) > P_2(i,r)$, then we have $\Gamma(P_1) < \Gamma(P_2)$. Also if we have $\Gamma(P_1) < \Gamma(P_2)$, we can obtain that $P_1(i,r) > P_2(i,r)$. The monotonically decreasing property will be used in the $H_2$ tracking controller design.

### 7.3.2 Robust $H_2$ Tracking Control

The design purpose in this section is to specify the control law in (7.9) to achieve the step tracking of the system in (7.14). First, we give the definition of $H_2$ norm of the system in (7.14) and then solve the robust $H_2$ tracking control problem via an iterative LMI approach.

**Definition 7.2.** *[24] The $H_2$ norm of the system in (7.14) is defined as*

$$\|H_{z\omega}\|_2^2 = \sum_{s=1}^{l}\sum_{i_0=0}^{\tau}\sum_{r_0=0}^{d}\alpha_{(i_0,r_0)}\|\mathcal{E}(z_{s,i_0,r_0})\|_2^2, \tag{7.19}$$

*where $z_{s,i_0,r_0}$ is the output sequence of the system in (7.14) when*

*(1) the input sequence is given by $\omega = (\omega(0), \omega(1), \ldots)$, $\omega(0) = e_s$, $\omega(k) = 0$, $k > 0$; $e_s$ is the unitary vector formed by one at the* s*th position and zero elsewhere;*

*(2) $\tau(0) = i_0$;*

*(3) $d(0) = r_0$.*

The initial distribution for $(\tau_0, d_0)$ is given by $\alpha = (\alpha_{(i_0,r_0)})$, where $i_0 \in \mathcal{M}$, $r_0 \in \mathcal{N}$ and $\sum_{i_0\in\mathcal{M},r_0\in\mathcal{N}}\alpha_{(i_0,r_0)} = 1$.

The following theorem represents a characterization of the $H_2$ norm based on the state-space model.

**Theorem 7.2.** *The $H_2$ norm of the system in(7.14) can be computed as follows.*

$$\|H_{z\omega}\|_2^2 = \sum_{i=0}^{\tau}\sum_{r=0}^{d}\sum_{j=0}^{\tau}\sum_{s=0}^{d}\alpha_{(i,r)}\lambda_{ij}\pi_{rs}\mathrm{tr}\left\{\bar{B}^{\mathrm{T}}S(j,s)\bar{B}\right\}, \tag{7.20}$$

*where $S(j,s) > 0$ is the solution obtained from the following discrete-time equation*

$$S(i,r) = \sum_{j=0}^{\tau}\sum_{s=0}^{d}\lambda_{ij}\pi_{rs}\bar{A}(i,r)^{\mathrm{T}}S(j,s)\bar{A}(i,r) + \bar{C}^{\mathrm{T}}\bar{C}, \tag{7.21}$$

*for $i \in \mathcal{M}, r \in \mathcal{N}$.*

*Proof.* Suppose $z = (z(0), z(1), \ldots)$ is an impulse response of the system in (7.14). Then for $k \geq 1$ and considering (7.21), we have

$$\begin{aligned}
&\mathcal{E}\{z(k)^{\mathrm{T}}z(k)\}\\
&= \mathcal{E}\{X(k)^{\mathrm{T}}\bar{C}^{\mathrm{T}}\bar{C}X(k)\}\\
&= \mathcal{E}\left\{X(k)^{\mathrm{T}}\left[S(i,r) - \sum_{j=0}^{\tau}\sum_{s=0}^{d}\lambda_{ij}\pi_{rs}\bar{A}(i,r)^{\mathrm{T}}S(j,s)\bar{A}(i,r)\right]X(k)\right\}\\
&= \mathcal{E}\left\{X(k)^{\mathrm{T}}S(i,r)X(k) - X(k+1)^{\mathrm{T}}\mathcal{S}X(k+1)\right\},
\end{aligned}$$

where

$$\mathcal{S} = \sum_{j=0}^{\tau}\sum_{s=0}^{d}\lambda_{ij}\pi_{rs}S(j,s). \tag{7.23}$$

By considering (7.21), $\bar{C}^{\mathrm{T}}\bar{C} \geq 0$ indicates that the condition in (7.17) is satisfied. Then the system in (7.14) is stochastically stable. Thus we have $\mathcal{E}(\|X(k)\|_2^2) \to 0$ as $k \to \infty$.

$$\begin{aligned}
&\|\mathcal{E}(z_{s,i_0,r_0})\|_2^2\\
&= \sum_{k=1}^{\infty}\mathcal{E}\left\{z_{s,i,r}(k)^{\mathrm{T}}z_{s,i,r}(k)\middle| i = i_0, r = r_0\right\}\\
&= \mathcal{E}\left\{X(1)^{\mathrm{T}}S(j,s)X(1)\middle| i = i_0, r = r_0\right\}\\
&= \sum_{j=0}^{\tau}\sum_{s=0}^{d}\lambda_{i_0,j}\pi_{r_0,s}e_s^{\mathrm{T}}\bar{B}^{\mathrm{T}}S(j,s)\bar{B}e_s.
\end{aligned}$$

From Definition 7.2,

$$\begin{aligned}\|H_{z\omega}\|_2^2 =& \sum_{s=1}^{l}\sum_{i_0=0}^{\tau}\sum_{r_0=0}^{d}\alpha_{(i_0,r_0)}\|\mathcal{E}(z_{s,i_0,r_0})\|_2^2 \\ =& \sum_{s=1}^{l}\sum_{i_0=0}^{\tau}\sum_{r_0=0}^{d}\alpha_{(i_0,r_0)}\sum_{j=0}^{\tau}\sum_{s=0}^{d}\lambda_{i_0,j}\pi_{r_0,s}e_s^{\mathrm{T}}\bar{B}^{\mathrm{T}}S(j,s)\bar{B}e_s.\end{aligned}$$

Noting that $\sum_{s=1}^{l} e_s^{\mathrm{T}}\bar{B}^{\mathrm{T}}S(j,s)\bar{B}e_s = \mathrm{tr}\left\{\bar{B}^{\mathrm{T}}S(j,s)\bar{B}\right\}$, we have

$$\|H_{z\omega}\|_2^2 = \sum_{i_0=0}^{\tau}\sum_{r_0=0}^{d}\sum_{j=0}^{\tau}\sum_{s=0}^{d}\alpha_{(i_0,r_0)}\lambda_{i_0,j}\pi_{r_0,s}\mathrm{tr}\left\{\bar{B}^{\mathrm{T}}S(j,s)\bar{B}\right\}.$$

Denote $i_0$ and $r_0$ by $i$ and $r$, respectively, which give a general form of the initial distribution for ($\tau_0$, $d_0$). After the changing of variables, the proof is thus completed. □

With the derived $H_2$ norm of the system, we can look into the $H_2$ control problem.

**Theorem 7.3.** *Under the proposed control law in (7.9), the closed-loop system in (7.14) is stable and $\|H_{z\omega}\|_2 < \beta$, if and only if there exist matrices $K(i,r)$ and symmetric matrices $\bar{X}(i,r) > 0$, $P(i,r) > 0$ satisfying the following inequalities with nonconvex constraints*

$$\sum_{i=0}^{\tau}\sum_{r=0}^{d}\sum_{j=0}^{\tau}\sum_{s=0}^{d}\alpha_{(i,r)}\lambda_{ij}\Pi_{rs}\mathrm{tr}\left\{\bar{B}^{\mathrm{T}}P(j,s)\bar{B}\right\} < \beta^2, \tag{7.24a}$$

$$\begin{bmatrix} -P(i,r) & \bar{A}(i,r)^{\mathrm{T}} & \bar{C}^{\mathrm{T}} \\ \bar{A}(i,r) & -\bar{X}(i,r) & 0 \\ \bar{C} & 0 & -I \end{bmatrix} < 0, \tag{7.24b}$$

$$\bar{X}(i,r)\left[\sum_{r=0}^{\tau}\sum_{s=0}^{d}\lambda_{ij}\Pi_{rs}P(j,s)\right] = I, \tag{7.24c}$$

*for all $i,j \in \mathcal{M}$ and $r,s \in \mathcal{N}$.*

*Proof.* From Schur complement and considering (7.24c), (7.24b) is equivalent to

$$\sum_{j=0}^{\tau}\sum_{s=0}^{d}\lambda_{ij}\Pi_{rs}\bar{A}(i,r)^{\mathrm{T}}P(j,s)\bar{A}(i,r) + \bar{C}^{\mathrm{T}}\bar{C} - P(i,r) < 0. \tag{7.25}$$

Then, from Theorem 7.1, (7.25) implies (7.17). Hence, the system in (7.14) is stochastically stable. Further, by comparing (7.20), (7.21), and (7.25) and considering the monotonicity property of (7.18), the proof can be readily completed. □

Finally, we summarize the $H_2$ step tracking control problem as follows.

The $H_2$ robust tracking control design can be accomplished by solving the following optimization problem:

$$\min_{K(i,r),P(i,r),\bar{X}(i,r)} \quad \beta \quad s.t. \quad (7.24). \tag{7.26}$$

### 7.3.3 Robust $H_\infty$ Tracking Control

This section is concerned with the $H_\infty$ tracking control problems. More specifically, we shall study the conditions under which the closed-loop system in (7.14) is stochastically stable and achieves the $H_\infty$ step tracking performance. We first provide the definition of $H_\infty$ norm and further give the theorem which shows that the $H_\infty$ tracking performance can be guaranteed if there exist some matrices satisfying certain matrix inequalities. This theorem will play an instrumental role in the controller design and finally the $H_\infty$ tracking problem is solved via an iterative LMI approach.

**Definition 7.3.** *[208] Assume the closed-loop system in (7.14) is stochastically stable. Let $X(0) = 0$ and the $H_\infty$ norm of systems in (7.14) is defined as*

$$\|H_{z\omega}\|_\infty = \sup_{\tau(0)\in\mathcal{M}} \sup_{d(0)\in\mathcal{N}} \sup_{\omega\in l_2(0,\infty)} \frac{\|z\|_2}{\|\omega\|_2}. \tag{7.27}$$

The following theorem is an adaption of the bounded real lemma for MJLSs [50, 208] to the closed-loop system in (7.14).

**Theorem 7.4.** *Under the proposed output feedback control law in (7.9), the closed-loop system in (7.14) is stochastically stable and $\|H_{z\omega}\|_\infty < \gamma$, if and only if there exist matrices $K(i,r)$ and symmetric matrices $\bar{X}(i,r) > 0$, $P(i,r) > 0$ satisfying the following inequalities*

$$\begin{bmatrix} \bar{A}(i,r) & \bar{B} \\ \bar{C} & 0 \end{bmatrix}^{\mathrm{T}} \begin{bmatrix} \bar{P}(i,r) & 0 \\ 0 & I \end{bmatrix} \begin{bmatrix} \bar{A}(i,r) & \bar{B} \\ \bar{C} & 0 \end{bmatrix} - \begin{bmatrix} P(i,r) & 0 \\ 0 & \gamma^2 I \end{bmatrix} < 0, \tag{7.28}$$

*for all* $i, j \in \mathcal{M}$ *and* $r, s \in \mathcal{N}$ *where*

$$\bar{P}(i,r) = \sum_{j=0}^{\tau} \sum_{s=0}^{d} \lambda_{ij} \pi_{rs} P(j,s). \tag{7.29}$$

*Proof.* According to the *Bounded Real Lemma* in [208], we can readily obtain the results. The detailed procedure is omitted here. □

In the following theorem, the sufficient and necessary condition for the $H_\infty$ tracking control problem is given in terms of LMIs with nonconvex constraints based on Theorem 7.4.

**Theorem 7.5.** *Under the proposed output feedback control law (7.9), the closed-loop system in (7.14) is stochastically stable and* $\|H_{z\omega}\|_\infty < \gamma$*, if and only if there exist matrices* $K(i,r)$ *and symmetric matrices* $\bar{X}(i,r) > 0$*,* $P(i,r) > 0$*, satisfying:*

$$\begin{bmatrix} -P(i,r) & 0 & \bar{C}^{\mathrm{T}} & \bar{A}(i,r)^{\mathrm{T}} \\ 0 & -\gamma^2 I & 0 & \bar{B}^{\mathrm{T}} \\ \bar{C} & 0 & -I & 0 \\ \bar{A}(i,r) & \bar{B} & 0 & -\bar{X}(i,r) \end{bmatrix} < 0, \tag{7.30a}$$

$$\bar{X}(i,r)\bar{P}(i,r) = I, \tag{7.30b}$$

*for all* $i, j \in \mathcal{M}$ *and* $r, s \in \mathcal{N}$*.*

*Proof.* Using the Schur complement and letting $\bar{X}(i,r) = \bar{P}(i,r)^{-1}$, this theorem can be readily completed. □

The $H_\infty$ robust tracking control design can be achieved by solving the following optimization problem:

$$\min_{K(i,r), P(i,r), \bar{X}(i,r)} \quad \gamma \quad s.t. \quad (7.30). \tag{7.31}$$

The conditions (7.24) and (7.30) contain nonconvex constraints. This can be solved by the product reduction algorithm (PRA) [209], which is an iterative LMI approach. Detailed procedure about how to apply PRA to solve the optimization problems in (7.26) and (7.31) can be referred to [210].

**Remark 7.6** In practice, it is difficult to obtain an exact mathematical model of the dynamic system. Therefore, the plant model in (7.1) with *norm-bounded uncertainties*

can be considered as follows:

$$\begin{aligned} x(k+1) =& (A + \Delta A(k))x(k) + (B + \Delta B(k))\left[\tilde{u}(k) + \omega(k)\right], \\ y(k) =& Cx(k), \end{aligned}$$

where $A$, $B$, and $C$ are known real-valued constant matrices, and $\Delta A(k)$ and $\Delta B(k)$ are real time-varying matrix functions representing parameter uncertainties. Also it is assumed that

$$[\Delta A(k) \quad \Delta B(k)] = M\Delta(k)[N_1 \quad N_2].$$

Here, $M$, $N_1$, and $N_2$ are known real constant matrices and $\Delta(k)$ is an unknown time-varying matrix function satisfying:

$$\|\Delta(k)\| \leq 1.$$

Using the similar augmentation technique in Section 7.3, the closed-loop system can be formulated as an MJLS with *norm-bounded uncertainties*. The relevant $H_2$ and $H_\infty$ control synthesis problems can be solved readily based on Theorem 7.3 and Theorem 7.5, respectively.

### 7.3.4 Mixed $H_2/H_\infty$ Tracking Control Design

In many practical applications, it often needs to make a compromise between $H_2$ and $H_\infty$ control performance. The compromise can be achieved by the mixed $H_2/H_\infty$ control synthesis: Set $H_\infty$ norm of the system to be a prescribed value, and minimize the $H_2$ norm of the system. The mixed $H_2/H_\infty$ tracking control for the system in (7.14) can be summarized as: Set $\gamma$ to be a prescribed value, and

$$\min_{K(i,r),P(i,r),\bar{X}(i,r)} \quad \beta \quad s.t. \ \text{(7.24) and (7.30)}. \tag{7.33}$$

## 7.4 Simulation and Experimental Results

In this section, simulations and experimental result on a vertical take-off and landing (VTOL) helicopter system and a DC motor system are provided.

### 7.4.1 Numerical Example on a VTOL System

In this sub-section, design examples on a VTOL helicopter [211] are given to demonstrate the applicability and effectiveness of the proposed methods. The discrete-time state-space model of the VTOL helicopter with sampling period of 0.01s is:

$$A = \begin{bmatrix} 0.9996 & 0.0003 & 0.0002 & -0.0046 \\ 0.0005 & 0.9900 & -0.0002 & -0.0400 \\ 0.0010 & 0.0036 & 0.9930 & 0.0141 \\ 0 & 0 & 0.0100 & 1.0001 \end{bmatrix}, \quad B = \begin{bmatrix} 0.0044 & 0.0018 \\ 0.0353 & -0.0755 \\ -0.0549 & 0.0446 \\ -0.0003 & 0.0002 \end{bmatrix},$$
$$C = \begin{bmatrix} 0 & 1 & 0 & 0 \end{bmatrix}.$$

The eigenvalues of $A$ are 0.9977, 0.9795, $1.0028 + 0.0026i$, and $1.0028 - 0.0026i$. Hence, the plant is unstable. The involved random delays in the NCS are assumed to be $\tau_k \in \{0, 1, 2\}$ and $d_k \in \{0, 1\}$ with the following transition probability matrices

$$\Lambda = \begin{bmatrix} 0.6 & 0.4 & 0 \\ 0.7 & 0.2 & 0.1 \\ 0.8 & 0.1 & 0.1 \end{bmatrix}, \quad \Pi = \begin{bmatrix} 0.5 & 0.5 \\ 0.7 & 0.3 \end{bmatrix}. \tag{7.34}$$

Here, the maximum C-A delay is $d = 1$. Considering the time-stamp information, the data portion of the transmission packet is

$$\underbrace{[\underbrace{(d+1)}_{\substack{\text{sequence} \\ \text{length}}} \times \underbrace{2}_{\dim\{u\}} + \underbrace{1}_{\text{timestamp}}]}_{\text{number of data}} \times \underbrace{4}_{\text{byte}} = 20 \text{ bytes}, \tag{7.35}$$

by using the IEEE 754 standard.

Take the network properties into the controller design procedure, then choose the following weighting matrices: $Q = C$, $R = [0.01 \quad 0.01]$. In the case when a higher level control performance is needed, heuristic methods can be employed to choose the weighting matrices $Q$ and $R$. The minimum $H_2$ norm $\beta_{\min}$ is 0.1225 and the proposed delay dependent controller is

$$K(0,0) = [-4.1629\ 5.6465]^{\mathrm{T}}, \quad K(0,1) = [-4.1774\ 5.6462]^{\mathrm{T}},$$
$$K(1,0) = [-1.8548\ 2.5818]^{\mathrm{T}}, \quad K(1,1) = [-1.1025\ 1.5065]^{\mathrm{T}},$$
$$K(2,0) = [-1.3368\ 1.8751]^{\mathrm{T}}, \quad K(2,1) = [-1.0764\ 1.4867]^{\mathrm{T}}.$$

The resulting step responses, corresponding to the proposed $H_2$ controller and a local $H_2$ controller, are shown in Figure 7.2. Here, the local $H_2$ controller gain is calculated as $[-56.0196 \quad -10.5998]^{\mathrm{T}}$ which is independent of the time delay. In this simulation, an impulse disturbance is added to the control signal at time instant 300. It can be seen from Figure 7.2 that the proposed $H_2$ controller has both better transient response and better disturbance rejection performance.

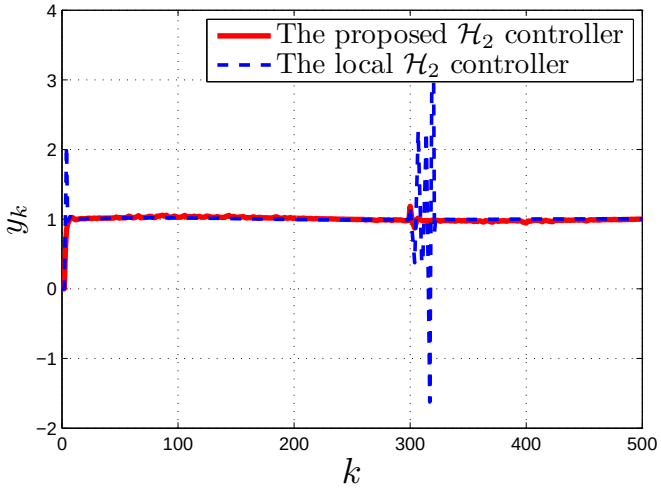


Figure 7.2: Step response in NCSs using the proposed robust $H_2$ controller and the local robust $H_2$ controller.

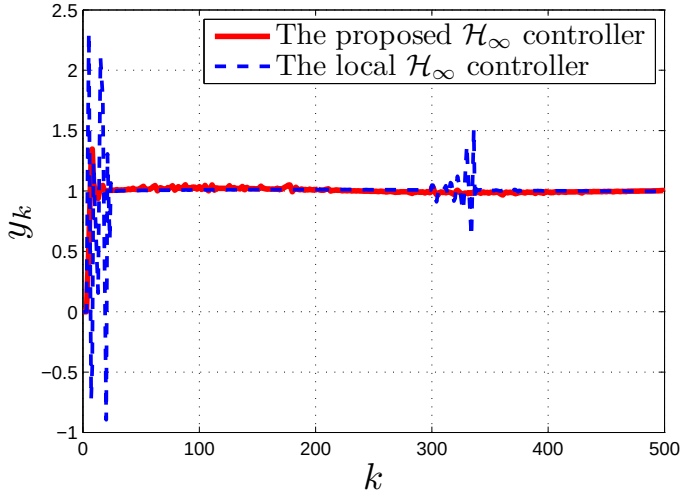


Figure 7.3: Step response using the proposed robust $H_\infty$ controller and the local robust $H_\infty$ controller.

Similarly, the $H_\infty$ controller can be designed by choosing the same weighting

matrices as those of the $H_2$ controller. The minimum $H_\infty$ norm $\gamma_{\min}$ is 0.3464 and the proposed delay dependent controller is

$$K(0,0) = [-5.6786\ 7.4750]^{\mathrm{T}}, \quad K(0,1) = [-6.5506\ 8.7246]^{\mathrm{T}},$$
$$K(1,0) = [-1.8669\ 2.5136]^{\mathrm{T}}, \quad K(1,1) = [-1.2499\ 1.6792]^{\mathrm{T}},$$
$$K(2,0) = [-1.0491\ 1.4216]^{\mathrm{T}}, \quad K(2,1) = [-0.9730\ 1.3288]^{\mathrm{T}}.$$

An impulse disturbance is also added at time instant 300. The comparison with a local $H_\infty$ controller for the step tracking is shown in Figure 7.3. It is observed that the proposed $H_\infty$ controller has both better transient response and better disturbance rejection performance. The total computation time of the two controllers are 8.23 hours on a PC (3.0 GHz, 2.0 GB of RAM memory). It is worth noting that the computation is done offline, and no online calculation is required to determine the controller parameters.

As a comparison, the sum of squared tracking errors are summarized in Table 7.1. The proposed controllers outperform the local ones which do not consider the network-induced delays.

Table 7.1: Sum of squared tracking errors over 0-5s (VTOL example).

| Proposed | | Local | |
|---|---|---|---|
| $H_2$ | $H_\infty$ | $H_2$ | $H_\infty$ |
| 0.0356 | 0.0512 | 0.3319 | 0.2051 |

### 7.4.2 Numerical Simulation on a Networked DC Motor System

In this sub-section, the design for a networked DC motor control system is presented to demonstrate the effectiveness of the proposed methods.

The identified model of the DC motor is

$$G(s) = \frac{172.38}{s(s+3.5287)},$$

where the input is the voltage and the output is the angular position of the motor. By

choosing the sampling period as 0.05s, the following state-space model is obtained:

$$A = \begin{bmatrix} 1.00021 & 0.00460 \\ 0.00460 & 0.00004 \end{bmatrix},\ B = \begin{bmatrix} 0.34868 \\ 7.68069 \end{bmatrix},$$
$$C = [1 \quad 0],\ D = 0.$$

The random delays in this NCS are assumed to be $\tau_k \in \{0, 1, 2\}$ and $d_k \in \{0, 1\}$ with the transition probability matrices in (7.34). The weighting matrices are chosen as $Q = C$, $R = 0.01$. By following the proposed controller design methods, the minimal $H_\infty$ norm $\gamma_{\min}$ is 17.4085 and the $H_\infty$ controller parameters are

$$\begin{aligned} &K(0,0) = -0.1576,\ K(0,1) = -0.1318, \\ &K(1,0) = -0.0878,\ K(1,1) = 0.0091, \\ &K(2,0) = -0.0342,\ K(2,1) = 0.0074. \end{aligned} \tag{7.36}$$

The minimal $H_2$ norm $\beta_{\min}$ is 5.0147 and the $H_2$ controller parameters are

$$\begin{aligned} &K(0,0) = -0.1980,\ K(0,1) = -0.1647, \\ &K(1,0) = -0.1232,\ K(1,1) = -0.0547, \\ &K(2,0) = -0.0747,\ K(2,1) = -0.0399. \end{aligned} \tag{7.37}$$

The total computation time of the two controllers are 1.93 hours on a PC (3.0 GHz, 2.0 GB of RAM memory).

The reference signal $\bar{r}$ is a step signal with the magnitude of 3 rad. A disturbance signal of 0.1 rad and length of 2 sampling periods is added at time instant 30s. The simulation results using the designed $H_\infty$ and $H_2$ controllers in (7.36) and (7.37) are shown in Figure 7.6 and Figure 7.7 (dashed lines). The simulation results confirm that the tracking performance is well achieved and the proposed design scheme is effective.

As a comparison, a Smith predictor is applied to the same networked motor system and the simulation result is shown in Figure 7.4 (red dashed line) [212]. The Smith predictor is used to compensate for the S-C delay, and the *send all, apply one* scheme is also applied to compensate for the C-A delay. From the simulation results, the responses by applying the proposed $H_\infty$ and $H_2$ controllers are faster than that by applying the Smith predictor. Yet, the drawback is that the overshot is greater by

applying the proposed $H_\infty$ and $H_2$ controllers. In addition, the proposed $H_\infty$ and $H_2$ controllers outperform the Smith predictor in terms of disturbance rejection.

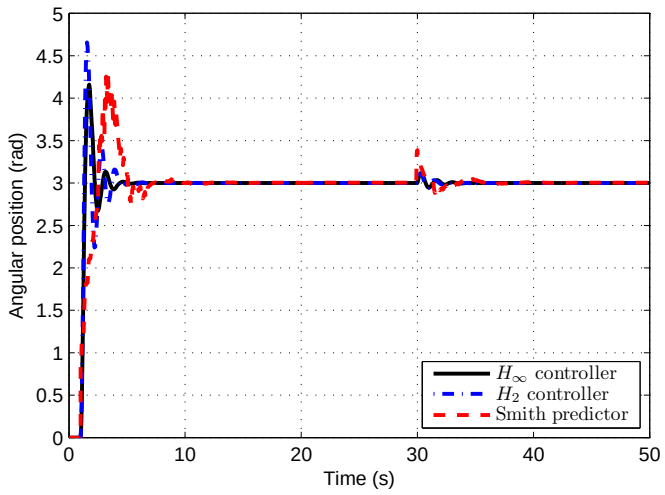


Figure 7.4: Simulation results using the proposed $H_\infty$ controller, $H_2$ controller, and Smith predictor for the networked DC motor system under a simulated network environment.

### 7.4.3 Experimental Test on the Networked DC Motor System

To further illustrate the effectiveness and applicability of the proposed methods, the hardware-in-the-loop (HIL) test on a networked DC motor system (Figure 7.5) is conducted. In order to demonstrate the agreement with the results in the numerical simulation, the sampling rate is also chosen as 0.05s.

The experimental apparatus consists of a PC, an interface board, and a DC motor with sensors. The networked controller is implemented in Matlab/Simulink on the PC. The function of the interface board is to: 1) convert the control signal from the PC into a pulse-width modulation signal to drive the motor; 2) convert the motor output signal from the sensor into digital format and send it to the PC. In the experimental test, the PC controller and the DC motor are linked by a simulated network where the random delays are characterized by the transition matrices in (7.34). The reference and disturbance signals are chosen as the same as in the simulation for the purpose of comparison.

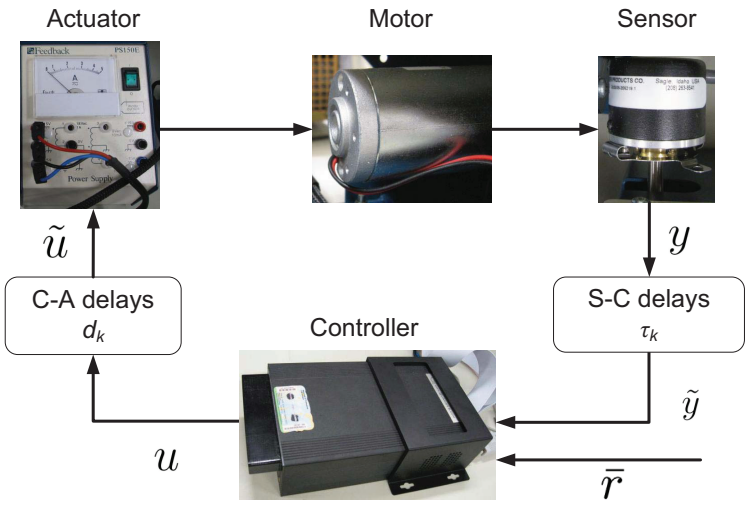


Figure 7.5: The experimental setup of the networked DC motor system.

A local $H_\infty$ control gain: $K = -0.4515$ is designed and applied in the HIL test. The simulation and experimental results by applying the local controller to the networked DC motor system are shown in Figure 7.8. By applying the $H_\infty$ and $H_2$ controllers in (7.36) and (7.37), the experimental results are shown in Figure 7.6 and Figure 7.7 (solid lines), respectively. Apparently, the proposed $H_\infty$ and $H_2$ controller outperform the local $H_\infty$ controller. Also, Figure 7.6 and Figure 7.7 indicate a good agreement between the simulation and the experiment showing that the proposed controller is indeed effective in the application.

The sum of squared tracking errors over 0-50s and 5-50s are listed in Table 7.2. By using the proposed controller, the control performance has been improved, especially during the time frame 5-50s.

Table 7.2: Sum of squared tracking errors (DC motor example).

| | Simulation | | | Experiment | | |
|---|---|---|---|---|---|---|
| Time | $H_\infty$ | $H_2$ | Local | $H_\infty$ | $H_2$ | Local |
| 0-50s | 11.29 | 11.65 | 12.11 | 15.14 | 14.57 | 16.16 |
| 5-50s | 0.0065 | 0.0055 | 0.0693 | 0.0295 | 0.0193 | 0.2989 |

**Remark 7.7** From the experimental results (the blue solid lines in Figure 7.6 and Figure 7.7), the steady-state error by applying the proposed $H_\infty$ and $H_2$ controllers are $-0.0348$ rad and 0.0172 rad, respectively, i.e. $-1.16\%$ and 0.57%. Though small, the steady-state errors in the experimental results come as no surprise because there

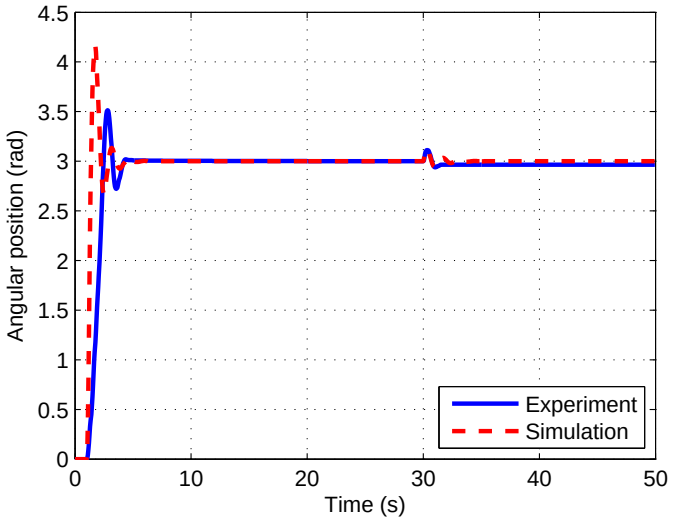


Figure 7.6: Experimental and simulation results using the proposed $H_\infty$ controller for the networked DC motor system under a simulated network environment.

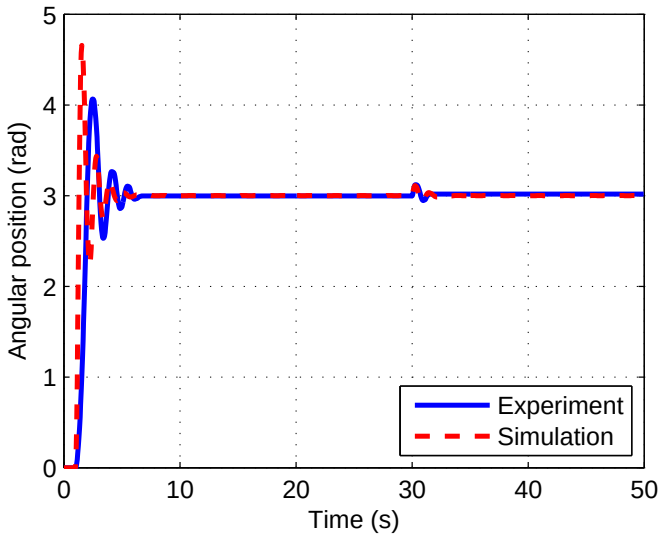


Figure 7.7: Experimental and simulation results using the proposed $H_2$ controller for the networked DC motor system under a simulated network environment.

are unavoidable modeling errors and also inevitable nonlinearities such as dead-zone and brush frictions in the experimental apparatus. It is worthwhile to look into the controller design for nonlinear NCSs considering the nonlinear frictions, which is still under research. It is also noticed that the dead-zone is an inherent property of the motor. To further enhance the steady-state tracking performance, other control

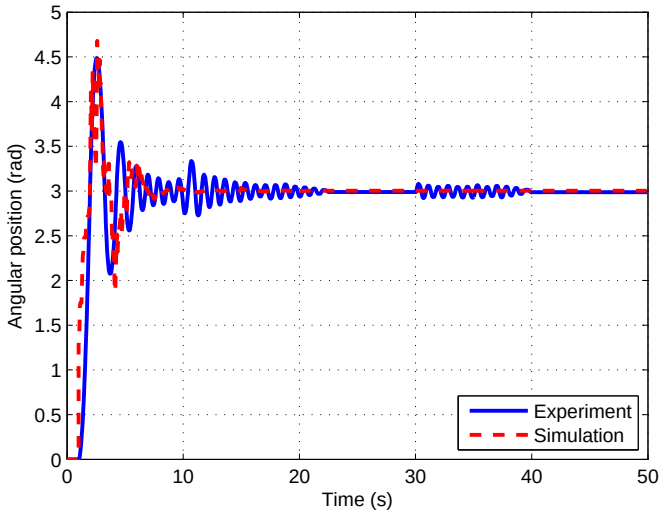


Figure 7.8: Simulation and experimental results using the local controller for the networked DC motor system under a simulated network environment.

techniques can be applied here, e.g., 1) a dynamic controller, or 2) feedback-plus-feedforward control design.

**Remark 7.8** Note that the simulated network in which the associated random delays are characterized by fixed (precisely known) transition matrices is employed in the experimental test. In practice, to identify the probability transition matrix of the Markov chain, we need to measure and record the network-induced delays and/or packet dropouts. Based on the analysis of the collected data, the number of modes should be firstly determined, and then the probability transition matrix will be identified. Furthermore, due to the difficulties in precise delay measurements, the identified probability transition matrix may not be accurate. Therefore, studying the effects of uncertainties and unknown parameters on the probability transition matrix is also a meaningful research area. Both of these topics deserve further research.

## 7.5 Conclusions

In this chapter, we investigate the step tracking problem for NCSs with both S-C and C-A delays modeled by Markov chains. The focus is on the design of the two-mode delay dependent controllers to achieve the step tracking and disturbance rejection. By employing the "send all, apply one" scheme, the controller is dependent on both

current S-C and C-A delays. Such a control scheme is more effective than those that cannot incorporate the current C-A delay into the controller design. The closed-loop system is transformed to the MJLS using the augmentation technique. The $H_2$ and $H_\infty$ tracking control problems are solved under the framework of the MJLS to achieve the disturbance rejection performance. Simulation and experimental results are given to demonstrate the effectiveness of the proposed approaches. It is worth noting that a more general way of employing semi-Markov process [213, 214] to model network-induced delays can better reflect network characteristics in practice. Accordingly, the resulting closed-loop NCSs fall into the generalized class of S-MJLSs.

# Chapter 8

# Conclusions and Future Work

This thesis investigates stabilization and control problems for S-MJLSs and discusses the networked dynamic system design via switching system approaches. Robust and optimal control problems for S-MJLSs are studied. Furthermore, analysis and design for networked dynamic systems have been conducted and verified by using numerical simulations and/or experiments. Nevertheless, based on the developed theorems in the thesis, more research topics deserve further research attention. In this chapter, a summary of the thesis is firstly provided, followed by some topics in the next research step in the future.

## 8.1 Summary of the Thesis

By examining the limitations of Markov processes and MJLSs, the semi-Markov process is revisited and jump linear systems depending on semi-Markov processes are studied. Compared with the existing results in the literature, this thesis focuses on the developments of results that could be used in practice. Some approaches in the literature rely on a solution of a set of integral equations which are hard to solve, so those approaches are not ready for engineering applications. Other approaches in the literature use Markov processes to approximate the semi-Markov processes and then deploy the results from Markov processes or MJLSs to solve the S-MJLS stabilization and control problems.

In this thesis, systematic numerically implementable methods are proposed for S-MJLSs for the first time. The procedure of the systematic stability analysis enables the designer to be aware that if an S-MJLS is stochastically stable. The thesis also

provides a standard procedure to design controllers for unstable S-MJLSs. In the engineering applications, mathematical models of dynamic systems or processes often suffer from uncertainties. Controller design problems for such uncertain systems are also studied. Compared with the existing results where Markov approximations are applied, the control performance is improved by applying the proposed control strategies in this thesis. The improvements are illustrated in numerical simulation results. In order to study the NCSs, the delayed S-MJLS is studied, where not only the stabilization conditions are obtained, but also the $H_\infty$ optimal controller is designed.

Two approaches have been developed to design controllers for NCSs in this thesis. One approach is to provide redundant control signals to the pre-configured smart actuator, then the smart actuator could determine the C-A delay and select the appropriate control signals. In this way, the C-A delays can be well compensated. The tracking controller by using this compensation technique is tested on networked DC motor devices. Similar experiments using different control laws have been conducted for the same networked DC motor device without compensating for the C-A delays. A clear improvement in control performance is observed by utilizing the control laws in this thesis. The other approach is to make the most of the historical information of the system state. In the literature, when the controller calculates the control signal, the outdated measurement of the plant was usually discarded and only the most recent available measurement was used. For certain special types of networked systems where multiple sensors are mounted to measure different states of the plant/process, we develop control strategies using not only the most recent data but also the historical measurement. After taking the historical data into account, a smoother transient response is obtained. The two aforementioned approaches developed in this thesis provide two hints on the controller design for NCSs: 1) Learn from the history; 2) plan for the future.

Since semi-Markov processes can naturally describe the "working" and "failure" status of system components, the semi-Markov processes are used in fault tolerant control analysis. In the thesis, a system whose component's life time follows non-exponential distributions is studied and fault tolerant control schemes are provided. The purpose of using semi-Markov processes is that the failure rate of the system components may not necessarily be constant, because the failure rate function could theoretically be in any shapes. As a matter of fact, the research from reliability engineering shows that the failure rate often exhibits bathtub shapes, i.e., time-varying functions. With the designed fault tolerant controller, the numerical simulation for a

VTOL vehicle with actuator failures is conducted. Improvements are observed using the proposed fault tolerant controllers.

The stochastic process is used to model a complex planar surface in the virtual environment. In the virtual environment, the avatar is moving with one-dimensional interaction on the virtual wall. The virtual wall consists of serval materials, so the random walking of the avatar results in a random interaction between the avatar and the wall. The random interaction is modeled by a stochastic process, so the resulting closed-loop system is a jump linear system. With the designed controller, the perception of a multi-material wall is realized and the multi-material wall is felt by the operator, therefore the virtual environment rendering is achieved.

## 8.2 Future Work

This thesis has solved some basic problems for a type of jump linear systems and has applied the results on NCSs and fault tolerant control systems. Nevertheless, we believe that lots of research problems have not been solved, especially the applications in NCSs. In the future, we will extend the current results to more general scenarios and practical situations.

### 8.2.1 S-MJLSs Applied in NCSs

For the NCSs in this thesis, the time delays are modeled by Markov processes; it is anticipated that the semi-Markov process could improve the precision of predicting the network-induced delays. So we propose to study the NCS stability and control problems where S-C and C-A delays are modeled by semi-Markov processes. This idea is a natural extension of the one used in Chapter 5. The historical information is used to capture the behavior of the system dynamics in Chapter 5, while in this proposed research topic, the historical information is applied to improve the precision of future communication delay predictions. As depicted in Figure 8.1, not only $\tau_{k-1}$ but also $\tau_{k-2}$, $\tau_{k-3}$, $\tau_{k-4}$, and so on are used to predict $\tau_k$; similarly, not only $d_{k-1}$ but also $d_{k-2}$, $d_{k-3}$, $d_{k-4}$, and so on are used to predict $d_k$. With the proposed problem formulation, it is expected that the control performance will be improved.

Several challenges under the aforementioned framework are: (1) Data packet disorder. If packet disorder happens, the prediction model will depend on an incomplete set of historical information. A potential technique to tackle this challenge is to con-

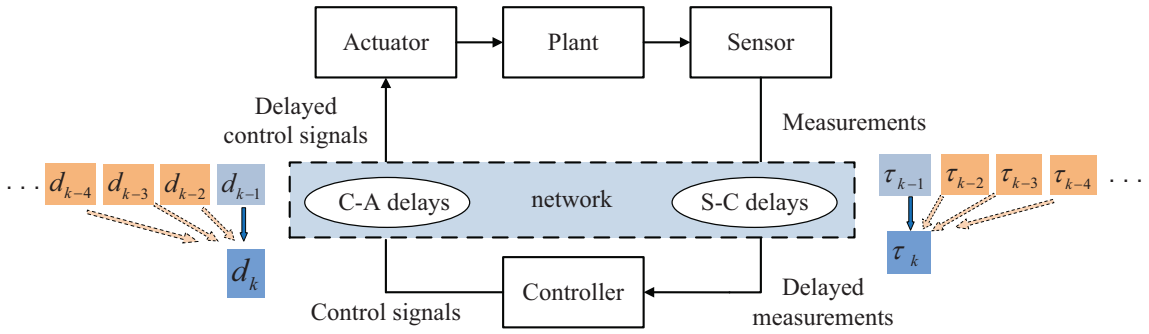


Figure 8.1: The idea illustration of the semi-Markov process based NCS.

struct a prediction model according to partially known delay values. (2) Data package dropout. It would also result in an incomplete set of previous delays. In the disorder case, the delayed packets will arrive at the controller or the actuator at a later time. In contrast, the lost packets will never arrive at the controller or the actuator in the packet dropout scenario. So it is preferable yet a challenge to distinguish the difference between the disorder and dropout. (3) Length of the historical data to be used. A too short history may not be able to capture the delay variation dynamics, while a too long history may cost too many computational resources with limited improvements in the prediction.

### 8.2.2 Event-Triggered S-MJLSs

The main purpose of using event-trigger scheme is to reduce the network load in communication networks [215, 216]. The idea is illustrated in Figure 8.2. Compared with the standard NCS setup in Figure 1.3, an additional system component *event-trigger switch* is added in the communication channel from sensors to the controller. Suppose that the process to be controlled is a chemical process, and the measured process value is the temperature in a reaction kettle. The thermocouple (i.e. sensor) detects the value from $k$ to $k+8$ and so on. When the state variation is not dramatic, we assume that the process preserves the same temperature and no control actions are required. Therefore, it is not necessary to send the redundant information when the network recourses are limited. For the example in Figure 8.2, the measurements at $k$, $k+4$, $k+7$, and $k+8$ contain more information. We call them *key measurements*.

The *event-trigger switch* is able to determine which measurements are critical and then labels them as key measurements, which would be transmitted to the controller. The non-key measurements would be discarded. A lot of research results discuss

the proper triggering schemes. The most popular ones are: 1) Magnitude based triggering with impulse control [217]; 2) error based triggering [218]; and 3) deadzone based triggering [219]. The triggering scheme shown in Figure 8.2 is of the second type.

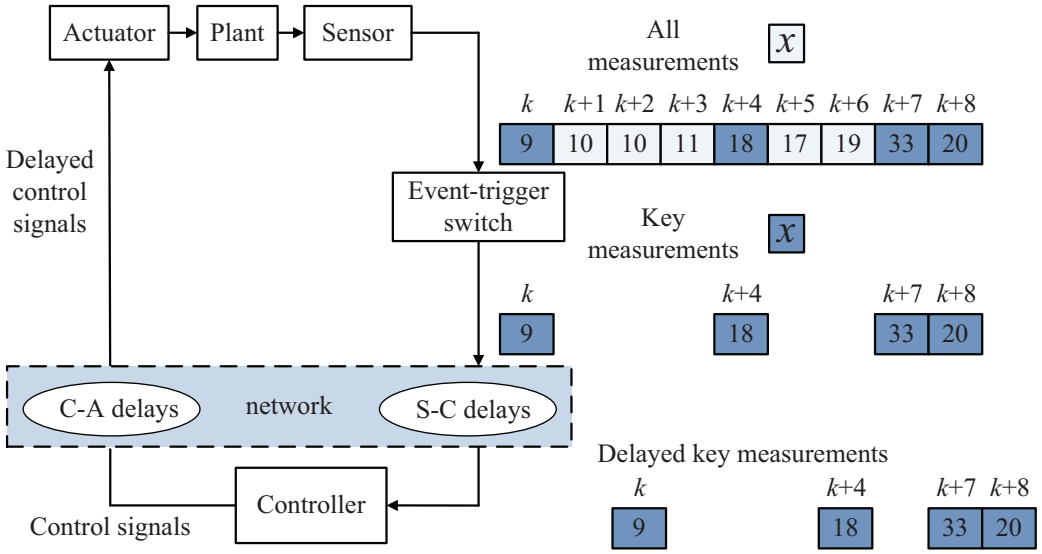


Figure 8.2: The idea illustration for event-trigger scheme based on the error between adjacent measurements.

In the system configuration, the time delays are assumed to follow semi-Markov processes. Several challenges are identified. (1) The controller should be able to predict the network-induced delays in several time steps. Two popular ways to predict the stochastic process mode in several steps are state augmentation and constructing a multi-step transition rate matrix. The flaw of using the state augmentation is that the dimension of the resulting stochastic process will increase drastically, so it is ideal to construct the multi-step transition rate matrix. In Markov chains, the $n$-step transition rate matrix has been studied in [56]. Therefore, the first challenge is to determine the stochastic process mode in a longer future. (2) The second challenge is to choose a proper event-trigger scheme. As mentioned before, several event-trigger schemes exist in the literature. It is crucial to select the most appropriate one that costs least communication load and guarantees satisfactory control performance. The second challenge is actually a network and control co-design problem.

# Bibliography

[1] C. Schwartz, "Control of semi-Markov jump linear systems with application to the bunch-train cavity interaction," Ph.D. dissertation, Northwestern University, 2003.

[2] C. Schwartz and A. Haddad, "Control of jump linear systems having semi-Markov sojourn times," in *Proceedings of the IEEE Conference on Decision and Control*, vol. 3, Maui, USA, 2003, pp. 2804–2805.

[3] R. Vidal, A. Chiuso, and S. Soatto, "Observability and identifiability of jump linear systems," in *Proceedings of the IEEE Conference on Decision and Control*, vol. 4, Las Vegas, USA, 2002, pp. 3614–3619.

[4] A. Willsky and H. Jones, "A generalized likelihood ratio approach to the detection and estimation of jumps in linear systems," *IEEE Transactions on Automatic Control*, vol. 21, no. 1, pp. 108–112, 1976.

[5] L. S. Vijay Gupta, Richard M. Murray and B. Sinopoli, *Networked Sensing, Estimation and Control Systems*. California Institute of Technology Report, 2009.

[6] Y. Wang, S. Ding, P. Zhang, W. Li, H. Ye, and G. Wang, "Fault detection of networked control systems with packet dropout," in *Proceedings of the World Congress on the International Federation of Automatic Control*, Seoul, Korea, 2008, pp. 8884–8889.

[7] D. Sworder, "Feedback control of a class of linear systems with jump parameters," *IEEE Transactions on Automatic Control*, vol. 14, no. 1, pp. 9–14, 1969.

[8] ——, "On the control of stochastic systems," *International Journal of Control*, vol. 6, no. 2, pp. 179–188, 1967.

[9] D. Sworder and R. Rogers, "An LQ-solution to a control problem associated with a solar thermal central receiver," *IEEE Transactions on Automatic Control*, vol. 28, no. 10, pp. 971–978, 1983.

[10] D. de Farias, J. Geromel, J. do Val, and O. Costa, "Output feedback control of Markov jump linear systems in continuous-time," *IEEE Transactions on Automatic Control*, vol. 45, no. 5, pp. 944–949, 2000.

[11] Y. Cao and J. Lam, "Robust $H_\infty$ control of uncertain Markovian jump systems with time-delay," *IEEE Transactions on Automatic Control*, vol. 45, no. 1, pp. 77–82, 2000.

[12] M. Mahmoud and P. Shi, "Robust stability, stabilization and $H_\infty$ control of time-delay systems with Markovian jump parameters," *International Journal of Robust and Nonlinear Control*, vol. 13, no. 8, pp. 755–784, 2003.

[13] A. Gonçalves, A. Fioravanti, and J. Geromel, "Filtering of discrete-time Markov jump linear systems with uncertain transition probabilities," *International Journal of Robust and Nonlinear Control*, vol. 21, no. 6, pp. 613–624, 2011.

[14] E. Dynkin, *Markov Processes*. Academic Press, 1965.

[15] H. Akaike, "A new look at the statistical model identification," *IEEE Transactions on Automatic Control*, vol. 19, no. 6, pp. 716–723, 1974.

[16] L. Zhang, E. Boukas, and J. Lam, "Analysis and synthesis of Markov jump linear systems with time-varying delays and partially known transition probabilities," *IEEE Transactions on Automatic Control*, vol. 53, no. 10, pp. 2458–2464, 2008.

[17] L. Zhang and J. Lam, "Necessary and sufficient conditions for analysis and synthesis of Markov jump linear systems with incomplete transition descriptions," *IEEE Transactions on Automatic Control*, vol. 55, no. 7, pp. 1695–1701, 2010.

[18] H. J. Kushner, *Stochastic Stability and Control*. Academic Press, 1967.

[19] A. Rosenbloom, J. Heilfron, and D. Trautman, "Analysis of linear systems with randomly varying inputs and parameters," in *IRE Convention Record*, vol. 106, London, England, 1955, p. 106.

[20] E. Boukas and Z. Liu, "Delay-dependent stabilization of singularly perturbed jump linear systems," *International Journal of Control*, vol. 77, no. 3, pp. 310–319, 2004.

[21] H. Shao, "New delay-dependent stability criteria for systems with interval delay," *Automatica*, vol. 45, no. 3, pp. 744–749, 2009.

[22] Y. Ji and H. Chizeck, "Controllability, stabilizability, and continuous-time Markovian jump linear quadratic control," *IEEE Transactions on Automatic Control*, vol. 35, no. 7, pp. 777–788, 1990.

[23] P. Gahinet, A. Nemirovskii, A. Laub, and M. Chilali, "The LMI control toolbox," in *Proceedings of the IEEE Conference on Decision and Control*, vol. 3, New Orleans, USA, 1995, pp. 2038–2041.

[24] O. L. V. Costa, J. B. R. do Val, and J. C. Geromel, "A convex programming approach to $H_2$ control of discrete-time Markovian jump linear systems," *International Journal of Control*, vol. 66, no. 4, pp. 557–579, 1997.

[25] O. Costa, E. Assumpção Filho, E. Boukas, and R. Marques, "Constrained quadratic state feedback control of discrete-time Markovian jump linear systems," *Automatica*, vol. 35, no. 4, pp. 617–626, 1999.

[26] E. Boukas and Z. Liu, "Robust stability and $H_\infty$ control of discrete-time jump linear systems with time-delay: An LMI approach," in *Proceedings of the IEEE Conference on Decision and Control*, vol. 2, Sydney, Australia, 2000, pp. 1527–1532.

[27] C. de Souza, "Robust stability and stabilization of uncertain discrete-time Markovian jump linear systems," *IEEE Transactions on Automatic Control*, vol. 51, no. 5, pp. 836–841, 2006.

[28] S. Boyd, L. El Ghaoui, E. Feron, and V. Balakrishnan, *Linear Matrix Inequalities in System and Control Theory*. Society for Industrial and Applied Mathematics, 1994, vol. 15.

[29] O. Costa and R. Marques, "Robust $H_2$-control for discrete-time Markovian jump linear systems," *International Journal of Control*, vol. 73, no. 1, pp. 11–21, 2000.

[30] N. Xiao, L. Xie, and M. Fu, "Kalman filtering over unreliable communication networks with bounded Markovian packet dropouts," *International Journal of Robust and Nonlinear Control*, vol. 19, no. 16, pp. 1770–1786, 2009.

[31] Z. Hou, J. Luo, and P. Shi, "Stochastic stability of linear systems with semi-Markovian jump parameters," *ANZIAM J*, vol. 46, no. 3, pp. 331–340, 2005.

[32] L. Gomes and S. Bogosyan, "Current trends in remote laboratories," *IEEE Transactions on Industrial Electronics*, vol. 56, no. 12, pp. 4744–4756, 2009.

[33] Y. Shi, H. Fang, and M. Yan, "Kalman filter-based adaptive control for networked systems with unknown parameters and randomly missing outputs," *International Journal of Robust and Nonlinear Control*, vol. 19, no. 18, pp. 1976–1992, 2009.

[34] D. de la Pena and P. Christofides, "Model-based control of nonlinear systems subject to sensor data losses: A chemical process case study," in *Proceedings of the IEEE Conference on Decision and Control*, New Orleans, USA, 2007, pp. 3333–3338.

[35] P. Ogren, E. Fiorelli, and N. Leonard, "Cooperative control of mobile sensor networks:adaptive gradient climbing in a distributed environment," *IEEE Transactions on Automatic Control*, vol. 49, no. 8, pp. 1292–1302, 2004.

[36] M. Mahvash, J. Gwilliam, R. Agarwal, B. Vagvolgyi, L.-M. Su, D. Yuh, and A. Okamura, "Force-feedback surgical teleoperator: Controller design and palpation experiments," *Symposium on Haptic Interfaces for Virtual Environment and Teleoperator Systems*, pp. 465–471, 2008.

[37] H. Takahashi, H. Nishi, and K. Ohnishi, "Autonomous decentralized control for formation of multiple mobile robots considering ability of robot," *IEEE Transactions on Industrial Electronics*, vol. 51, no. 6, pp. 1272–1279, 2004.

[38] G. Walsh, H. Ye, and L. Bushnell, "Stability analysis of networked control systems," *IEEE Transactions on Control Systems Technology*, vol. 10, no. 3, pp. 438–446, 2002.

[39] R. S. Stansbury, M. A. Vyas, and T. A. Wilson, *Unmanned Aircraft Systems*. Springer, 2009.

[40] J. Baillieul and P. J. Antsaklis, "Control and communication challenges in networked real-time systems," *Proceedings of the IEEE*, vol. 95, no. 1, pp. 9–28, 2007.

[41] S. Petersen and S. Carlsen, "Wirelesshart versus ISA100.11a: The format war hits the factory floor," *IEEE Industrial Electronics Magazine*, vol. 5, no. 4, pp. 23–34, 2011.

[42] M. Branicky, S. Phillips, and W. Zhang, "Scheduling and feedback co-design for networked control systems," in *Proceedings of the IEEE Conference on Decision and Control*, vol. 2, Las Vegas, USA, 2002, pp. 1211–1217.

[43] L. Zhang and D. Hristu-Varsakelis, "Communication and control co-design for networked control systems," *Automatica*, vol. 42, no. 6, pp. 953–958, 2006.

[44] P. Martí, J. Yépeza, M. Velasco, R. Villà, and J. M. Fuertes, "Managing quality-of-control in network-based control systems by controller and message scheduling co-design," *IEEE Transactions on Industrial Electronics*, vol. 51, no. 6, pp. 1159–1167, 2004.

[45] H. Zhang, "Robust tracking control and signal estimation for networked control systems," Ph.D. dissertation, University of Victoria, 2012.

[46] J. Nilsson, "Real-time control systems with delays," Ph.D. dissertation, Lund Institute of Technology, Sweden, 1998.

[47] L. Xiao, A. Hassibi, and J. P. How, "Control with random communication delays via a discrete-time jump system approach," in *American Control Conference*, vol. 3, Chicago, USA, 2000, pp. 2199–2204.

[48] O. L. V. Costa and M. D. Fragoso, "Stability results for discrete-time linear systems with Markovian jumping parameters," *Journal of Mathematical Analysis and Applications*, vol. 179, no. 1, pp. 154–178, 1993.

[49] E. K. Boukas and H. Yang, "Stability of discrete-time linear systems with Markovian jumping parameters," *Mathematics of Control, Signals, and Systems*, vol. 8, no. 4, pp. 390–402, 1995.

[50] P. Seiler and R. Sengupta, "An $H_\infty$ approach to networked control," *IEEE Transactions on Automatic Control*, vol. 50, no. 3, pp. 356–364, 2005.

[51] K. Gu, V. Kharitonov, and J. Chen, *Stability of Time-Delay Systems*. Birkhauser, 2003.

[52] D. Huang, "Robust control for uncertain networked control systems with random delays," Ph.D. dissertation, University of Auckland, 2008.

[53] Y. Shi and B. Yu, "Output feedback stabilization of networked control systems with random delays modeled by Markov chains," *IEEE Transactions on Automatic Control*, vol. 54, no. 7, pp. 1668–1674, 2009.

[54] J. Wu and T. Chen, "Design of networked control systems with packet dropouts," *IEEE Transactions on Automatic Control*, vol. 52, no. 7, pp. 1314–1319, 2007.

[55] L. Zhang, Y. Shi, T. Chen, and B. Huang, "A new method for stabilization of networked control systems with random delays," *IEEE Transactions on Automatic Control*, vol. 50, no. 8, pp. 1177–1181, 2005.

[56] Y. Shi and B. Yu, "Robust mixed $H_2/H_\infty$ control of networked control systems with random time delays in both forward and backward communication links," *Automatica*, vol. 47, no. 4, pp. 754–760, 2011.

[57] G. Zhai and H. Lin, "Controller failure time analysis for symmetric control systems," *International Journal of Control*, vol. 77, no. 6, pp. 598–605, 2004.

[58] K. Narendra and J. Balakrishnan, "A common Lyapunov function for stable LTI systems with commuting $A$-matrices," *IEEE Transactions on Automatic Control*, vol. 39, no. 12, pp. 2469–2471, 1994.

[59] H. Lin and P. Antsaklis, "Stability and stabilizability of switched linear systems: A survey of recent results," *IEEE Transactions on Automatic control*, vol. 54, no. 2, pp. 308–322, 2009.

[60] J. Lofberg, "YALMIP: A toolbox for modeling and optimization in MATLAB," in *2004 IEEE International Symposium on Computer Aided Control Systems Design*, Taipei, 2004, pp. 284–289.

[61] M. García-Rivera and A. Barreiro, "Analysis of networked control systems with drops and variable delays," *Automatica*, vol. 43, no. 12, pp. 2054–2059, 2007.

[62] M. Cloosterman, N. van de Wouw, M. Heemels, and H. Nijmeijer, "Robust stability of networked control systems with time-varying network-induced delays," in *Proceedings of the IEEE Conference on Decision and Control*, San Diego, USA, 2006, pp. 4980–4985.

[63] L. Hu, T. Bai, P. Shi, and Z. Wu, "Sampled-data control of networked linear control systems," *Automatica*, vol. 43, no. 5, pp. 903–911, 2007.

[64] Z. Wu, P. Shi, H. Su, and J. Chu, "Passivity analysis for discrete-time stochastic Markovian jump neural networks with mixed time delays," *IEEE Transactions on Neural Networks*, vol. 22, no. 10, pp. 1566–1575, 2011.

[65] L. Wu, P. Shi, H. Gao, and C. Wang, "$H_\infty$ filtering for 2D Markovian jump systems," *Automatica*, vol. 44, no. 7, pp. 1849–1858, 2008.

[66] D. Yue, J. Fang, and S. Won, "Delay-dependent robust stability of stochastic uncertain systems with time delay and Markovian jump parameters," *Circuits, Systems, and Signal Processing*, vol. 22, no. 4, pp. 351–365, 2003.

[67] J. Liu, Z. Gu, and S. Hu, "$H_\infty$ filtering for Markovian jump systems with time-varying delays," *International Journal of Innovative Computing, Information and Control*, vol. 7, no. 3, pp. 1299–1310, 2011.

[68] Q. Ding and M. Zhong, "On designing $H_\infty$ fault detection filter for Markovian jump linear systems with polytopic uncertainties," *International Journal of Innovative Computing, Information and Control*, vol. 6, no. 3, pp. 995–1004, 2010.

[69] X. Luan, F. Liu, and P. Shi, "Neural network based stochastic optimal control for nonlinear Markov jump systems," *International Journal of Innovative Computing, Information and Control*, vol. 6, no. 8, pp. 3715–3724, 2010.

[70] H. Li and Y. Shi, "Robust filtering for nonlinear stochastic systems with uncertainties and Markov delays," *Automatica*, vol. 48, no. 1, pp. 159–166, 2012.

[71] H. Zhang, Y. Shi, and A. Mehr, "Robust static output feedback control and remote PID design for networked motor systems," *IEEE Transactions on Industrial Electronics*, vol. 58, no. 12, pp. 5396–5405, 2011.

[72] S. M. Ross, *Introduction to Probability Models.* Academic Press, 2006.

[73] N. Limnios, B. Ouhbi, and A. Sadek, "Empirical estimator of stationary distribution for semi-Markov processes," *Communications in Statistics-Theory and Methods*, vol. 34, no. 4, pp. 987–995, 2005.

[74] L. Zhang, "$H_\infty$ control of a class of piecewise homogeneous Markov jump linear systems," in *Asian Control Conference*, Hong Kong, China, 2009, pp. 197–202.

[75] B. Johnson, *Design and Analysis of Fault-Tolerant Digital Systems*. Addison-Wesley Reading, MA, 1989.

[76] M. Xie and C. Lai, "Reliability analysis using an additive Weibull model with bathtub-shaped failure rate function," *Reliability Engineering & System Safety*, vol. 52, no. 1, pp. 87–93, 1996.

[77] H. Li and Q. Zhao, "Reliability evaluation of fault tolerant control with a semi-Markov fault detection and isolation model," *Proceedings of the Institution of Mechanical Engineers, Part I: Journal of Systems and Control Engineering*, vol. 220, no. 5, pp. 329–338, 2006.

[78] Z. Hou, J. Luo, P. Shi, and S. Nguang, "Stochastic stability of Ito differential equations with semi-Markovian jump parameters," *IEEE Transactions on Automatic Control*, vol. 51, no. 8, pp. 1383–1387, 2006.

[79] E. Shmerling and K. Hochberg, "Stability of stochastic jump-parameter semi-Markov linear systems of differential equations," *Stochastics: An International Journal of Probability and Stochastic Processes*, vol. 80, no. 6, pp. 513–518, 2008.

[80] R. Barlow, F. Proschan, and L. Hunter, *Mathematical Theory of Reliability*. Society for Industrial Mathematics, 1996.

[81] E. Gershon and U. Shaked, "Robust $H_\infty$ output-feedback control of retarded state-multiplicative stochastic systems," *International Journal of Robust and Nonlinear Control*, vol. 21, no. 11, pp. 1283–1296, 2011.

[82] M. Liu, P. Shi, L. Zhang, and X. Zhao, "Fault-tolerant control for nonlinear Markovian jump systems via proportional and derivative sliding mode observer technique," *IEEE Transactions on Circuits and Systems I: Regular Papers*, vol. 58, no. 11, pp. 2755–2764, 2011.

[83] Z. Fei, H. Gao, and P. Shi, "New results on stabilization of Markovian jump systems with time delay," *Automatica*, vol. 45, no. 10, pp. 2300–2306, 2009.

[84] J. Qiu, G. Feng, and H. Gao, "Approaches to robust $H_\infty$ static output feedback control of discrete-time piecewise-affine systems with norm-bounded uncertainties," *International Journal of Robust and Nonlinear Control*, vol. 21, no. 7, pp. 790–814, 2011.

[85] D. Yue and J. Lam, "Reliable memory feedback design for a class of non-linear time-delay systems," *International Journal of Robust and Nonlinear Control*, vol. 14, no. 1, pp. 39–60, 2004.

[86] Y. He, Y. Zhang, M. Wu, and J. She, "Improved exponential stability for stochastic Markovian jump systems with nonlinearity and time-varying delay," *International Journal of Robust and Nonlinear Control*, vol. 20, no. 1, pp. 16–26, 2010.

[87] A. Svishchuk, *Random Evolutions and Their Applications: New Trends*. Springer, 2000.

[88] J. Huang and Y. Shi, "Stochastic stability of semi-Markov jump linear systems: An LMI approach," in *Proceedings of the IEEE Conference on Decision and Control*, Orlando, USA, 2011, pp. 4668–4673.

[89] E. K. Boukas and Z. K. Liu, "Robust stability and $H_\infty$ control of discrete-time jump linear systems with time-delay: An LMI approach," *Journal of Dynamic Systems, Measurement, and Control*, vol. 125, no. 2, pp. 271–277, 2003.

[90] J. Wen and F. Liu, "Receding horizon control for constrained Markovian jump linear systems with bounded disturbance," *Journal of Dynamic Systems, Measurement, and Control*, vol. 133, no. 1, p. 011005, 2011.

[91] N. E. Wu, "Coverage in fault-tolerant control," *Automatica*, vol. 40, no. 4, pp. 537–548, 2004.

[92] M. Mariton, *Jump Linear Systems in Automatic Control*. New York: M. Dekker, 1990.

[93] K. Zhou and J. Doyle, *Essentials of Robust Control*. Prentice Hall New Jersey, 1998, vol. 104.

[94] W.-H. Chen, Z.-H. Guan, and P. Yu, "Delay-dependent stability and $H_\infty$ control of uncertain discrete-time Markovian jump systems with mode-dependent time delays," *Systems & Control Letters*, vol. 52, no. 5, pp. 361–376, 2004.

[95] E. Boukas and Z. Liu, "Robust $H_\infty$ control of discrete-time Markovian jump linear systems with mode-dependent time-delays," *IEEE Transactions on Automatic Control*, vol. 46, no. 12, pp. 1918–1924, 2001.

[96] J. Gao, B. Huang, and Z. Wang, "LMI-based robust $H_\infty$ control of uncertain linear jump systems with time-delays," *Automatica*, vol. 37, no. 7, pp. 1141–1146, 2001.

[97] D.-J. Wang, "A new approach to delay-dependent $H_\infty$ control of linear state-delayed systems," *Journal of Dynamic Systems, Measurement, and Control*, vol. 126, no. 1, pp. 201–205, 2004.

[98] Q. Wang, J. Lam, S. Xu, and L. Zhang, "Delay-dependent $\gamma$-suboptimal $H_\infty$ model reduction for neutral systems with time-varying delays," *Journal of Dynamic Systems, Measurement, and Control*, vol. 128, no. 2, pp. 394–399, 2006.

[99] H. Gao, T. Chen, and J. Lam, "A new delay system approach to network-based control," *Automatica*, vol. 44, no. 1, pp. 39–52, 2008.

[100] P. Muliere, P. Secchi, and S. G. Walker, "Reinforced random processes in continuous time," *Stochastic Processes and their Applications*, vol. 104, no. 1, pp. 117–130, 2003.

[101] E. Boukas, *Stochastic Switching Systems: Analysis and Design.* Birkhauser, 2006.

[102] I. Amri, D. Soudani, and M. Benrejeb, "Robust state-derivative feedback LMI-based designs for time-varying delay system," in *2011 International Conference on Communications, Computing and Control Applications (CCCA)*, Hammamet, Tunisia, 2011, pp. 1–6.

[103] X. Luan, F. Liu, and P. Shi, "Finite-time stabilization of stochastic systems with partially known transition probabilities," *Journal of Dynamic Systems, Measurement, and Control*, vol. 133, p. 014504, 2011.

[104] D. Henry, S. Simani, and R. Patton, "Fault detection and diagnosis for aeronautic and aerospace missions," *Fault Tolerant Flight Control*, pp. 91–128, 2010.

[105] Y. Zhang and J. Jiang, "Bibliographical review on reconfigurable fault-tolerant control systems," *Annual Reviews in Control*, vol. 32, no. 2, pp. 229–252, 2008.

[106] B. Jiang, K. Zhang, and P. Shi, "Less conservative criteria for fault accommodation of time-varying delay systems using adaptive fault diagnosis observer," *International Journal of Adaptive Control and Signal Processing*, vol. 24, no. 4, pp. 322–334, 2010.

[107] J. Chen, R. J. Patton, and Z. Chen, "Active fault-tolerant flight control systems design using the linear matrix inequality method," *Transactions of the Institute of Measurement and Control*, vol. 21, no. 2–3, pp. 77–84, 1999.

[108] G. Gagliardi, A. Casavola, and D. Famularo, "A fault detection and isolation filter design method for Markov jump linear parameter-varying systems," *International Journal of Adaptive Control and Signal Processing*, vol. 26, no. 3, pp. 241–257, 2012.

[109] F. Tao and Q. Zhao, "Synthesis of active fault-tolerant control based on Markovian jump system models," *IET Control Theory & Applications*, vol. 1, no. 4, pp. 1160–1168, 2007.

[110] P. Shi, E. K. Boukas, S. K. Nguang, and X. Guo, "Robust disturbance attenuation for discrete-time active fault tolerant control systems with uncertainties," *Optimal Control Applications and Methods*, vol. 24, no. 2, pp. 85–101, 2003.

[111] R. Srichander and K. W. Bruce, "Stochastic stability analysis for continuous-time fault tolerant control systems," *International Journal of Control*, vol. 57, no. 2, pp. 433–452, 1993.

[112] M. Mahmoud, J. Jiang, and Y. M. Zhang, "Stochastic stability analysis for fault tolerant control systems with multiple failure processes," *International Journal of Systems Science*, vol. 33, no. 1, pp. 55–65, 2002.

[113] Y. Yin, P. Shi, and F. Liu, "Gain-scheduled robust fault detection on time-delay stochastic nonlinear systems," *IEEE Transactions on Industrial Electronics*, no. 99, pp. 4908–4916, 2011.

[114] A. A. G. Siqueira, M. H. Terra, and C. Buosi, "Fault-tolerant robot manipulators based on output-feedback controllers," *Robotics and Autonomous Systems*, vol. 55, no. 10, pp. 785–794, 2007.

[115] M. Finkelstein, *Failure Rate Modeling for Reliability and Risk*. Springer Verlag, 2008.

[116] N. Gebraeel, A. Elwany, and J. Pan, "Residual life predictions in the absence of prior degradation knowledge," *IEEE Transactions on Reliability*, vol. 58, no. 1, pp. 106–117, 2009.

[117] P. Goupil, "Oscillatory failure case detection in the A380 electrical flight control system by analytical redundancy," *Control Engineering Practice*, vol. 18, no. 9, pp. 1110–1119, 2010.

[118] R. Hayama, M. Higashi, S. Kawahara, S. Nakano, and H. Kumamoto, "Fault-tolerant automobile steering based on diversity of steer-by-wire, braking and acceleration," *Reliability Engineering & System Safety*, vol. 95, no. 1, pp. 10–17, 2010.

[119] F. Grabski, "The reliability of an object with semi-Markov failure rate," *Applied Mathematics and Computation*, vol. 135, no. 1, pp. 1–16, 2003.

[120] K. Hochberg and E. Shmerling, "Stability and optimal control for semi-Markov jump parameter linear systems," *Recent Advances in Applied Probability*, pp. 205–221, 2005.

[121] J. Widder, M. Biely, G. Gridling, B. Weiss, and J.-P. Blanquart, "Consensus in the presence of mortal Byzantine faulty processes," *Distributed Computing*, vol. 24, no. 6, pp. 299–321, 2012.

[122] V. A. Ugrinovskii and I. R. Petersen, "Absolute stabilization and minimax optimal control of uncertain systems with stochastic uncertainty," *SIAM Journal on Control and Optimization*, vol. 37, no. 4, pp. 1089–1122, 1999.

[123] E. Kiyak, O. Cetin, and A. Kahvecioglu, "Aircraft sensor fault detection based on unknown input observers," *Aircraft Engineering and Aerospace Technology: An International Journal*, vol. 80, no. 5, pp. 545–548, 2008.

[124] B. Yu, Y. Shi, and J. Huang, "Modified generalized predictive control of networked systems with application to a hydraulic position control system," *Journal of Dynamic Systems, Measurement, and Control*, vol. 133, no. 3, p. 031009, 2011.

[125] V. Gupta, B. Hassibi, and R. Murray, "Optimal LQG control across packet-dropping links," *Systems & Control Letters*, vol. 56, no. 6, pp. 439–446, 2007.

[126] A. D'Innocenzo, G. Weiss, R. Alur, A. Isaksson, K. Johansson, and G. Pappas, "Scalable scheduling algorithms for wireless networked control systems," in *IEEE International Conference on Automation Science and Engineering*, Bangalore, India, 2009, pp. 409–414.

[127] P. Baronti, P. Pillai, V. Chook, S. Chessa, A. Gotta, and Y. Hu, "Wireless sensor networks: A survey on the state of the art and the 802.15.4 and ZigBee standards," *Computer Communications*, vol. 30, no. 7, pp. 1655–1695, 2007.

[128] ISA100. ISA-SP100 Wireless Systems for Automation Website. [Online]. Available: http://www.isa.org/isa100 28 Nov. 2011.

[129] P. Chen, C. Ramesh, and K. Johansson, "Network estimation and packet delivery prediction for control over wireless mesh networks," *Arxiv preprint arXiv:1103.5405*, 2011.

[130] Y. Liang, T. Chen, and Q. Pan, "Multi-rate stochastic $H_\infty$ filtering for networked multi-sensor fusion," *Automatica*, vol. 46, no. 2, pp. 437–444, 2010.

[131] M. Seron, X. Zhuo, J. De Doná, and J. Martínez, "Multisensor switching control strategy with fault tolerance guarantees," *Automatica*, vol. 44, no. 1, pp. 88–97, 2008.

[132] R. Luo, T. Lin, and K. Su, "Multisensor based security robot system for intelligent building," *Robotics and Autonomous Systems*, vol. 57, no. 3, pp. 330–338, 2009.

[133] E. Besada-Portas, J. Lopez-Orozco, J. Besada, and J. De La Cruz, "Multisensor out of sequence data fusion for estimating the state of discrete control systems," *IEEE Transactions on Automatic Control*, vol. 54, no. 7, pp. 1728–1732, 2009.

[134] I. Petersen, "Robust output feedback guaranteed cost control of nonlinear stochastic uncertain systems via an IQC approach," *IEEE Transactions on Automatic Control*, vol. 54, no. 6, pp. 1299–1304, 2009.

[135] H. Zhang, D. Yang, and T. Chai, "Guaranteed cost networked control for T-S fuzzy systems with time delays," *IEEE Transactions on Systems, Man, and Cybernetics, Part C*, vol. 37, no. 2, pp. 160–172, 2007.

[136] L. Wu, J. Lam, X. Yao, and J. Xiong, "Robust guaranteed cost control of discrete-time networked control systems," *Optimal Control Applications and Methods*, vol. 32, no. 1, pp. 95–112, 2011.

[137] R. Wang, G. Liu, W. Wang, D. Rees, and Y. Zhao, "Guaranteed cost control for networked control systems based on an improved predictive control method," *IEEE Transactions on Control Systems Technology*, vol. 18, no. 5, pp. 1226–1232, 2010.

[138] X. Guan and C. Chen, "Delay-dependent guaranteed cost control for TS fuzzy systems with time delays," *IEEE Transactions on Fuzzy Systems*, vol. 12, no. 2, pp. 236–249, 2004.

[139] C. Chen, A. Molin, and S. Hirche, "Guaranteed cost control over quality-of-service networks," in *European Control Conference*, Budapest, Hungary, 2009, pp. 1–7.

[140] X. Fang and J. Wang, "Stochastic observer-based guaranteed cost control for networked control systems with packet dropouts," *IET Control Theory & Applications*, vol. 2, no. 11, pp. 980–989, 2008.

[141] Y. Tipsuwan and M. Chow, "Control methodologies in networked control systems," *Control Engineering Practice*, vol. 11, no. 10, pp. 1099–1111, 2003.

[142] E. Candes and M. Wakin, "An introduction to compressive sampling," *IEEE Signal Processing Magazine*, vol. 25, no. 2, pp. 21–30, 2008.

[143] R. Baraniuk, "Compressive sensing," *IEEE Signal Processing Magazine*, vol. 24, no. 4, pp. 118–121, 2007.

[144] G. Fiore, V. Ercoli, A. Isaksson, K. Landernas, and M. Di Benedetto, "Multi-hop multi-channel scheduling for wireless control in WirelessHART networks,"

in *Proceedings of the IEEE Conference on Emerging Technologies & Factory Automation*, Mallorca, Spain, 2009, pp. 758–765.

[145] Y. Wang, S. Ding, H. Ye, L. Wei, P. Zhang, and G. Wang, "Fault detection of networked control systems with packet based periodic communication," *International Journal of Adaptive Control and Signal Processing*, vol. 23, no. 8, pp. 682–698, 2009.

[146] R. Gupta, A. Agarwal, M. Chow, and W. Wang, "Characterization of data-sensitive wireless distributed networked-control-systems," in *IEEE/ASME International Conference on Advanced Intelligent Mechatronics*, Zurich, Switzerland, 2007, pp. 1–6.

[147] M. Nagahara and D. Quevedo, "Sparse representations for packetized predictive networked control," in *Proceedings of the 18th IFAC World Congress*, vol. 18, Milano, Italy, 2011, pp. 84–89.

[148] H. Zhang, Y. Shi, and A. Mehr, "Robust $H_\infty$ PID control for multivariable networked control systems with disturbance/noise attenuation," *International Journal of Robust and Nonlinear Control*, vol. 22, no. 2, pp. 183–204, 2012.

[149] L. El Ghaoui, F. Oustry, and M. AitRami, "A cone complementarity linearization algorithm for static output-feedback and related problems," *IEEE Transactions on Automatic Control*, vol. 42, no. 8, pp. 1171–1176, 1997.

[150] K. Kim, J. Colgate, J. Santos-Munné, A. Makhlin, and M. Peshkin, "On the design of miniature haptic devices for upper extremity prosthetics," *IEEE/ASME Transactions on Mechatronics*, vol. 15, no. 1, pp. 27–39, 2010.

[151] M. Ferre, I. Galiana, R. Wirz, and N. Tuttle, "Haptic device for capturing and simulating hand manipulation rehabilitation," *IEEE/ASME Transactions on Mechatronics*, vol. 16, no. 5, pp. 808–815, 2011.

[152] P. Griffiths, R. Gillespie, and J. Freudenberg, "Performance/stability robustness tradeoffs induced by the two-port virtual coupler," in *the Proceedings of the 14th Symposium on Haptic Interfaces for Virtual Environment and Teleoperator Systems*, Alexandria, USA, 2006, pp. 193–200.

[153] J. Kim, J. Kim, C. Seo, and J. Ryu, "A directionally transparent energy bounding approach for multiple degree-of-freedom haptic interaction," *International Journal of Control, Automation and Systems*, vol. 8, no. 2, pp. 352–360, 2010.

[154] D. Lawrence, "Stability and transparency in bilateral teleoperation," *IEEE Journal of Robotics and Automation*, vol. 9, no. 5, pp. 624–637, 1993.

[155] D. Lawrence, L. Pao, M. Salada, and A. Dougherty, "Quantitative experimental analysis of transparency and stability in haptic interfaces," in *the Proceedings of ASME Dynamic Systems and Control Division*, vol. 58, Altanta, USA, 1996, pp. 441–449.

[156] H. Son, T. Bhattacharjee, and H. Hashimoto, "Enhancement in operator's perception of soft tissues and its experimental validation for scaled teleoperation systems," *IEEE/ASME Transactions on Mechatronics*, vol. 16, no. 6, pp. 1096–1109, 2011.

[157] M. Minsky, O. Ming, O. Steele, F. Brooks Jr, and M. Behensky, "Feeling and seeing: Issues in force display," in *the Proceedings of Symposium on Interactive 3D Graphics*, New York, USA, 1990, pp. 235–243.

[158] B. Miller, J. Colgate, R. Freeman, C. Inc, and C. Goleta, "Guaranteed stability of haptic systems with nonlinear virtual environments," *IEEE Journal of Robotics and Automation*, vol. 16, no. 6, pp. 712–719, 2000.

[159] J. Colgate and G. Schenkel, "Passivity of a class of sampled-data systems: Application to haptic interfaces," *Journal of Robotic Systems*, vol. 14, no. 1, pp. 37–47, 1997.

[160] P. Naghshtabrizi and J. Hespanha, "Designing transparent stabilizing haptic controllers," in *the Proceedings of American Control Conference*, Minneapolis, USA, 2006, pp. 2475–2480.

[161] M. Tabbara, D. Nesic, and A. Teel, "Stability of wireless and wireline networked control systems," *IEEE Transactions on Automatic Control*, vol. 52, no. 9, pp. 1615–1630, 2007.

[162] K. Walker, Y. Pan, and J. Gu, "Bilateral teleoperation over networks based on stochastic switching approach," *IEEE/ASME Transactions on Mechatronics*, vol. 14, no. 5, pp. 539–554, 2009.

[163] M. Drew, X. Liu, A. Goldsmith, and K. Hedrick, "Networked control system design over a Wireless LAN," in *Proceedings of the IEEE Conference on Decision and Control*, Seville, Spain, 2005, pp. 6704–6709.

[164] J. Colandairaj, W. Scanlon, and G. Irwin, "Understanding wireless networked control systems through simulation," *Computing Control Engineering Journal*, vol. 16, no. 2, pp. 26–31, 2005.

[165] C. Tang, P. Miller, V. Krovi, J. Ryu, and S. Agrawal, "Differential-flatness-based planning and control of a wheeled mobile manipulator – theory and experiment," *IEEE/ASME Transactions on Mechatronics*, vol. 16, no. 4, pp. 768–773, 2011.

[166] T. Kim, E. Kim, and J. Kim, "Development of a humanoid walking command system using a wireless haptic controller," in *International Conference on Control, Automation and Systems*, Seoul, Korea, 2008, pp. 1178–1183.

[167] J. Troy, C. Erignac, and P. Murray, "System for haptics-enabled teleoperation of vehicles," 2010, US Patent 7885732.

[168] I. Polushin, P. Liu, and C. Lung, "A force-reflection algorithm for improved transparency in bilateral teleoperation with communication delay," *IEEE/ASME Transactions on Mechatronics*, vol. 12, no. 3, pp. 361–374, 2007.

[169] Y. Ye and P. Liu, "Improving trajectory tracking in wave-variable-based teleoperation," *IEEE/ASME Transactions on Mechatronics*, vol. 15, no. 2, pp. 321–326, 2010.

[170] Z. Yang, L. Lian, and Y. Chen, "Haptic function evaluation of multi-material part design," *Computer-Aided Design*, vol. 37, no. 7, pp. 727–736, 2005.

[171] M. Bergamasco, A. Frisoli, and F. Barbagli, "Haptics technologies and cultural heritage applications," in *the Proceedings of Computer Animation*, Geneva, Switzerland, 2002, pp. 25–32.

[172] A. Menciassi, A. Eisinberg, M. Carrozza, and P. Dario, "Force sensing microinstrument for measuring tissue properties and pulse in microsurgery," *IEEE/ASME Transactions on Mechatronics*, vol. 8, no. 1, pp. 10–17, 2003.

[173] N. Dahotre and S. Harimkar, *Laser Fabrication and Machining of Materials*. Springer Verlag, 2008.

[174] M. Jackson, *Machining with Abrasives*. Springer Verlag, 2010.

[175] Y. Kwon, N. Saito, and I. Shigematsu, "Friction stir process as a new manufacturing technique of ultrafine grained aluminum alloy," *Journal of Naterials Science Letters*, vol. 21, no. 19, pp. 1473–1476, 2002.

[176] J. Colgate, P. Grafing, M. Stanley, and G. Schenkel, "Implementation of stiff virtual walls in force-reflecting interfaces," in *the Virtual Reality Annual International Symposium*, Seattle, USA, 1993, pp. 202–208.

[177] B. Miller, J. Colgate, and R. Freeman, "Passive implementation for a class of static nonlinear environmentsin haptic display," in *the Proceedings of IEEE International Conference on Robotics and Automation*, vol. 4, Detroit, USA, 1999, pp. 2937–2942.

[178] K. Hale and K. Stanney, "Deriving haptic design guidelines from human physiological, psychophysical, and neurological foundations," *IEEE Computer Graphics and Applications*, vol. 24, no. 2, pp. 33–39, 2004.

[179] Y. Cao and J. Lam, "Stochastic stabilizability and $H_\infty$ control for discrete-time jump linear systems with time delay," *Journal of the Franklin Institute*, vol. 336, no. 8, pp. 1263–1281, 1999.

[180] M. Fukuda and M. Kojima, "Branch-and-cut algorithms for the bilinear matrix inequality eigenvalue problem," *Computational Optimization and Applications*, vol. 19, no. 1, pp. 79–105, 2001.

[181] J. VanAntwerp and R. Braatz, "A tutorial on linear and bilinear matrix inequalities," *Journal of Process Control*, vol. 10, no. 4, pp. 363–385, 2000.

[182] R. Gupta and M. Chow, "Networked control system: Overview and research trends," *IEEE Transactions on Industrial Electronics*, vol. 57, no. 7, pp. 2527–2535, 2010.

[183] A. Onat, T. Naskali, E. Parlakay, and O. Mutluer, "Control over imperfect networks: Model-based predictive networked control systems," *IEEE Transactions on Industrial Electronics*, vol. 58, no. 3, pp. 905–913, 2011.

[184] J. García, F. R. Palomo, A. Luque, C. Aracil, J. M. Quero, D. Carrión, F. Gámiz, P. Revilla, J. Pérez-Tinao, M. Moreno, P. Robles, and L. G. Franquelo, "Reconfigurable distributed network control system for industrial plant automation," *IEEE Transactions on Industrial Electronics*, vol. 51, no. 6, pp. 1168–1180, 2004.

[185] R. Gupta, A. Masoud, and M. Chow, "A delay-tolerant potential field-based, network implementation of an integrated navigation system," *IEEE Transactions on Industrial Electronics*, vol. 57, no. 2, pp. 769–783, 2010.

[186] H. Gao and T. Chen, "$H_\infty$ estimation for uncertain systems with limited communication capacity," *IEEE Transactions on Automatic Control*, vol. 52, no. 11, pp. 2070–2084, 2007.

[187] R. Wirz, R. Marin, M. Ferre, J. Barrio, J. Claver, and J. Ortego, "Bidirectional transport protocol for teleoperated robots," *IEEE Transactions on Industrial Electronics*, vol. 56, no. 9, pp. 3772–3781, 2009.

[188] S. Canovas and C. Cugnasca, "Implementation of a control loop experiment in a network-based control system with LonWorks technology and IP networks," *IEEE Transactions on Industrial Electronics*, vol. 57, no. 11, pp. 3857–3867, 2010.

[189] R. Zurawski, *Embedded Systems Handbook: Networked Embedded Systems*. CRC Press, 2009, vol. 2.

[190] R. Wang, G. Liu, W. Wang, D. Rees, and Y. Zhao, "$H_\infty$ control for networked predictive control systems based on the switched Lyapunov function method," *IEEE Transactions on Industrial Electronics*, vol. 57, no. 10, pp. 3565–3571, 2010.

[191] M. Chow and Y. Tipsuwan, "Gain adaptation of networked DC motor controllers based on QoS variations," *IEEE Transactions on Industrial Electronics*, vol. 50, no. 5, pp. 936–943, 2003.

[192] M. Liu, D. W. Ho, and Y. Niu, "Stabilization of Markovian jump linear system over networks with random communication delay," *Automatica*, vol. 45, no. 2, pp. 416–421, 2009.

[193] N. van de Wouw, P. Naghshtabrizi, M. Cloosterman, and J. P. Hespanha, "Tracking control for networked control systems," in *Proceedings of the IEEE Conference on Decision and Control*, New Orleans, USA, 2007, pp. 4441–4446.

[194] W. Wu, G. Liu, and D. Rees, "Event-driven networked predictive control," *IEEE Transactions on Industrial Electronics*, vol. 54, no. 3, pp. 1603–1613, 2007.

[195] H. Gao and T. Chen, "Network-based $H_\infty$ output tracking control," *IEEE Transactions on Automatic Control*, vol. 53, no. 3, pp. 655–667, 2008.

[196] Y.-L. Wang and G.-H. Yang, "Output tracking control for networked control systems with time delay and packet dropout," *International Journal of Control*, vol. 81, no. 11, pp. 1709–1719, 2008.

[197] H. Li, M.-Y. Chow, and Z. Sun, "EDA-based speed control of a networked DC motor system with time delays and packet losses," *IEEE Transactions on Industrial Electronics*, vol. 56, no. 5, pp. 1727–1735, 2009.

[198] W. Kim, K. Ji, and A. Ambike, "Networked real-time control strategy dealing with stochastic time delays and packet losses," *Journal of Dynamic Systems, Measurement, and Control*, vol. 128, no. 3, pp. 681–685, 2006.

[199] D. Georgiev and D. M. Tilbury, "Packet-based control: The $H_2$-optimal solution," *Automatica*, vol. 42, no. 1, pp. 137–144, 2006.

[200] Y.-B. Zhao, G. Liu, and D. Rees, "Improved predictive control approach to networked control systems," *IET Control Theory & Applications*, vol. 2, no. 8, pp. 675–681, 2008.

[201] H. Lin and P. Antsaklis, "Stability and persistent disturbance attenuation properties for a class of networked control systems: Switched system approach," *International Journal of Control*, vol. 78, no. 18, pp. 1447–1458, 2005.

[202] D. Quevedo and D. Nesic, "Input-to-state stability of packetized predictive control over unreliable networks affected by packet-dropouts," *IEEE Transactions on Automatic Control*, vol. 56, no. 2, pp. 370–375, 2011.

[203] J. R. Broussard and M. J. O'Brien, "Feedforward control to track the output of a forced model," *IEEE Transactions on Automatic Control*, vol. 25, no. 4, pp. 851–853, 1980.

[204] R. W. Benson, W. E. Schmiteiidorf, and R. M. Dolphiis, "Feedforward tracking for uncertain systems," in *Proceedings of the IEEE Conference on Decision and Control*, vol. 3, Tucson, USA, 1992, pp. 2635–2639.

[205] D. Yue, J. Lam, and Z. Wang, "Persistent disturbance rejection via state feedback for networked control systems," *Chaos, Solitons and Fractals*, vol. 40, no. 1, pp. 382–391, 2009.

[206] O. Kim, S. Lee, and D. Han, "Positioning performance and straightness error compensation of the magnetic levitation stage supported by the linear magnetic bearing," *IEEE Transactions on Industrial Electronics*, vol. 50, no. 2, pp. 374–378, 2003.

[207] Y. Ji, H. J. Chizeck, X. Feng, and K. Loparo, "Stability and control of discrete-time jump linear systems," *Control Theory and Advanced Technology*, vol. 7, no. 2, pp. 247–270, 1991.

[208] P. Seiler and R. Sengupta, "A bounded real lemma for jump systems," *IEEE Transactions on Automatic Control*, vol. 48, no. 9, pp. 1651–1654, 2003.

[209] M. C. de Oliveira and J. C. Geromel, "Numerical comparison of output feedback design methods," in *American Control Conference*, vol. 1, Albuquerque, USA, 1997, pp. 72–76.

[210] L. Zhang, B. Huang, and J. Lam, "$H_\infty$ model reduction of Markovian jump linear systems," *Systems & Control Letters*, vol. 50, no. 2, pp. 103–118, 2003.

[211] Y.-Y. Cao, J. Lam, and Y.-X. Sun, "Static output feedback stabilization–An ILMI approach," *Automatica*, vol. 34, no. 12, pp. 1641–1645, 1998.

[212] C. Santacesaria and R. Scattolini, "Easy tuning of Smith predictor in presence of delay uncertainty," *Automatica*, vol. 29, no. 6, pp. 1595–1597, 1993.

[213] L. White, R. Mahony, and G. Brushe, "Lumpable hidden Markov models-model reduction and reduced complexity filtering," *IEEE Transactions on Automatic Control*, vol. 45, no. 12, pp. 2297–2306, 2000.

[214] V. Girardin, "Entropy maximization for Markov and semi-Markov processes," *Methodology and Computing in Applied Probability*, vol. 6, no. 1, pp. 109–127, 2004.

[215] M. Mazo and P. Tabuada, "On event-triggered and self-triggered control over sensor/actuator networks," in *Proceedings of the IEEE Conference on Decision and Control*, Cancun, Mexico, 2008, pp. 435–440.

[216] ——, "Decentralized event-triggered control over wireless sensor/actuator networks," *IEEE Transactions on Automatic Control*, vol. 56, no. 10, pp. 2456–2461, 2011.

[217] K. Astrom and B. Bernhardsson, "Comparison of Riemann and Lebesgue sampling for first order stochastic systems," in *Proceedings of the IEEE Conference on Decision and Control*, vol. 2, Las Vegas, USA, 2002, pp. 2011–2016.

[218] J. Lunze and D. Lehmann, "A state-feedback approach to event-based control," *Automatica*, vol. 46, no. 1, pp. 211–215, 2010.

[219] W. Heemels, J. Sandee, and P. Van Den Bosch, "Analysis of event-driven controllers for linear systems," *International Journal of Control*, vol. 81, no. 4, pp. 571–590, 2008.

# Appendix

## Publications

- **Journal Articles (published and accepted)**

  J1. **J. Huang** and Y. Shi, "Stochastic stability and robust stabilization of semi-Markov jump linear systems," *International Journal of Robust and Nonlinear Control*, accepted and in press in 2012.

  J2. **J. Huang** and Y. Shi, "$H_\infty$ state-feedback control for semi-Markov jump linear systems with time-varying delays," *ASME Journal of Dynamic Systems, Measurement, and Control*, accepted in 2013.

  J3. Y. Shi, **J. Huang**, and B. Yu, "Robust tracking control of networked control systems: Application to a networked DC motor," *IEEE Transactions on Industrial Electronics*, accepted in 2012.

  J4. **J. Huang**, Y. Shi, and J. Wu, "Transparent virtual coupler design for networked haptic systems with a mixed virtual wall," *IEEE/ASME Transactions on Mechatronics*, vol. 17, no. 3, pp. 480–487, 2012.

  J5. **J. Huang**, Y. Shi, H. Huang, and Z. Li "$l_2 - l_\infty$ filtering for multirate nonlinear sampled-data systems using T-S fuzzy models," *Digital Signal Processing*, vol. 23, no. 1, pp. 418–426, 2013.

  J6. **J. Huang** and Y. Shi, "Active fault tolerant control systems by the semi-Markov model approach," *International Journal of Adaptive Control and Signal Processing*, accepted in 2013.

  J7. B. Yu, Y. Shi, and **J. Huang**, "Modified generalized predictive control of networked systems with application to a hydraulic position control system," *ASME Journal of Dynamic Systems, Measurement, and Control*, vol. 133, no. 3, p. 031009, 2011.

  J8. J. Wu, Y. Shi, **J. Huang**, and D. Constantinescu. "Stochastic stabiliza-

tion for bilateral teleoperation over networks with probabilistic delays," *Mechatronics*, vol. 22, no. 8, pp. 1050–1059, 2012.

J9. F. Liu, **J. Huang**, Y. Shi, and D. Xu, "Fault detection for discrete-time systems with randomly occurring nonlinearity and data missing: A quadrotor vehicle example," *Journal of The Franklin Institute*, accepted in 2013.

- **Conference Papers**

C1. **J. Huang** and Y. Shi, "Guaranteed cost control for multi-sensor networked control systems using historical data," *31st American Control Conference*, Montreal, Canada, June 27–29, 2012.

C2. **J. Huang** and Y. Shi, "Stochastic stability of semi-Markov jump linear systems: An LMI approach," *50th IEEE Conference on Decision and Control and European Control Conference*, Orlando, Florida, USA, Dec. 12–15, 2011.

C3. B. Yu, Y. Shi, and **J. Huang**, "Step tracking control with disturbance rejection for networked control systems with random time delays," *48th IEEE Conference on Decision and Control and 28th Chinese Control Conference*, Shanghai, China, Dec. 16–18, 2009.

C4. Y. Shi, B. Yu, and **J. Huang**, "Mixed $H_2/H_\infty$ control of networked control systems with random delays modeled by Markov chains," *28th American Control Conference*, St. Louise, Missouri, USA, June 10–12, 2009.